Engineering of Protein Glycosylation in Chinese Hamster Ovary Cells

Thesis by

Pablo Umaña

In Partial Fulfillment of the Requirements

for the Degree of

Doctor of Philosophy

California Institute of Technology
Pasedena, California
1998

(Submitted April 6, 1998)

ACKNOWLEDGEMENTS

I would first like to thank my advisor, Prof. Jay Bailey, for introducing me to this exciting area of research, for providing me with intellectual freedom, and for his constant encouragement and financial support.

Next, I would like to thank Joël Jean-Mairet, a close friend and research partner, who contributed significantly to this work. Collaborating with such an inquisitive, hard working, understanding person, has been the most rewarding part of my doctoral studies.

Various persons in the Bailey group have taught me many useful things and stimulated interesting scientific discussions. Special thanks in this regard go to Peter Licari, Miguel Alvarez, Vassily Hatzimanikatis, Wolfgang Krömer, Pauli Kallio, and Wolfgang Minas. I also thank the latin-crew and adopted members - Adriana, Lisa, Roberto, Patrick, Tobias, and Claudia, for providing a very joyful environment in and out of the lab.

People who helped directly in specific parts of the work presented here are acknowledged in the appropriate chapters.

I would like to express my gratitude to my family and to Fiona for their support and patience. Their love and understanding have helped to keep my feet on the ground during this difficult process. Besides her immense personal support, discussions with Fiona helped me to keep my research focused, and without her careful proofreading, there would certainly be many more errors in this thesis.

ABSTRACT

Improved versions of therapeutic glycoproteins may be produced by manipulation of their glycosylation patterns. Engineering of glycoform biosynthesis in CHO cells is studied here as a route to produce new variants of a recombinant, therapeutic protein and to maximize the proportion of beneficial glycoforms within the glycoform population. An anti-neuroblastoma monoclonal antibody (chCE7) was used as a model therapeutic glycoprotein, and the target glycoforms were those carrying bi-antennary complex N-linked oligosaccharides modified with a bisecting N-acetylglucosamine (GlcNAc).

A mathematical model of N-linked glycoform biosynthesis was constructed and used to simulate the qualitative effects of overexpression of GlcNAc-transferase III (GnTIII), the enzyme catalyzing the transfer of a bisecting GlcNAc to various oligosaccharide substrates. These simulations indicated a maximum level for bisected complex oligosaccharides, and accumulation of hybrid bisected oligosaccharides.

To investigate the effects of GnTIII overexpression experimentally, a CHO cell line with tetracycline-regulated overexpression of a rat GnTIII cDNA was established. Expressed GnTIII was localized in the Golgi complex of CHO cells by means of immunoelectron microscopy using an antibody against a peptide epitope tag added to the carboxy-terminus of the enzyme. The enzyme concentrated on one side of the Golgi, mainly in cisternal compartments.

Using the experimental system, it was found that overexpression of GnTIII to high levels led to growth inhibition and was toxic to the cells. Another CHO cell line with tetracycline-regulated overexpression of GnTV, a distinct glycosyltransferase, showed the same inhibitory effect, indicating that this may be a general feature of glycosyltransferase overexpression. The growth effect set an upper limit to glycosyltransferase overexpression and may therefore also limit the extent to which poorly accessible glycosylation sites can be modified by engineering of glycosylation pathways.

A set of chCE7 mAb samples differing in their glycoform distributions was produced by controlling GnTIII expression in a range between basal and toxic levels. Measurement of the ADCC activity of these samples showed an optimal range of GnTIII expression for maximal chCE7 *in vitro* biological activity. The activity correlated with the level of Fc-associated bisected, complex oligosaccharides. Expression of GnTIII within the biotechnologically practical range, i.e., where no significant growth inhibition and toxicity are observed, led to a consumption of more than 90% of non-bisected, non-galactosylated bi-antennary complex oligosaccharides, but, at most, 50% was converted to the target bisected, complex structures for this set of chCE7 samples. The pattern of oligosaccharide peaks in MALDI/TOF-mass spectrometric analysis of samples produced at high levels of GnTIII, indicate that a significant proportion of potential GnTIII substrates is diverted to bisected hybrid oligosaccharide by-products. Minimization of these by-products by further engineering of the pathway could therefore be valuable.

The new optimized variants of chCE7 are promising candidate reagents for the treatment of neuroblastoma. The strategy presented here may also be applicable to other therapeutic IgGs.

TABLE OF CONTENTS

ACKNOWLEDGEMENTS iii

ABSTRACT iv

CHAPTER I Introduction 1

1.1 Production of Therapeutic Glycoproteins in Animal Cells 2

1.2 Thesis Motivation 5

1.3 Thesis Scope 8

1.4 References 10

CHAPTER II A Mathematical Model of N-linked Glycoform Biosynthesis 13

2.1 Summary 14

2.2 Introduction 15

2.3 Physical Model 18

2.4 Mathematical Model 25

2.5 Model Parameters 32

2.6 Solution Strategy 43

2.7 Results and Discussion 44

2.8 Acknowledgements 51

2.9 References 52

2.10 Tables 63

2.11 Figures 67

CHAPTER III Tetracycline-Regulated Overexpression of Glycosyltransferases in Chinese Hamster Ovary Cells 78

3.1 Summary 79

3.2 Introduction 80

3.3 Materials and Methods 82

3.4 Results and Discussion 93

3.5 Acknowledgements 100

3.6 References 101

3.7 Figures 103

CHAPTER IV Engineering the Glycosylation of a Therapeutic Antibody in Chinese Hamster Ovary Cells 115

4.1 Summary 116

4.2 Introduction 117

4.3 Materials and Methods 120

4.4 Results and Discussion 129

4.5 Acknowledgements 136

4.6 References 137

4.7 Figures 141

CHAPTER V Conclusions 151

5.1 Summary of Findings and Recommendations for Future Work 152

5.2 References 154

CHAPTER I

Introduction

1.1 Production of Therapeutic Glycoproteins in Animal Cells

Glycoproteins carry oligosaccharides covalently attached at specific sites of the polypeptide chain. They make up the majority of non-cytosolic proteins in eucaryotic organisms and mediate essential catalytic, structural, and molecular recognition functions (Lis and Sharon, 1993; Rademacher et al., 1988; Varki, 1993; Wyss and Wagner, 1996). Many glycoproteins can be exploited for therapeutic purposes, and during the last two decades, recombinant versions of naturally-occurring, secreted glycoproteins have been the major product of the biotechnology industry. Examples of these are erythropoietin (EPO), therapeutic monoclonal antibodies (therapeutic mAbs), tissue plasminogen activator (tPA), interferon-β (IFN-β), granulocyte-macrophage colony stimulating factor (GM-CSF), and human chorionic gonadotrophin (hCG) (Bailey et al., 1998; Cumming, 1991; Lis and Sharon, 1993).

The oligosaccharide component can significantly affect properties relevant to the efficacy of a therapeutic glycoprotein, including physical stability, resistance to protease attack, interactions with the immune system, pharmacokinetics, and specific biological activity. Such properties may depend not only on the presence or absence, but also on the specific structures, of oligosaccharides. Some generalizations between oligosaccharide structure and glycoprotein function can be made. For example, certain oligosaccharide structures mediate rapid clearance of the glycoprotein from the bloodstream through interactions with specific carbohydrate binding proteins, while others can be bound by antibodies and trigger undesirable immune reactions. However, the relationship between oligosaccharide structure and glycoprotein biological activity is unique to each glycoprotein (Bailey et al., 1998; Jenkins et al., 1996).

Glycoproteins are produced by expression of their corresponding genes in a cellular host. Oligosaccharides are attached post-translationally to aspargine residues, within specific glycosylation sites of the polypeptide, during translocation of the protein into the

first secretory compartment of the cell, the endoplasmic reticulum (ER). These oligosaccharides are said to be N-linked to the protein. Subsequently, as glycoprotein molecules travel through the ER and then through the next series of compartments, called the Golgi complex (Golgi), on their way out of the cell, the oligosaccharides are modified by a complex network of reactions catalyzed by many glycosyltransferase and glycosidase enzymes residing in those compartments. In the Golgi, a different type of oligosaccharide may also be linked to particular serine or threonine residues of the protein and subsequently modified. The resultant oligosaccharides are referred to as O-linked. The end product of the process is a heterogeneous population of glycoforms of the secreted protein, i.e., molecules sharing the same polypeptide backbone but having different occupancy of their glycosylation sites and different oligosaccharide structures attached to each site (Kornfeld and Kornfeld, 1985; Rademacher et al., 1988).

The types of glycoforms produced and their relative proportions depend on the specific glycoprotein, the type of host cell used for production, and the external cellular environment. The polypeptide backbone of each glycoprotein controls to some extent the outcome of the process by modulating the rates of glycosyltransferase- and glycosidase-catalyzed reactions. This implies that individual glycoproteins, or distinct glycosylation sites located in separate regions of a single glycoprotein, can have different glycoform distributions when produced in the same type of cell under identical external conditions. The type of cell used for production of the glycoprotein can also have a profound influence on the glycoform distribution, since the composition of the glycosylation machinery, e.g., which enzymes are present and their levels, can vary with organism, tissue and developmental stage. Finally, the external cellular environment can affect the process by modulating the expression glycosylation-related enzymes, or by directly altering specific catalytic and molecular transport events, e.g., by affecting the concentration of enzyme co-substrates or inhibitors, or the pH inside the secretory compartments. In addition, glycoproteins secreted out of the cell may be modified further by extracellular glycosidases

(Bailey et al., 1998; Cumming, 1991; Kornfeld and Kornfeld, 1985; Rademacher et al., 1988).

Mammalian cells are the preferred hosts for production of therapeutic glycoproteins, due to their capability to glycosylate proteins in the most compatible form for human application (Bailey et al., 1998; Cumming, 1991; Jenkins et al., 1996). Bacteria do not glycosylate proteins, and other types of common hosts, such as yeasts, filamentous fungi, insect and plant cells, yield glycosylation patterns associated with rapid clearance from the bloodstream, undesirable immune interactions, and in some specific cases, reduced biological activity. Among mammalian cells, Chinese hamster ovary (CHO) cells have been most commonly used during the last two decades. In addition to giving suitable glycosylation patterns, these cells allow consistent generation of genetically-stable, highly productive clonal cell lines. They can be cultured to high densities in simple bioreactors using serum-free media, and permit the development of safe and reproducible bioprocesses. Other commonly used animal cells include baby hamster kidney (BHK) cells, NSO-, and SP2/0-mouse myeloma cells. More recently, production from transgenic animals has also been tested (Bailey et al., 1998; Jenkins et al., 1996).

1.2 Thesis Motivation

Although CHO and other mammalian cells glycosylate proteins in a manner adequate for therapeutic applications, there may be some glycoforms with superior properties, which are either not produced by these hosts or are produced at relatively low levels within the glycoform population. In such cases, improved versions of a glycoprotein could be produced by manipulation of the glycosylation pattern (Bailey, 1991; Bailey et al., 1998; Stanley, 1992). For example, "second generation" EPO and tPA glycoproteins, obtained through changes in the glycosylation pattern of earlier versions, are now advancing through clinical trials. The new versions of these two drugs were produced, respectively, by enrichment of superior glycoforms during the purification of the final product (Fürst, 1997), and by introduction of mutations in the polypeptide chain, which shifted the position of the oligosaccharide within the protein and led to a different glycosylation pattern (Keyt et al., 1994). In both cases, biosynthesis of the superior glycoforms was achieved with the standard glycosylation apparatus of normal CHO cells.

An alternative, complementary route for production of improved glycoproteins, is through genetic manipulation of the host glycosylation pathway (Bailey, 1991). New glycoforms or glycoform distributions can be generated by introduction of glycosyltransferase and glycosidase genes into the host cells. This is an attractive route for synthesis of new glycoforms since it does not add major costs to the process, and the required stable genetic changes can be introduced into the host cells using reliable and efficient technology already tested for production of glycoprotein drugs.

Previous work has shown that incorporation of new glycosyltransferase activities into animal cells can yield novel oligosaccharide structures on recombinant glycoproteins (Bailey et al., 1998). The application of this technology to generate potentially improved therapeutic products has only recently begun to be reported. Only those oligosaccharide modifications which influence the pharmacokinetic behaviour of the glycoprotein have thus

far been studied. It would be valuable to extend this technology to more glycoproteins, and to target other types of properties. This must be done case by case due to the specificity of oligosaccharide-structure/glycoprotein-function relationships.

Another important question yet to be addressed, is how the proportion of superior glycoforms within the glycoform population of a therapeutic glycoprotein can be maximized. Achieving this goal could require manipulation of a number of heterologous and/or endogenous enzymes that participate in the glycosylation reaction network. Due to the complexitiy of glycosylation pathways, a comprehensive description of the system and its characteristics would be useful. At several points, a single intermediate can be modified by multiple enzymes, sometimes blocking subsequent reactions by other enzymes. Moreover, some single enzymes can modify several substrates again yielding some products which cannot be subsequently modified by other enzymes. In addition, some enzymes have different, but overlapping, spatial distributions within the various compartments where the reactions take place.

An important group of glycoproteins to which glycosylation engineering may be applied are therapeutic, unconjugated monoclonal antibodies (mAbs). MAbs target viruses and undesirable cells for destruction by the immune system. They consist of a variable region that varies in sequence between antibodies, and a constant region whose sequence is common among many antibodies. The variable region mediates specific, high-affinity binding to the target, e.g., to a certain type of cancer cell; while the constant region is recognized by special proteins of the immune system which trigger a lytic attack on the target cell. Unconjugated mAbs are not linked to toxic molecules or radioactive compounds, and therefore depend to a large extent on recognition by the immune system to yield a therapeutic effect (Dillman, 1997; Wright and Morrison, 1997). Glycosylation of the constant region is essential for this molecular recognition event (Lund et al., 1996; Wright and Morrison, 1997).

Although the glycosylation pattern of mAbs produced by CHO cells is suitable for their therapeutic application (Reff et al., 1994), these cells do not add certain types of monosaccharide residues that are present in naturally-occurring antibodies of humans and animals (Lifely et al., 1995; Wormald et al., 1997). Some evidence suggests that one of these residues could play a significant role in the recognition of the constant region by the immune system receptors (Lifely et al., 1995). Therefore, it could prove valuable to engineer glycoform biosynthesis in CHO cells to produce therapeutic antibodies carrying this special monosaccharide residue, and if new the glycoforms do have superior activity, to try to maximize their proportion.

1.3 Thesis Scope

The aim of this thesis is to engineer glycoform biosynthesis in CHO cells to produce new variants of a cloned, therapeutic protein, and to study the extent to which the glycosylation reaction network can be manipulated in an attempt to maximize the proportion of certain glycoforms within the population. An anti-cancer mAb is used as a model therapeutic glycoprotein, and the target glycoforms are those carrying a special class of carbohydrate; namely, bi-antennary complex N-linked oligosaccharides modified with a bisecting N-acetylglucosamine (GlcNAc). The glycosyltransferase that adds a bisecting GlcNAc to various types of N-linked oligosaccharides, GlcNAc-transferase III (GnTIII), is not normally produced by CHO cells (Stanley and Campbell, 1984).

Chapter II describes the development of a mathematical model of N-linked glycoform biosynthesis to enable calculation of the expected qualitative trends in the oligosaccharide distribution that would result from changes in the levels of one or more enzymes involved in the glycosylation reaction network. The effect of overexpression of GnTIII in CHO cells is simulated under different conditions, including during co-overexpression of other enzymes in the network. The spatial distribution of GnTIII within the different Golgi sub-compartments is unknown, and the impact of this variable is also evaluated.

The simulations in Chapter II indicate that there could be an optimal range of GnTIII overexpression for the maximization of complex N-linked oligosaccharides carrying a bisecting GlcNAc, and that this range can be affected by the spatial distribution of the enzyme. To investigate the effects of GnTIII overexpression experimentally, a CHO cell line with tetracycline-regulated overexpression of GnTIII was established (Chapter III). The experimental system permits control of GnTIII expression level in CHO cells by simply changing the concentration of tetracycline added to the extracellular environment. Parallel cultures of the cell line, grown at different tetracycline concentrations, allow rigorous correlations to be made between expression of the GnTIII gene and different

response variables. One relevant issue for metabolic engineering of the system is how overproduction of the catalysts affects the cellular hosts. This was studied for GnTIII and another glycosyltransferase, GnTV. The results are described in Chapter III together with an investigation of the spatial distribution of GnTIII within the Golgi of CHO cells.

The experimental system was used to produce a set of anti-cancer mAb samples differing in their glycoform distributions. The biological activity of these samples correlates with the expression level of the GnTIII gene in CHO cells. These results are presented in Chapter IV. The extent to which the network can be manipulated to maximize bisected, complex glycoforms of the mAb was determined and is also presented in this chapter.

1.4 References

Bailey, J. E. 1991. Toward a science of metabolic engineering. Science **252:** 1668- 1675.

Bailey, J. E., Prati, E., Jean-Mairet, J., et al. 1998. Engineering Glycosylation in Animal Cells. p. In: Merten, O. (ed.), Animal Cell Technology. Kluwer, Amsterdam. (In press).

Cumming, D. A. 1991. Glycosylation of recombinant protein therapeutics: control and functional implications. Glycobiology **1:** 115-130.

Dillman, R. O. 1997. Magic bullets at last! Finally-approval of a monoclonal antibody for the treatment of cancer!!! Cancer Biother. & Radiopharm. **12:** 223-225.

Fürst, I. 1997. Amgen's NESP heats up competiton in lucrative erythropoietin market. Nature Biotech. **15:** 940.

Jenkins, N., Parekh, R. B. and James, D. C. 1996. Getting the glycosylation right: implications for the biotechnology industry. Nature Biotechnol. **14:** 975-981.

Keyt, B. A., Paoni, N. F., Refino, C. J., et al. 1994. A faster-acting and more potent form of tissue plasminogen activator. Biochemistry **91:** 3670-3674.

Kornfeld, R. and Kornfeld, S. 1985. Assembly of asparagine- linked oligosaccharides. Ann. Rev. Biochem. **54:** 631- 664.

Lifely, R. M., Hale, C., Boyce, S., et al. 1995. Glycosylation and biological activity of CAMPATH-1H expressed in different cell lines and grown under different culture conditions. Glycobiology **318:** 813- 822.

Lis, H. and Sharon, N. 1993. Protein glycosylation: Structural and functional aspects. Eur. J. Biochem. **218:** 1-27.

Lund, J., Takahashi, N., Pound, J. D., et al. 1996. Multiple interactions of IgG with its core oligosaccharide can modulate recognition by complement and human Fcγ receptor I and influence the synthesis of its oligosaccharide chains. J. Immunol. **157:** 4963-4969.

Rademacher, T. W., Parekh, R. B. and Dwek, R. A. 1988. Glycobiology. Annu. Rev. Biochem. **57:** 785-838.

Reff, M. E., Carner, K., Chambers, K. S., et al. 1994. Depletion of B cells in vivo by a chimeric mouse human monoclonal antibody to CD20. Blood **83:** 435-445.

Stanley, P. 1992. Glycosylation engineering. Glycobiology **2:** 99-107.

Stanley, P. and Campbell, C. A. 1984. A dominant mutation to ricin resistance in Chinese hamster ovary cells induces UDP- GlcNac: Glycopeptide β-4-N- Acetylglucosaminyl-transferase III activity. J. Biol. Chem. **261:** 13370- 13378.

Varki, A. 1993. Biological roles of oligosaccharides: all theories are correct. Glycobiology **3:** 97-130.

Wormald, M. R., Rudd, P. M., Harvey, D. J., et al. 1997. Variations in oligosaccharide-protein interactions in immunoglobulin G determine the site-specific glycosylation profiles and modulate the dynamic motion of the oligosaccharides. Biochemistry **36:** 1370-1380.

Wright, A. and Morrison, S. L. 1997. Effect of glycosylation on antibody function: implications for genetic engineering. Tibtech **15:** 26-31.

Wyss, D. F. and Wagner, G. 1996. The structural role of sugars in glycoproteins. Current Opinion Biotechnol. **7:** 409-416.

CHAPTER II

A Mathematical Model of N-linked Glycoform Biosynthesis

Source: Umaña, P., Bailey, J. E. 1997. Biotechnology and Bioengineering **55**: 890-908

2.1 Summary

Metabolic engineering of N-linked oligosaccharide biosynthesis to produce novel glycoforms or glycoform distributions of a recombinant glycoprotein can potentially lead to an improved therapeutic performance of the glycoprotein product. Effective engineering of this pathway to maximize the fractions of beneficial glycoforms within the glycoform population of a target glycoprotein can be aided by a mathematical model of the N-linked glycosylation process. A mathematical model is presented here, whose main function is to calculate the expected qualitative trends in the N-linked oligosaccharide distribution resulting from changes in the levels of one or more enzymes involved in the network of enzyme-catalyzed reactions which accomplish N-linked oligosaccharide biosynthesis. It consists of mass balances for 33 different oligosaccharide species N-linked to a specified protein that is being transported through the different compartments of the Golgi complex. Values of the model parameters describing Chinese hamster ovary (CHO) cells were estimated from literature information. A basal set of kinetic parameters for the enzyme-catalyzed reactions acting on free oligosaccharide substrates was also obtained from the literature. The solution of the system for this basal set of parameters gave a glycoform distribution consisting mainly of complex-galactosylated oligosaccharides, distributed in structures with different numbers of antennae in a fashion similar to that observed for various recombinant proteins produced in CHO cells. Other simulations indicate that changes in the oligosaccharide distribution could easily result from alteration in glycoprotein productivity within the range currently attainable in industry. The overexpression of N-acetylglucosaminyltransferase III (GnTIII) in CHO cells was simulated under different conditions to test the main function of the model. These simulations allow a comparison of different strategies, such as simultaneous overexpression of several enzymes or spatial relocation of enzymes, when trying to optimize a particular glycoform distribution.

2.2 Introduction

Glycosylation is an important post-translational modification for many recombinant therapeutic proteins. Several properties of glycoproteins can be affected by their carbohydrates, including physical stability, resistance to protease attack, antigenicity, pharmacokinetics, tissue distribution, and specific biological activity (Cumming, 1991; Jenkins et al., 1996). These properties depend not only on the presence or absence, but also on the specific structures, of the carbohydrates.

Glycoproteins occur as heterogeneous populations of molecules, called glycoforms, that share the same polypeptide backbone but have different oligosaccharides at, or different occupancy of, the glycosylation sites (Cumming, 1991). Diverse oligosaccharide structures are synthesized by a network of enzyme-catalyzed reactions taking place as the protein is transported through a series of compartments of the secretory apparatus of the cell. Novel glycoforms or glycoform distributions, accessible through metabolic engineering of the reaction network, could potentially lead to an improved therapeutic performance of the glycoprotein (Stanley, 1992; Bailey, 1991).

Incorporation of new glycosyltransferase activities in cell lines has been reported to yield novel oligosaccharide structures on endogenous (Lee et al., 1989) or recombinant (Minch et al., 1995) glycoproteins. In the majority of the studies carried out to date, the new enzymes either modify the final products of the endogenous reaction network or compete with the last reaction step. In general, less attention has been paid to genetic manipulation of enzymes already present in a cell line. One of the few attempts to overexpress an endogenous enzyme did not produce any detectable change in the oligosaccharide distribution (Youakim and Shur, 1993).

Besides producing novel glycoforms, another important goal for metabolic engineering of glycosylation is to maximize the mole fractions of beneficial glycoforms within the glycoform population of a desired glycoprotein. This could be crucial for some glycoproteins, for example therapeutic antibodies, which must be produced in large amounts by the biotechnology industry (Bibila and Robinson, 1995). To achieve this, various novel or endogenous enzymes acting at different points in the pathway might need to be manipulated. The efficacy of such manipulations can be enhanced by a careful consideration of the complexity of the system. This complexity arises from the number of enzymes involved, their distribution at different levels in various cellular compartments, and the multiple competing reactions catalyzed by some of them. Since other complex biochemical systems have been better understood in the past through their mathematical modelling (Domach et al., 1984; Lee and Bailey, 1984; Starbuck and Lauffenburger, 1992), such a mathematical modelling approach may also guide metabolic engineering efforts to achieve a desired glycoform distribution. For this purpose, a mathematical model of the N-linked glycosylation process has been developed and is presented here. The main function of the model is to calculate the expected qualitative trends in the N-linked oligosaccharide distribution resulting from changes in the levels of one or more enzymes involved in the network of enzyme-catalyzed reactions which accomplish N-linked oligosaccharide biosynthesis.

The present mathematical model consists of mass balances for 33 different oligosaccharide species N-linked to a specified protein that is being transported through the different compartments of the Golgi complex. These equations relate the oligosaccharide mole fractions to the amounts of the different enzymes, the kinetic constants of the reactions, the distribution of enzymes in the different compartments, the half-life of the protein in the Golgi, the volume of the compartments, and the specific glycoprotein productivity. Values for the parameters in the model and their normal ranges can either be found in the literature

or estimated from literature information. Some of the parameters are specific for each cell line. Those describing Chinese hamster ovary (CHO) cells were used here, since CHO cells are currently the most common host for the industrial production of therapeutic glycoproteins. Numerical simulations of the model with these values of the parameters gave glycoform distributions similar to those observed for some proteins produced in CHO cells.

One characteristic of the glycosylation pathway makes its modelling different from that of other biochemical pathways. Oligosaccharides have some degree of conformational flexibility and, through interactions with the polypeptide chain, certain conformations can be preferentially stabilized (Wyss and Gerhard, 1996). In addition, the polypeptide backbone around the glycosylation site may limit the access of the catalytic sites of the enzymes to the oligosaccharide (Shao and Wold, 1995). As a result, a particular glycosylation site can have its own set of values for the kinetic constants of the enzyme-catalyzed reactions. These values can be different from those of other glycosylation sites in the same or other proteins. The occurrence of this phenomenom can be inferred from numerous examples where very different oligosaccharide distributions have been observed for different glycosylation sites of the same protein, even though all other system variables were identical for all sites during biosynthesis. Nevertheless, the range of values of the kinetic constants for oligosaccharides on some glycoproteins lies close to the corresponding range for soluble oligosaccharides (Do et al., 1994; Rao and Mendicino, 1978; Gross et al., 1990). Motivated by this observation, the constants for the latter were used as an initial approach to test the model and to study some aspects of its general behaviour.

2.3 Physical Model

The N-linked glycosylation pathway consists of enzyme-catalyzed reactions which first attach a common oligosaccharide precursor to appropiate glycosylation sites in a polypeptide and then modify the linked oligosaccharides to produce a heterogenous set of glycoforms (Kornfeld and Kornfeld, 1985). Potential glycosylation sites are asparagine residues in the sequence Asn-X-Ser/Thr. The reactions take place in the endoplasmic reticulum (ER) and in the Golgi complex (Golgi) as proteins are transported through these cellular compartments *en route* to their final destinations. These destinations may be, for example, the ER or Golgi themselves, the plasma membrane, or the extracellular space.

The initial covalent attachment of the oligosaccharide precursor to the protein takes place during translocation of the latter into the lumen of the ER. Not all the translocated molecules acquire oligosaccharides in their potential glycosylation sites, and the fraction that does may vary between sites. The type of glycoform heterogeneity which thus results is called glycoform macro-heterogeneity (Shelikoff et al., 1996). Once in the ER the N-linked oligosaccharides are trimmed down by glycosidases which can sequentially remove three molecules of glucose and, sometimes, one of mannose. The glycoproteins are then transported to the Golgi where a different set of glycosidases and glycosyltransferases act on the N-linked oligosaccharides and lead to a diversity of structures. Such type of heterogeneity in the identity of the attached oligosaccharides is referred to as glycoform micro-heterogeneity.

A mathematical model of glycoform macro-heterogeneity has been published recently (Shelikoff et al., 1996). It incorporates different factors that determine the extent of the first transfer reaction of the pathway. In contrast, the model presented below is concerned with glycoform micro-heterogeneity. More specifically, it deals with a set of eight Golgi-

localized enzymes which together determine the distribution of oligosaccharides into the following major structural classes: high mannose, hybrid, bi-, tri-, tri'-, and tetra-antennary complex, bisected hybrid, and bisected bi-, tri-, tri'-, and tetra-antennary complex oligosaccharides (Figs. 1 and 2). Thirty-three different oligosaccharide species are involved in 33 reactions catalyzed by these enzymes; including 5 high-mannose, 3 hybrid, 3 hybrid-galactosylated, 4 complex (bi-, tri-, tri', and tetra-antennary complex), 4 complex-galactosylated, and the 14 bisected counterparts of the hybrid and complex oligosaccharides. The products of this set of reactions can be processed further in the Golgi through more transferase-catalyzed reactions that increase glycoform micro-heterogeneity.

The major elements of the physical model are: (a) the different Golgi compartments where the reactions take place and the transport of proteins between them, (b) the central network of enzyme-catalyzed reactions, and (c) the spatial distribution of these enzymes in the different Golgi compartments.

a) Golgi compartments

The Golgi complex consists of a series of distinct, membrane-bounded compartments. Proteins destined to the extracellular space, plasma membrane, lysosomes, endosomes, or secretory storage vesicles are transported from the ER to the first Golgi compartment, the cis-Golgi network (CGN). From there they travel in sequential order through the remaining compartments of the series; the cis-, medial-, and trans-Golgi cisternae, which together comprise the Golgi stack; and then to the trans-Golgi network (TGN), the final sorting place (Rothman and Orci, 1992). There is some controversy about the number of cisternae in the Golgi stack, but in the present model only three are considered.

Proteins are transported between compartments by vesicles which bud off from the membrane of one compartment and fuse to the next in the series (Rothman and Wieland, 1996). Secreted and plasma membrane proteins appear to go through the Golgi by a "bulk flow" mechanism. These proteins enter vesicles by default, i.e., in the absence of specific transport or retention signals, and therefore at their bulk concentration in the donor compartment. Proteins which reside in the ER or Golgi require retention signals that allow them to be concentrated in the appropiate compartments. Such residency is not permanent and their relative concentration in a particular region is also aided by retrieval-vesicles that recognize transport signals in escaped proteins and return them to previous compartments.

For the physical model, four of the five Golgi compartments mentioned above are considered as a system of four reactors in series. The modelled compartments are the cis-, medial-, and trans-Golgi cisternae, and the TGN. This selection is based on immuno-electron microscopy studies that localize the enzymes included in the present model to these compartments (Nilsson et al., 1993; Rabouille et al., 1995). The chemical reactions catalyzed by these enzymes are described next.

b) Central reaction-network

The N-linked glycosylation pathway of mammalian cells has been deduced by a combination of *in vitro* and *in vivo* biosynthetic studies (Kornfeld and Kornfeld, 1985; Schachter, 1986). Although many enzymes participate in the pathway, a subset of them determines the distribution of oligosaccharides into 33 different species which together define the high mannose, hybrid, hybrid-bisected, complex, and complex-bisected types. The network of reactions catalyzed by this subset is called here "central reaction network" (CRN). The CRN considered in the present model is depicted in Figure 2.

The first enzyme of the CRN is Golgi α1,2-mannosidase I (ManI), which can cleave α1,2-linked mannose residues from M_9 - M_6 to finally produce M_5 (see nomenclature in Figure 1), corresponding to reactions 1 to 4 in Figure 2. All eukaryotic cells have an α1,2-mannosidase in the ER that can also catalyze reaction 1. Therefore, the initial substrate for the Golgi CRN is a mixture of M_9 and M_8 oligosaccharides. Compounds M_9 to M_5 constitute the high-mannose class of N-linked oligosaccharides. The synthesis of hybrid and complex oligosaccharides then follows as described below.

An N-acetylglucosamine (GlcNAc) can be transferred to the α1,3-mannose branch of M_5 by β1,2-N-acetylglucosaminyltransferase I (GnTI) to yield M_5Gn, the first hybrid oligosaccharide. M_5Gn is a substrate for α-mannosidase II (ManII), which catalyzes the removal of two mannose residues resulting in hybrids M_4Gn (reaction 6) and M_3Gn (reaction 7). The free α1,6-mannose branch of M_3Gn is then available for extension by GnTII to produce M_3Gn_2, a complex bi-antennary oligosaccharide. M_3Gn_2 may be branched further by GnTIV or GnTV. GnTIV adds a GlcNAc in a β1,4-linkage to the α1,6-mannose branch, leading to the tri-antennary complex oligosaccharide M_3Gn_3. GnTV catalyzes a GlcNAc transfer in a β1,6-linkage to the α1,3-mannose branch and

produces the tri'-antennary complex oligosaccharide M_3Gn_3'. The tetra-antennary complex compound M_3Gn_4 can be synthesized both by GnTIV from M_3Gn_3' (reaction 11) and by GnTV from M_3Gn_3 (reaction 12).

All hybrid and complex oligosaccharides contain non-reducing-end GlcNAcs which may be extended by β1,4-galactosyltransferase (GalT, reactions 13 to 19). Once a galactose residue is transferred, the modified oligosaccharide is no longer a biosynthetic substrate for any of the remaining GnTs or for ManII (Schachter, 1986). All of the branches in any complex oligosaccharide serve as substrates for GalT, but do so with different affinities (Paquet et al., 1984). In the present model these reactions are lumped together in single steps which remove the compound from the flux through reactions 1 to 12.

The reactions mentioned to this point take place in common industrial cell lines, such as CHO cells and baby hamster kidney (BHK) cells, used for the production of recombinant glycoproteins (Jenkins et al., 1996). An additional set of reactions (20 to 33) is also important for determining the major classes of N-linked oligosaccharides in cell lines expressing GnTIII. Examples of these cell lines are a glycosylation mutant of CHO cells named Lec 10 (Stanley and Campbell 1984) and rat myeloma (Y0) cells (Lifely et al., 1995). As indicated in reactions 20 to 26, GnTIII can modify any non-galactosylated hybrid or complex oligosaccharide by transferring a GlcNAc residue in a β1,4-linkage to the core mannose. The transferred residue is called a bisecting GlcNAc (Gn^b), and the products of these reactions are referred to as bisected oligosaccharides. GalT cannot extend the Gn^b residue, but it may modify all the other non-reducing-end GlcNAcs of any bisected oligosaccharide (reactions 27 to 33).

The final products of the CRN are usually modified further in the Golgi by the addition of sialic acids, poly-N-acetyllactosamine, fucose, N-acetylgalactosamine, sulphate, and α1,3-

linked galactose. Wild type CHO cells only add sialic acids (in α2,3-linkages to galactose), fucose (α1,6-linked to the oligosacharide core, see R in Fig. 1), and poly-N-acetyllactosamine (to various antennae but preferentially to that synthesized by GnTV). The addition of fucose to the core of oligosaccharides can take place at any point after reaction 5 of the CRN, but it is also blocked by the modifications that GalT or GnTIII introduce. Core-fucosylated oligosaccharides can go through the rest of the CRN in the same way as their non-fucosylated counterparts, although minor alterations in some of the kinetic parameters may occur (Gu et al., 1992).

Other reactions which could participate in the CRN have been identified. For example, GnTIV-modified hybrid compounds and a GnTVI activity towards tri'- and tetra-antennary oligosaccharides have both been identified in hen oviduct microsomes (Brockhausen et al., 1992). Also, some types of mammalian cells have α-mannosidases which can act on M_9 to M_4 or on glucose-containing M_9 substrates and produce M_3 oligosaccharides (Moremen et al., 1994). None of these activities are included in the present model, which considers only a standard network of well-characterized reactions explaining the common types of N-linked oligosaccharides.

All the transferase-catalyzed reactions of the CRN use sugar-nucleotide co-substrates; UDP-GlcNAc for the GnTs and UDP-galactose (UDP-Gal) for GalT. The co-substrates are synthesized in the cytoplasm and access the lumen of the Golgi compartments by means of specific membrane transporters (Hirschberg and Snider, 1987). The by-product of all these transfer reactions is UDP, which is degraded into UMP and inorganic phosphate by a Golgi-nucleoside diphosphatase. The membrane transporters function as antiporters that accumulate co-substrates to high concentrations inside the compartments and at the same time export UMP.

c) Spatial distribution of the enzymes

The glycosidases and glycosyltransferases mentioned above are type II integral membrane proteins and reside permanently in the Golgi complex. They consist of a short N-terminal cytoplasmic tail followed a hydrophobic transmembrane domain, a lumenal stalk region, and a large lumenal catalytic domain (Paulson and Colley, 1989). The retention signal is transplantable and is found in the transmembrane domain and its two flanking regions (Nilsson et al., 1996). However, the mechanism by which residence is achieved in the presence of a continuous flow of other membrane proteins and lipids is not yet understood (Cole et al., 1996; Rothman and Wieland, 1996). It seems that oligomerization of the enzymes through their transmembrane domains and stalk regions (Nilsson et al., 1994), stabilizing interactions between the transmembrane domain and lipids of Golgi membranes (Bretscher and Munro, 1993), and interactions between the cytoplasmic tail and cytoskeletal proteins (Yamaguchi and Fukuda, 1995), are all involved in the retention mechanism. Retrieval signals have not been identified yet for these enzymes, but there is some evidence for their retrograde vesicular transport (Rothman and Wieland, 1996). Additionally, a recent study suggests that the enzymes can diffuse very rapidly within Golgi membranes (Cole et al., 1996).

The steady-state distribution of the enzymes has been determined by immuno-electron microscopy (Dunphy et al., 1985; Nilsson et al., 1993). Typically, the enzymes are distributed as peaks which occupy mainly two cisternae. GalT is mainly localized in the trans-Golgi cisterna and TGN, while the other enzymes are mainly found in the medial- and trans-Golgi cisternae. This spatial distribution has an important effect on N-linked oligosaccharide biosynthesis; it reduces the competition of GalT with the rest of the enzymes and thus favors flux through reactions 1 to 12 of the CRN. The interplay between

the different elements of the physical model is described quantitatively by the mathematical model.

2.4 Mathematical Model

The mathematical model consists of mass balance equations for a soluble glycoprotein that is being secreted to the extracellular space, and for the oligosaccharide species N-linked to it. Mass balance equations are derived for each of four Golgi compartments. Glycoprotein transport through the Golgi is modelled in the same fashion as in previous successful models of protein traffic through the secretory apparatus of a cell (Bibila and Flickinger, 1991; Sambanis et al., 1991). Three basic assumptions are thus made:

(A.1) intercompartmental protein transfer follows first order kinetics

(A.2) the contents of a compartment are spatially homogeneous

(A.3) there is no loss of protein during transport through the Golgi.

The mass balance equation for a glycoprotein in the first compartment is:

$$\frac{dp_1}{dt} = q_p - k_G p_1 \qquad (1)$$

where p_1 is the amount of protein in compartment 1 (moles per compartment), t is the time (h), q_p is the specific rate of protein transport into the first compartment (moles cell^{-1} h^{-1}), and k_G is the kinetic constant for protein transport in the Golgi (h^{-1}). The last term on the right-hand side of equation (1) corresponds to the rate of protein transport out of compartment 1 and into compartment 2.

An additional assumption has been made in equation (1), and it is also used for all mass balance equations of this model:

(A.4) the dilution of compartamental components due to cell growth is negligible.

Glycoproteins require approximately 20 minutes to go through all of the Golgi compartments (Bibila and Flickinger, 1991), while typical doubling times of mammalian cells in culture are around 1000 minutes (Arathoon and Birch, 1986). This implies that glycoproteins experience a practically constant volume of the compartments during their processing in the Golgi. Moreover, introduction of a dilution term due to cell growth does not change the form of any mass balance equation of this model; it only contributes a perturbation to the k_G coefficient of less than 0.5% (see model parameters section below).

The mass balances for the remaining compartments are:

$$\frac{dp_j}{dt} = k_G(p_{j-1} - p_j) \; ; \; 2 \le j \le 4 \qquad (2)$$

where index j denotes the compartment number. As mentioned in the previous section, four compartments are considered; the cis-, medial-, and trans-Golgi cisternae, denoted with values of j equal to 1, 2, and 3, respectively, and the TGN, with j equal to 4. The steady-state solution for equations (1) and (2) is:

$$p_j = \frac{q_p}{k_G} \; ; \; 1 \le j \le 4 \quad (3)$$

and q_p is equal to the specific productivity of a secreted glycoprotein observed for steady-state conditions.

For the oligosaccharide mass balance equations described below, the amount of an N-linked oligosaccharide in a compartment is expressed as the product of its mole fraction and the amount of glycoprotein in that compartment. These equations include the transport rates in and out of the compartments, and the rates of oligosaccharide consumption and generation by the reactions of the CRN. In addition to the simplifying assumptions mentioned above, the following are made:

(A.5) *in vivo* enzyme-catalyzed reaction rates can be described by Michaelis-Menten type kinetics

(A.6) the catalytic sites of the GnT and GalT enzymes are saturated with sugar-nucleotide co-substrates UDP-GlcNAc and UDP-Gal, respectively

(A.7) product inhibition of the reactions is insignificant.

Various experimental observations support assumption (A.5). Glycosyltransferase reaction kinetics have been shown to be well modelled by a random equilibrium mechanism (Rearick et al., 1979), which reduces to common Michaelis-Menten kinetics under co-substrate saturation. Most of the kinetic data reported in the literature have been obtained under this condition, fitted to the Michaelis-Menten rate expression, and reported as apparent maximal velocities and dissociation constants (Schachter et al., 1989). The use of these rate expressions to describe the *in vivo* reactions is further justified (Albe et al., 1990) by concentrations of enzymes in the compartments which are much lower than those of their substrates (see model parameters section).

Assumption (A.6) is supported by data which indicates that sugar-nucleotides are accumulated in the compartments to concentrations in the millimolar range (Briles et al., 1979), while the values of apparent dissociation constants for many glycosyltransferases

are in the micromolar range (Schachter et al., 1989). It should be noted, however, that changes in the N-linked glycosylation of rat hepatocytes have been recently reported to occur when the intracellular concentration of UDP-GlcNAc is artificially increased by incubating the cells with high extracellular levels of uridine (Pels Rijcken et al., 1995). Finally, the presence of a nucleoside diphosphatase activity that hydrolyses UDP in the Golgi, and of a UMP export mechanism, favour the use of assumption (A.7).

A mass balance for the M_9 N-linked oligosaccharide in compartment 1 is presented below in order to illustrate the type of equations which result and to introduce the nomenclature. ManI, the enzyme which catalyzes the consumption of M_9, participates in multiple reactions on different substrates (Fig. 2). All of these substrates may be present in one compartment at the same time, and therefore the reaction rate expression must be modified for the case of multiple substrates competing for a common binding site. The same is true for ManII, GnT III, GnTIV, GnTV, and GalT. However, this competition is momentarily ignored to simplify the following exposition. The mass balance for M_9 is:

$$\frac{d(p_1 x_{1,1})}{dt} = q_p x_{1,0} - \frac{v_{m,1,1} p_1 x_{1,1}}{K_{m,1} V_{G,1} + p_1 x_{1,1}} - k_G p_1 x_{1,1} \quad (4)$$

where $x_{1,1}$ is the mole fraction of oligosaccharide 1 (corresponding to M_9) in compartment 1, $x_{1,0}$ is the mole fraction of oligosaccharide 1 on the glycoprotein before it enters compartment 1 but after it has exited the ER, $v_{m1,1}$ is the apparent maximal velocity for reaction 1 (numbered as in Fig. 2) in compartment 1, $K_{m,1}$ is the apparent dissociation constant for reaction 1, and $V_{G,1}$ is the volume of compartment 1. In general, $x_{i,j}$ represents the mole fraction of oligosaccharide i in compartment j; $v_{m,k,j}$, the apparent maximal velocity for reaction k in compartment j; and $K_{m,k}$, the apparent dissociation constant for reaction k. Although the compartments are numbered 1 through 4, index j takes a value of zero to represent the oligosaccharide composition of the glycoprotein feed

to compartment 1. There are 33 different oligosaccharide species in this model (Fig. 2) and the values of index i assigned to each species are shown in Table I.

From equations (1) and (4), and after the introduction of dimensionless variables and parameters, the mass balance of oligosaccharide 1 can be written as:

$$\frac{dx_{1,1}}{d\bar{t}} = \frac{(x_{1,0} - x_{1,1})}{\bar{p}_j} - \frac{\bar{v}_{m,1,1}x_{1,1}}{\bar{K}_{m,1,1} + \bar{p}_1 x_{1,1}} \qquad (5)$$

with dimensionless terms defined as:

$$\bar{t} = tk_G \qquad (6)$$

$$\bar{p}_j = p_j k_G / q_p \qquad (7)$$

$$\bar{v}_{m,k,j} = v_{m,k,j} / q_p \qquad (8)$$

$$\bar{K}_{m,k,j} = K_{m,k} k_G V_{G,j} / q_p \qquad (9)$$

In equations (5) to (9) the time has been scaled by the inverse of the kinetic constant for protein transport through the Golgi; the amount of protein in a compartment by its steady-state value; the apparent maximal velocity by the specific glycoprotein productivity under steady-state conditions; and the apparent dissociation constant by the steady-state volumetric concentration of glycoprotein in compartment j .

For steady-state conditions equation (5) reduces to:

$$x_{1,0} = x_{1,1} + \frac{\bar{v}_{m,1,1}x_{1,1}}{\bar{K}_{m,1,1} + x_{1,1}} \qquad (10)$$

Equation (10) can be extended to any compartment as:

$$x_{1,j-1} = x_{1,j} + \frac{\bar{v}_{m,1,j} x_{1,j}}{\bar{K}_{m,1,j} + x_{1,j}}; \quad 1 \leq j \leq 4 \quad (11)$$

The dimensionless apparent maximal velocity for a reaction in a particular compartment can be expressed as:

$$\bar{v}_{m,k,j} = \bar{v}_{m,k} e_{k,j} \quad (12)$$

where $\bar{v}_{m,k}$ is the dimensionless apparent maximal velocity for reaction k based on the total amount (in the Golgi) of the enzyme catalyzing reaction k, and $e_{k,j}$ is the fraction of this enzyme in compartment j.

As mentioned above, the reaction rate expressions for ManI, ManII, GnTIII, GnTIV, GnTV, and GalT must be modified since these enzymes act on multiple substrates which compete for one binding site. The general form of these rate expressions is:

$$\bar{r}_{k,j} = \frac{\bar{v}_{m,k} e_{k,j} x_{i_k,j}}{\bar{K}_{m,k,j}\left[1 + \bar{p}_j \sum_l \left(x_{i_l,j} \Big/ \bar{K}_{m,l,j}\right)\right]} \quad (13)$$

where subindex l sums over all the reactions catalyzed by the enzyme involved in reaction k, including reaction k; $x_{i_k,j}$ is the mole fraction, in compartment j, of an oligosaccharide i which is the substrate for reaction k; and $x_{i_l,j}$ is the mole fraction, in compartment j, of an oligosaccharide i which is the substrate for reaction l. For the steady-state case, $\bar{p}_j$ takes a value of one. For example, in a steady-state, the rate expression for reaction 10 is:

$$\bar{r}_{10,j} = \frac{\bar{v}_{m,10} e_{10,j} x_{9,j}}{\bar{K}_{m,10,j}\left[1 + (x_{9,j}/\bar{K}_{m,10,j}) + (x_{11,j}/\bar{K}_{m,11,j})\right]}$$

In total, the mole fractions of 33 oligosaccharide species in 4 compartments are described by a set of 132 oligosaccharide mass balance equations. In a steady-state, it is a system of non-linear algebraic equations of the type:

$$x_{i,j-1} = x_{i,j} - \sum_{k=1}^{33} (\vartheta_{k,i} \bar{r}_{k,j}); \quad 1 \le i \le 33; \; 1 \le j \le 4 \qquad (14)$$

where $\vartheta_{k,i}$ is the stoichiometric coefficient of oligosaccharide i in reaction k. For example, the mass balance equations for M_3Gn_2 are:

$$x_{9,j-1} = x_{9,j} - \bar{r}_{8,j} + \bar{r}_{9,j} + \bar{r}_{10,j} + \bar{r}_{16,j} + \bar{r}_{23,j}; \quad 1 \le j \le 4$$

Glycoproteins entering the cis-Golgi carry only M_9 and M_8 oligosaccharides (see preceeding section). Therefore, the system of equations is subject to the following conditions:

$$\begin{aligned} x_{1,0} &= 1 - \alpha; \; 0 \le \alpha \le 1 \\ x_{2,0} &= \alpha \\ x_{i,0} &= 0; \; 3 \le i \le 33 \end{aligned} \qquad (15)$$

where α is the extent of the mannosidase-catalyzed reaction in the ER.

2.5 Model Parameters

The parameters needed to solve the model equations for the oligosaccharide mole fractions include the inlet composition into the Golgi, which depends only on parameter α in equation (15), and the dimensionless apparent maximal velocities and dissociation constants for each reaction in every compartment. Estimation of these parameters in turn involves knowledge of the values of: (1) the kinetic constant for protein transport in the Golgi, (2) the specific glycoprotein productivity under steady-state conditions, (3) the volume of the Golgi compartments, (4) the spatial distribution of enzymes in the Golgi, (5) the apparent dissociation constant for each reaction, (6) the apparent maximal velocity for each reaction. The normal ranges of values for all of the parameters were sought in the literature.

1. Kinetic constant for protein transport in the Golgi (k_G)

The half-life for protein transport in the Golgi, obtained from pulse-chase experiments, can be used to calculate the kinetic constant k_G (Bibila and Flickinger, 1991). The transport of a pulse of protein through the system of four well-mixed compartments in series is described by equations (1) and (2). The transport half-life is defined as the time required for half of the protein in the pulse to be transported out the Golgi complex. The solution to equations (1) and (2) for a pulsed input of protein can be combined with the definition of transport half-life to yield:

$$\sum_{j=1}^{4}\left[\frac{(k_G t_{1/2})^{j-1} e^{-k_G t_{1/2}}}{(j-1)!}\right] = 1/2 \qquad (16)$$

where j is the compartment number and $t_{1/2}$ is the half-life for protein transport in the Golgi. Equation (16) can then be solved for the k_G that corresponds to an experimentally observed $t_{1/2}$. The latter is usually between 15 and 20 minutes for the majority of constitutively secreted proteins (Bibila and Flickinger, 1991). A $t_{1/2}$ of 20 minutes, which gives a k_G of 0.18 min^{-1}, is used for the simulations presented here.

2. Specific glycoprotein productivity (q_p)

The purpose of the model is to describe the glycosylation of recombinant proteins. However, endogenous glycoproteins are also being processed in the same compartments and at the same time as the recombinants. Depending on the relative levels of expression and dissociation constants, these will compete for the active sites of the CRN enzymes. A single glycoprotein is considered below, neglecting these host cell glycoprotein interactions. Further discussion on the modification of the model to take into account the glycosylation of endogeneous proteins is present at the end.

The specific productivity of a recombinant, secreted glycoprotein varies for different types of protein and is also dependant on the cell line and vector used for expression. For CHO cells, the highest productivities reported in the literature are between 80 and 110 $\mu g(10^6 \text{ cells})^{-1}(24h)^{-1}$, in all cases for recombinant IgG molecules expressed from stably integrated cassettes with constitutive promoters (Page and Sydenham, 1991; Fouser et al., 1992; Reff et al., 1994). An example of low productivities in this system is that of interferons, which normally give around 1 $\mu g(10^6 \text{ cells})^{-1}(24h)^{-1}$ (Rossmann et al., 1996). The oligosaccharide mass balance equations presented above can be used to describe a glycoprotein with a single N-linked glycosylation site or the average oligosaccharide composition of a glycoprotein with multiple sites. In the second case, the equivalent q_p for

the simulations would be the real one multiplied by the number of sites. Since IgG antibodies contain at least two glycosylation sites and their molecular mass is around 150 kDa, the highest equivalent value of q_p reported for CHO cells is approximately 1500 pmol(10^6 cells)$^{-1}$(24h)$^{-1}$. The q_p for interferons would be around 100 pmol(10^6 cells)$^{-1}$(24h)$^{-1}$. For the present simulations, values of q_p between 1 and 2000 pmol(10^6 cells)$^{-1}$(24h)$^{-1}$ are used.

3. Volume of the compartments (V_G)

The volume of the Golgi, estimated from electron microscopy studies, has been reported in the literature for BHK cells (Griffiths et al., 1989) and for a murine B cell line (Wiest et al., 1990). The volume of the Golgi stack, including the cisternal part of the TGN, was 20 ± 5 μm^3 for BHK cells. B cells had a volume of 5 ± 1.5 μm^3 for a "Golgi exclusion zone" containing both the stack and the TGN. This volume increased to 17 ± 5 μm^3 upon B cell differentiation. No data has been published on the volume of individual cisternae. A total volume of 10 μm^3, divided equally into four compartments, is used for the simulations.

4. Spatial distribution of the enzymes ($e_{k,j}$)

Quantitative data on the spatial distribution of the enzymes participating in the CRN has been obtained from immunoelectron microscopy studies in HeLa cells (Nilsson et al., 1993; Rabouille et al., 1995). ManII and GnTI co-distributed along the Golgi as peaks which localized mainly to the medial- and trans-Golgi cisternae and tailed-off to the adjacent cisternae, while most of GalT was found in the trans-Golgi cisterna and in the TGN. These studies agree with quantitative data on the distribution of enzyme activities in

Golgi membrane fractions derived from CHO cells and separated by density gradient centrifugation (Dunphy and Rothman, 1983). In the latter study it was found that ManI, ManII, GnTI, and GnTII activities co-distributed along the Golgi. Their peak activities could be resolved in this type of gradient from the corresponding GalT activity, but a significant portion of the activities still overlapped.

Besides the density gradient centrifugation results mentioned above, other data also support a similar distribution of enzymes between CHO and HeLa cells. Qualitative immunoelectron microscopy studies in CHO cells have localized the endogenous ManII in two or three Golgi cisternae immediatly after the CGN (Velasco et al., 1993), and a stably expressed bovine GalT in two or three cisternae on the trans-side of the Golgi (Russo et al., 1992).

GnTIV has been found to co-distribute with GnTI and ManII in Golgi fractions of mouse lymphoma cells separated by density gradient centrifugation (Goldberg and Kornfeld, 1983). No data has been published yet on the localization of GnTIII and GnTV. For the simulations presented here, it is assumed that GnTIII, GnTIV, and GnTV co-distribute with GnTI.

The quantitative enzyme distribution data from the immuno-electron microscopy study of HeLa cells (Rabouille et al., 1995) is used for the present simulations. The rounded-off average values between ManII and GnTI are used for all enzymes except GalT. These values are:

$$e_{k,1} = 0.15,\ e_{k,2} = 0.45,\ e_{k,3} = 0.30,\ e_{k,4} = 0.10$$

The corresponding values for GalT are:

$$e_{k,1} = 0,\ e_{k,2} = 0.05,\ e_{k,3} = 0.20,\ e_{k,4} = 0.75$$

5. Apparent dissociation constants ($K_{m,k}$)

As mentioned in the introduction, the variability in the values of the kinetic parameters between different glycosylation sites in the same or different glycoproteins is a special characteristic of protein glycosylation. The phenomenom can result from multiple influences of the polypeptide backbone around the glycosylation site. These include relative stabilization of a few of all the potential oligosaccharide conformations, limited accessibility of the catalytic site of the enzyme to the oligosaccharide substrate, and protein-protein interactions between the surfaces around the catalytic and glycosylation sites (Shao and Wold, 1995; Wyss and Gerhard, 1996). Clearly, for a given glycosylation site, different reactions can be affected to a different extent (Shao and Wold, 1988).

Some kinetic constants for a small number of the CRN reactions have been determined for a few glycoprotein acceptors that have minimal or well characterized heterogeneity. For example, apparent dissociation constants of GnTV (Do et al., 1994), GalT (Rao and Mendicino, 1978), and a sialyltransferase (Gross et al., 1990) for glycoprotein acceptors are in the range of 10 to 350 μM (in terms of moles of the appropiate N-linked oligosaccharide substrates). The corresponding values for glycopeptides derived from these proteins are in the range of 250 to 10,000 μM. The values for the glycoprotein acceptors are close to those observed for the preferred, soluble oligosaccharide acceptors of the glycosyltransferases and glycosidases of the CRN, which are typically around 150 μM. Motivated by this observation, the data available for soluble oligosaccharides is used here to conduct tests of the model.

Soluble oligosaccharide acceptors offer easier determination of the kinetic constants, and there is more data available for them. Apparent dissociation constants for soluble oligosaccharides are presented in Table II along with the source of the enzymes and the respective references. Although there is data for most of the enzymes, the kinetics on alternative substrates of a single enzyme have usually not been fully characterized. For example, ManI catalyzes reactions 1 to 4 of the CRN, but only $K_{m,2}$ for the M_8 oligosaccharide substrate is available. For the simulations, the same K_m value is used for reactions 1 to 4. The estimation of the remaining dissociation constants is described next. In general, many of these estimates require the use of pseudo-first-order kinetic constants reported in the literature, and also the assumption that, for a particular enzyme, reactions on different substrates behave in the same way once the substrate is bound; i.e., the dissociation constants vary much more between different oligosaccharide substrates than the corresponding catalytic constants do. Therefore:

(A.8) variations in the maximal velocities between different reactions catalyzed by the same enzyme are neglected.

$K_{m,5}$ for GnTI has been determined experimentally for different sources of enzyme. The value shown in Table II is for CHO cell microsomes in the presence of a non-ionic detergent, but very similar values have been obtained for other sources and conditions. For example, the highly purified enzyme from rabbit liver has a K_m of 250 μM (Schachter et al., 1989). In the case of ManII, the information available for oligosaccharides substrates shows that the pseudo-first-order kinetic constant for reaction 7 in microsomes has twice the value of the corresponding constant for reaction 6 (Harpaz and Schachter, 1980). For the simulations presented here, the K_m of 100 μM for ManI (Tabas and Kornfeld, 1979) is

also used for reaction 7 catalyzed by ManII. By assuming identical catalytic constants for the ManII reactions, a value of 200 μM is estimated for reaction 6.

For GnTIII, $K_{m,23}$ for the bi-antennary substrate has been determined (Taniguchi et al., 1989). There is a report comparing the activity on this substrate and that on the hybrid substrate M_3Gn, at defined initial concentrations of substrate (Narasimhan, 1982). By assuming identical catalytic constants, a value of 4000 μM is obtained for $K_{m,22}$. The same value is used here for reactions 20 and 21. For the tri-, tri'-, and tetra-antennary substrates the value of $K_{m,23}$ is used. In the case of GnTV, the activities for reactions 9 and 12 have been measured and $K_{m,9}$ has been determined (Gu et al., 1992). By assuming identical catalytic constants, $K_{m,12}$ can be estimated to be 90 μM. For GnTIV only $K_{m,10}$ has been measured. The same value is used for reaction 11.

GalT is a special case: not only does it modify different substrates of the CRN, but it can also catalyze multiple reactions on any oligosaccharide having more than one non-reducing-end GlcNAc; i.e., on all substrates but the hybrids. However, the model is used to determine the distribution of oligosaccharides of the CRN and not the details of which or how many branches have been galactosylated. In this model, any GalT reaction on a complex, non-galactosylated oligosaccharide substrate represents the consumption of that substrate independent of the position and number of transferred galactose residues. Such "total" GalT reaction lumps all possible galactose transfer reactions on the non-galactosylated oligosaccharide substrate. It proceeds at a rate equal to the sum of the rates of all possible reactions. The "total" GalT reaction is characterized by a lumped dissociation constant in terms of moles of non-galactosylated oligosaccharide substrate. In fact, the data on GalT shown in Table II was experimentally determined for this type of lumped reaction scheme.

The kinetic constants for GalT acting on the disaccharide and trisaccharide soluble fragments, normally present at the non-reducing end of the bi, tri-, tri'-, and tetra-antennary substrates, have been determined for a purified form of the enzyme (Elices and Goldstein, 1988). Values of 160, 340, and 940 μM were reported for the apparent dissociation constants of the Gnβ1,6-(Gnβ1,2-)Man trisaccharide, the Gnβ1,4-(Gnβ1,2-)Man trisaccharide, and the Gnβ1,2-Man disaccharide, respectively. The corresponding values of the catalytic constants were 26, 29, and 19 μmol of galactose transferred per minute per mg of purified GalT. The experimental data on the trisaccharides were determined for lumped reaction schemes. To estimate how these values are modified once the fragments are covalently attached in α1,3- and α1,6-linkages to the oligosaccharide core (R in Figure 1), experimental data on the branch specificity of GalT (acting on the bi-antennary substrate) are employed (Paquet et al., 1984). The pseudo-first-order kinetic constant for the α1,3-branch was reported to be 5.4 times larger than the corresponding constant for the α1,6-branch. For pseudo-first-order kinetics and identical catalytic constants, the inverse of the apparent lumped dissociation constant for the non-galactosylated substrate is equal to the sum of the inverses of the apparent dissociation constants for each branch:

$$K_{m,L} = \frac{K_{m,\alpha 3} K_{m,\alpha 6}}{K_{m,\alpha 3} + K_{m,\alpha 6}} \qquad (17)$$

where $K_{m,L}$ is the lumped dissociation constant for the "total" reaction, while $K_{m,\alpha 3}$ and $K_{m,\alpha 6}$ are the dissociation constants for the individual α1,3- and α1,6-branch, respectively. Using equation (17), a value of 130 μM ($K_{m,16}$ in Table II) for the $K_{m,L}$, a ratio of pseudo-first-order constants of 5.4, and assuming identical catalytic constants, values of 150 and 830 μM can be estimated for $K_{m,\alpha 3}$ and $K_{m,\alpha 6}$, respectively. These can then be compared with the experimental value of 940 μM for the corresponding, free Gnβ1,2-Man disaccharide. By extrapolating these effects upon core attachment to the soluble trisaccharides and using equation (17), values of 50, 70, and 40 μM can be estimated for

the lumped dissociation constants of the "total" reactions on the tri-, tri'-, and tetra-antennary acceptors, respectively.

Estimates for the equivalent, bisected substrates of GalT can be obtained with the procedure described above, together with experimental information on the pseudo-first-order constants for each branch of the bisected and the non-bisected bi-antennary substrates (Narasimhan et al., 1985). These data show that, when the core is bisected, the α1,3-branch has a 4.6 times lower kinetic constant, while the α1,6-branch shows only a two-fold reduction. The estimated lumped dissociation constants are: 500, 200, 220, and 140 μM for the bisected bi-, tri-, tri'-, and tetra-antennary substrates.

No kinetic data is available for GalT acting on soluble, hybrid oligosaccharides. GnTIII acts on the same substrates, and the absence of a GlcNAc residue on the α1,6-branch seems to have a very disruptive effect on its activity towards the soluble bi-antennary acceptor (Narasimhan, 1982). Both bisected and non-bisected hybrid oligosaccharides are relatively uncommon in glycoproteins (Sheares and Robbins, 1986). One potential reason for this is the relatively high dissociation constants for hybrids. The dissociation constant of 4000 μM estimated above for GnTIII acting on hybrid oligosaccharides is also used here for GalT.

A summary of all the dissociation constants used for the simulations is presented in Table IV. Specific glycoprotein productivities in the order of 10^2 pmol$(10^6$ cells$)^{-1}(24h)^{-1}$, the normal range used in the model, lead to compartmental concentrations of glycoprotein in the order of 10^2 μM, and therefore to dimensionless apparent dissociation constants of order 1.

6. Apparent maximal velocities ($V_{m,k}$)

The values of experimentally determined apparent maximal velocities for CHO cells are presented in Table III. These values represent the total activity found in assays of nucleus-clarified cell lysates, carried in the presence of a non-ionic detergent and under optimal pH and co-factor (divalent metal ion) concentration. Data for similar assays performed on many different types of cells are widespread in the literature, and in general, the values are in the range shown in Table III (Dennis et al., 1987; Palcic et al., 1990; Easton et al., 1991). In most cases the data is based on the total protein content of the cell lysate. However, the references (Dunphy et al., 1981; Dunphy and Rothman, 1983) for GnTI and GnTII provide information on the number of cells used for the lysates and thereby allow estimation of the average maximal velocities per cell. These are the values required for the present model. The estimates, assuming lysis of all cells, are also shown in Table III. The conversion applied for GnTI and GnTII has been extrapolated to the other enzymes, since all the velocities were determined for lysates prepared by essentially the same procedure. Another study which also reports the number of cells used for the lysates, gives a similar value of maximal velocity, 200 pmol$(10^6$ cells$)^{-1}$(h)$^{-1}$, for a sialyltransferase acting on N-linked oligosaccharides (Gross et al., 1990).

The GnTIV maximal velocity has not been reported for CHO cells. However, in many cell types, the maximal velocities for GnTIV and GnTV are in the same range, usually between one and two orders of magnitude lower than those of the other CRN enzymes (Dennis et al., 1987; Ohno et al., 1992). Therefore, the GnTV value is also used for GnTIV in the simulations. The maximal velocities for ManI and ManII are always reported in terms of special activity units (Dunphy and Rothman, 1983), but there is no information available in the literature to convert these units to absolute values in terms of moles of hydrolysed oligosaccharide. Data in purification tables indicates that the amounts of the Golgi

mannosidases are similar to those of GnTI (Nilsson et al., 1994), but this comparison is in terms of weight percent of protein in the Golgi. The average of the maximal velocity values between GnTI and GnTII is used for both ManI and ManII in the present simulations.

The compartmental concentrations of enzyme can be estimated in order to verify if they are much lower than those of their substrates (see assumption A.5). For example, a value of 1 μM can be estimated for GnTI, based on a specific activity for the purified enzyme of 20 μmol of GlcNAc(min)$^{-1}$(mg of enzyme)$^{-1}$ and a molecular mass of 45 kDa (Schachter et al., 1989). This value is two orders of magnitude lower than the typical compartmental substrate concentrations used here.

The total set of apparent maximal velocities used in the simulations is shown in Table IV. Assumptions (A.6) and (A.8) have been applied in the assignment of these values.

7. Inlet oligosaccharide composition

Glycoproteins entering the Golgi will carry a mixture of M_9 and M_8 oligosaccharides depending on the extent of the mannosidase-catalyzed reaction in the ER. Since the extent will vary between proteins, a value of 50% (α=0.5) is used for the test simulations.

2.6 Solution Strategy

The N-linked oligosaccharide distribution of a secreted glycoprotein, produced under steady-state conditions, is determined by solving the system of 132 non-linear algebraic equations (14) with the parameters presented above. A FORTRAN 77 program was implemented for the following solution strategy:

1. The reaction rates are calculated with linear expressions corresponding to pseudo-first-order kinetics, and the resulting system of linear equations is solved (IMSL subroutine DLINRG is used to calculate the inverse of the matrix).
2. The system of non-linear equations with the full reaction rate expressions, evaluated at a small value of q_p, is solved iteratively. The outlet oligosaccharide distribution from step 1 is used as the initial guess. The problem is simplified by solving "backwards" the mass balance equations for the inlet oligosaccharide distribution. In each iteration, IMSL subroutine DNEQNF uses the differences between the 33 calculated and "real" mole fractions in the inlet to the first compartment, in order to calculate the next guess for the 33 mole fractions in the outlet of the last compartment.
3. Parameter q_p is increased by a small amount and step 2 is repeated using the previous solution as the initial guess. Step 3 is repeated until the desired value of q_p is reached.

If a continuous variation in a parameter other than q_p is being studied, the system is first solved for the initial value of the parameter using steps 1 to 3. Step 3 is then repeated, but at q_p constant and instead slowly increasing the value of the parameter of interest.

2.7 Results and Discussion

The parameter values described above are estimates of the typical range of values found in the biosynthesis of N-linked glycoforms in CHO cells. Since the kinetic constants for the reactions were estimated for free oligosaccharide substrates, they are not expected to fit a particular glycoprotein substrate. However, the range of their values also corresponds to that observed for some real glycoproteins. Therefore, solving the system of equations with this set of parameters and comparing the resulting oligosaccharide distribution to those of glycoproteins expressed by this host should give a general idea of how reasonable the model is.

The steady-state oligosaccharide distribution for a secreted glycoprotein in the absence of GnTIII activity, i.e., for wild-type CHO cells, was calculated using the values of the parameters and solution strategy described above. The distribution obtained for pseudo-first order kinetics consisted mainly of complex bi- and tri'-antennary oligosaccharides: 72 and 24%, respectively. A small amount, 3%, of hybrid oligosaccharides was also obtained, while the remaining types were present below 1%. All the oligosaccharides were galactosylated. This is a reasonable distribution considering that many glycoproteins produced in CHO cells, for example β-interferon (Kagawa et al., 1988), EPO (Watson et al., 1994), and humanized IgGs (Lifely et al., 1995), contain mainly complex oligosaccharides. Most complex oligosaccharides produced by these cells are fully galactosylated, those of IgGs being an exception.

The system was then solved at increasing values of glycoprotein productivity (Fig. 3). At low values of glycoprotein productivity, the distribution of most of the oligosaccharides into bi- and tri'-antennary did not change significantly. This distribution is similar to that of β-interferon produced in CHO cells: 68% bi- and 31% tri'-antennary, all galactosylated

(Kagawa et al., 1988). Since the same maximal velocities were used for GnTV and GnTIV, this result reflects the relatively high dissociation constant of GnTIV for its soluble oligosaccharide substrate. This constant is one order of magnitude higher than the rest. Although this is consistent with the oligosaccharide distribution of β-interferon, many other glycoproteins produced in CHO cells contain significant amounts of tri- and tetra-antennary oligosaccharides. Use of a dissociation constant value of 150 μM for both GnTIV reactions, a typical value for the rest of CRN, yields a 10.6 : 1.9 : 2.4 : 1 ratio of bi- : tri- : tri'- : tetra-antennary oligosaccharides. This ratio is comparable to those found in the two glycosylation sites which carry complex oligosaccharides in recombinant tPA produced by CHO cells: 9.0 : 4.5 : 1.4 : 1 and 7.5 : 1.6 : 2.1 : 1, respectively (Spellman et al., 1989).

When the glycoprotein productivity is increased towards the middle of the range used in the simulations, a decline in the flux from bi- to tri'-antennary oligosaccharides is observed (Fig. 3), while the small hybrid fraction remains practically constant. However, at the highest glycoprotein productivities, the flux into bi-antennary structures starts to decrease and compounds occurring earlier in the pathway, the high-mannose and hybrid oligosaccharides, begin to accumulate slowly. Non-bisected hybrid oligosaccharides are relatively uncommon (Kornfeld and Kornfeld, 1985). One potential reason for this is that hybrid oligosaccharides in most glycoproteins, and perhaps also in solution, have more unfavourable kinetic constants for GalT than those assumed here. Nevertheless, some proteins do carry non-bisected hybrid oligosaccharides; for example, CHO cell-produced tPA carries 3% (Spellman et al., 1989), and recombinant ovalbumin, produced in a cell line lacking GnTIII activity, carries predominantly hybrid oligosaccharides (Sheares and Robbins, 1986).

The accumulation of high-mannose and hybrid oligosaccharides may depend to some extent on the maximal velocities for ManI and ManII, levels of which were estimated between those for GnTI and GnTII for these simulations. Figure 4 shows that at the estimated value of maximal activity for ManI, the accumulation of high-mannose structures is insignificant in the middle range of glycoprotein productivities (using a dissociation constant for soluble oligosaccharides). However, at one third of this velocity these structures start to accumulate significantly. Therefore, the model suggests that glycosylation patterns of some recombinant glycoproteins, expressed at different levels from a series of CHO clones, may easily show significant differences around the highest range of specific productivities currently attainable in the biotechnology industry.

The main function of the model, to simulate qualitative trends in the oligosaccharide distribution resulting from the overexpression of one or more enzymes, is illustrated here for the overexpression of GnTIII. This is a case of recent biotechnological relevance. IgG antibodies expressed in CHO cell lines lack the bisecting GlcNAc found in low amounts in human and animal serum IgG antibodies (Lifely et al., 1995). In contrast, a humanized IgG1 (CAMPATH-1H) produced in rat myeloma cell line, carried a bisecting GlcNAc in some of its glycoforms. The rat cell-derived antibody reached a similar *in vitro* ADCC activity as CAMPATH-1H antibodies produced in CHO cell lines, but at significantly lower antibody concentrations (Lifely et al., 1995). Therefore, overexpression of GnTIII in CHO cell lines already producing this target glycoprotein is an attractive alternative for synthesis of glycoforms which may have a superior specific biological activity.

However, overexpression of GnTIII can have a major effect on the entire oligosaccharide distribution. It acts at several points in the pathway (see Figure 2), and its bisected products can no longer be processed by the remaining CRN enzymes, with the exception of GalT.

Therefore, it is difficult to anticipate the consequences of GnTIII overexpression without the guidance of this type of mathematical representation for the complete network.

The effects of GnTIII overexpression on the bisected oligosaccharide distribution, as simulated with the model for basal parameter set, are presented in Figure 5. A maximum of about 60% in the fraction of bisected-complex oligosaccharides is observed around 300 pmol(10^6 cells)$^{-1}$(h)$^{-1}$. This value of activity is in the typical range of apparent maximal activities for different enzymes in CHO cell lysates. Moreover, it is evident that, in this range of GnTIII activities, the amount of product can be significantly controlled with small changes in the enzyme activity. At high GnTIII activity levels, bisected hybrid oligosaccharides start to accumulate. These are considered here as undesirable products due to the rapid clearance from circulation which they can cause (Cumming, 1991; Jenkins et al., 1996) and also due to the negative side-effects they could potentially induce through the formation of antibody aggregates with a mannose-binding protein (Malhorta et al., 1995). The highest activity used in these simulations corresponds to the estimate of the highest value reported in the literature, found in mouse melanoma cells stably transfected with a GnTIII expression vector (Yoshimura et al., 1995). For reference, the GnTIII activity, estimated for the CHO cell mutant Lec10, is between 80 and 130 pmol(10^6 cells)$^{-1}$(h)$^{-1}$ (Table III).

Important questions pertaining to this example can be addressed by exploring some aspects of the behaviour of the model when various parameters are changed around their typical values, as illustrated below.

In the synthesis of hybrid oligosaccharides, GnTIII competes (reactions 20 to 22) with ManII and GnTII (reactions 6 to 8). In all these simulations it has been assumed that GnTIII co-distributes with these other enzymes along the Golgi, as has been observed for

ManI, and GnTI (see model parameters section). However, the quantitative spatial distribution of this enzyme could be different, and the model can help to evaluate the impact this can have in the oligosaccharide distribution. In addition, it is technically possible to engineer the spatial distribution of this enzyme by exchanging its transmembrane and flanking domains with those of GalT. This should relocate the enzyme, leading to a spatial distribution similar to that of GalT (Russo et al., 1992), and could potentially reduce the competition with ManII and GnTII and consequently the amount of resulting bisected-hybrids. On the other hand this relocation would increase the competition between GnTIII and GalT for complex oligosaccharide acceptors. A simulation of GnTIII engineered in such a way is presented in Figure 6. Once again, the maximum value of the bisected-complex fraction is hardly altered, but a much higher amount of enzyme is required to achieve it.

However, the objective may be not only to maximize complex-bisected oligosaccharides, but at the same time to minimize potentially harmful hybrid structures. In this case it is interesting to make a plot of the selectivity, defined as the ratio of desired products to the sum of desired plus undesired products. This is shown in Figure 7. At the activities which lead to maximum amount of the desired product, the "wild-type" and re-located GnTIIIs give a similar selectivity. Nonetheless, the selectivity of the reaction network containing the re-located enzyme is much less sensitive to changes in activity.

Another alternative to be explored in a strategy to maximize complex-bisected oligosaccharides is the overexpression of GnTII and ManII. The model predicts that, for the basal set of parameter values, the maximum fraction of bisected complex oligosaccharides can be increased from about 60% to 70% with a five-fold overexpression of GnTII (Fig. 8). An additional five-fold overexpression of GnTII does not increase this value any further, while an equivalent increase in ManII takes the maximum fraction to

approximately 85%. In this last case, the sensitivity in the complex fraction to variations in GnTIII activity, at high activity levels, is also significantly reduced.

Different glycoprotein substrates can modulate in different ways the values of the kinetic constants for the reactions. For example, the accessibility of the oligosaccharides in an IgG molecule to the active sites of the enzymes could be significantly restricted (Malhorta et al., 1995), increasing the values of the Michaelis constants. This can be different for different oligosaccharides. Figure 9 shows that a ten-fold increase in the Michaelis constants of all GnTIII-catalyzed reactions increases about seven- to eight-fold the amount of GnTIII activity required to achieve the maximum fraction. However, the maximum value of the bisected-complex oligosaccharide fraction remains practically constant.

To tailor the simulations to a specific target glycoprotein, Michaelis constants for its glycosylation sites and estimates of all the relevant apparent maximal velocities are required. However, direct (*in vitro*) experimental determination of the kinetic constants of each reaction of the CRN for a particular glycosylation site is a difficult task. Protein-linked oligosaccharide substrates for many of the reactions would have to be generated either by the production of the glycoprotein in glycosylation mutants, the *in vitro* use of glycosyltransferases and glycosidases, or a combination of both. These experiments are further complicated by the partial denaturation of the glycoprotein substrate under the conditions required for *in vitro* remodelling with glycosidases (Do et al., 1994). As long as enough protein-linked oligosaccharide substrate is available, mixtures of glycoforms can be used, but a structural analysis of the oligosaccharides is required to correctly process the kinetic data. Site-specific information for a glycoprotein with multiple glycosylation sites would require post-assay proteolysis and separation of the glycopeptide products.

A different approach is proposed here for this problem. It consists of collecting a set of oligosaccharide distributions associated with different expression levels of a glycosyltransferase of interest. Together with measurements of apparent maximal velocities for the different enzymes, this set of data would enable calculation of protein-specific parameters. The new parameters would help to design other metabolic engineering experiments where additional glycosyltransferases, or the localization of these enzymes, are manipulated.

The present model can also be easily extended to include more Golgi-localized transfer reactions that increase oligosaccharide micro-heterogeneity. However, other extensions should be studied first. Competition between different glycosylation sites in the same recombinant glycoprotein and in endogenous glycoproteins can be incorporated by writing parallel mass balances for a lumped recombinant glycosylation site and a lumped endogenous glycosylation site. Clearly, the three types of mole fractions must be included in all of the reaction rates. This triples the size of the problem, but the solution strategy developed here can still easily handle this. Finally, once there is data available for the kinetics of sugar-nucleotide import into the Golgi, nucleoside diphosphate degradation, and nucleoside monophosphate export out of the Golgi, mass balances for these compounds can be included and the concentrations of sugar-nucleotides used in calculating the reaction velocities. For the guidance of metabolic engineering efforts, it would be important to know how significantly the steady-state levels of these compounds are changed by overexpression of glycosyltransferases.

2.8 Acknowledgements

This research was supported by the Swiss Priority Program in Biotechnology (SPP BioTech). In addition, the authors wish to thank Dr. V. Hatzimanikatis for helpful discussions and advice and Dr. Dana C. Andersen for suggesting important references for this manuscript.

2.9 References

Albe, K. R., Butler, M. H. and Wright, B. E. 1990. Cellular concentrations of enzymes and their substrates. J. Theor. Biol. **143**: 163-196.

Arathoon, W. R. and Birch, J. R. 1986. Large-scale cell culture in biotechnology. Science **232**: 1390-1395.

Bailey, J. E. 1991. Toward a science of metabolic engineering. Science **252**: 1668- 1675.

Bibila, T. A. and Flickinger, M. C. 1991. A model of interorganelle monoclonal antibody transport and secretion in mouse hybridoma cells. Biotechnol. Bioeng. **38**: 767-780.

Bibila, T. A. and Robinson, D. K. 1995. In pursuit of the optimal fed-batch process for monoclonal antibody production. Biotechnol. Prog. **11**: 1-13.

Bretscher, M. S. and Munro, S. 1993. Cholesterol and the Golgi apparatus. Science **261**: 1280-1281.

Briles, E. B., Li, E. and Kornfeld, S. 1979. Isolation of wheat germ agglutinin-resistant clones of Chinese hamster ovary cells deficient in membrane sialic acid and galactose. J. Biol. Chem. **252**: 1107-1116.

Brockhausen, I., Moller, G., Yang, J. M., et al. 1992. Control of glycoprotein synthesis. Carbohydr. Res. **236**: 281-299.

Chaney, W. and Stanley, P. 1986. Lec1A Chinese hamster ovary cell mutants appear to arise from a structural alteration in N-acetylglucosaminyltransferase I. J. Biol. Chem. **261**: 10551-20557.

Cole, N. B., Smith, C. L., Sciaky, N., et al. 1996. Diffusional mobility of Golgi proteins in membranes of living cells. Science **273**: 797-801.

Cumming, D. A. 1991. Glycosylation of recombinant protein therapeutics: control and functional implications. Glycobiology **1**: 115-130.

Dennis, J. W., Laferte, S., Waghorne, C., et al. 1987. Beta 1-6 branching of Asn-linked oligosaccharides is directly associated with metastasis. Science **236**: 582-585.

Do, K. Y., Fregien, N., Pierce, M., et al. 1994. Modification of glycoproteins by N-acetylglucosaminyltransferase V is greatly influenced by accessibility of the enzyme to oligosaccharide acceptors. J. Biol. Chem. **269**: 23456-23464.

Domach, M. M., Leung, S. K., Cahn, R. E., et al. 1984. Computer model for glucose-limited growth of a single cell of *Escherichia coli* B/r-A. Biotechnol. Bioeng. **26**: 203-216.

Dunphy, W. G., Brands, R. and Rothman, J. E. 1985. Attachment of terminal N-acetylglucosamine to asparagine-linked oligosaccharides occurs in central cisternae of the Golgi stack. Cell **40**: 463-472.

Dunphy, W. G., Fries, E., Urbani, L. J., et al. 1981. Early and late functions associated with the Golgi apparatus reside in distinct compartments. Proc. Natl. Acad. Sci. USA **78**: 7453-7457.

Dunphy, W. G. and Rothman, J. E. 1983. Compartmentation of asparagine-linked oligosaccharide processing in the Golgi apparatus. J. Cell Biol. **97**: 270-275.

Easton, E. W., Bolscher, J. G. and van den Eijnden, D. H. 1991. Enzymatic amplification involving glycosyltransferases forms the basis for the increased size of asparagine-linked glycans at the surface of NIH 3T3 cells expressing the N-ras proto-oncogene. J. Biol. Chem. **266**: 21674-21680.

Elices, M. J. and Goldstein, I. J. 1988. Ehrlich ascites tumor cell UDP-Gal:N-acetyl-D-glucosamine beta(1,4)-galactosyltransferase. Purification, characterization, and topography of the acceptor-binding site. J. Biol. Chem. **263**: 3354-3362.

Fouser, L. A., Swanberg, S. L., Lin, B. Y., et al. 1992. High level expression of a chimeric anti-ganglioside GD2 antibody: genomic kappa sequences improve expression in COS and CHO cells. Bio/Technology **10**: 1121-1127.

Goldberg, D. E. and Kornfeld, S. 1983. Evidence for extensive subcellular organization of aspargine-linked oligosaccharide processing and lysosomal enzyme phosphorylation. J. Biol. Chem. **258**: 3159-3165.

Griffiths, G., Fuller, S. D., Back, R., et al. 1989. The dynamic nature of the Golgi complex. J. Cell Biol. **108**: 277-298.

Gross, H. J., Sticher, U. and Brossmer, R. 1990. A highly sensitive fluorometric assay for sialyltransferase activity using CMP-9-fluoresceinyl-NeuAc as donor. Anal. Biochem. **186**: 127-134.

Gu, J., Nishikawa, A., Tsuruoka, N., et al. 1993. Purification and characterization of UDP-N-acetylglucosamine: alpha-6-D-mannoside beta 1-6N-acetylglucosaminyltransferase (N-acetylglucosaminyltransferase V) from a human lung cancer cell line. J. Biochem. **113**: 614-619.

Harpaz, N. and Schachter, H. 1980. Control of glycoprotein synthesis. J. Biol. Chem. **255**: 4894-4902.

Heffernan, M., Lotan, R., Amos, B., et al. 1993. Branching b-1-6N-acetylglucosaminyltransferases and polylactosamine expression in mouse F9 teratocarcinoma cells and differentiated counterparts. J. biol. Chem. **268**: 1242-1251.

Hirschberg, C. B. and Snider, M. D. 1987. Topography of glycosylation in the rough endoplasmic reticulum and Golgi apparatus. Annu. Rev. Biochem. **56**: 63-87.

Jenkins, N., Parekh and R. B., James, D. C. 1996. Getting the glycosylation right: implications for the biotechnology industry. Nature Biotechnol. **14**: 975-981.

Kagawa, Y., Takasaki, S., Utsumi, J., et al. 1988. Comparative study of the asparagine-linked sugar chains of natural human interferon-beta 1 and recombinant human interferon-beta 1 produced by three different mammalian cells. J. Biol. Chem. **263**: 17508-17515.

Kornfeld, R. and Kornfeld, S. 1985. Assembly of asparagine-linked oligosaccharides. Annu. Rev. Biochem. **54**: 631- 664.

Lee, E. U., Roth, J. and Paulson, J. C. 1989. Alteration of terminal glycosylation sequences on N-linked oligosaccharides of Chinese hamster ovary cells by expression of beta-galactoside alpha 2,6-sialyltransferase. J. Biol. Chem. **264**: 13848-13855.

Lee, S. B. and Bailey, J. E. 1984. Analysis of growth rate effects on productivity of recombinant *E. coli* populations using molecular mechanism models. Biotechnol. Bioeng. **26**: 66-73.

Lifely, R. M., Hale, C., Boyce, S., et al. 1995. Glycosylation and biological activity of CAMPATH-1H expressed in different cell lines and grown under different culture conditions. Glycobiology **318**: 813- 822.

Malhorta, R., Wormald, M. R., Rudd, P. M., et al. 1995. Glycosylation changes of IgG associated with rheumatoid arthritis can activate complement via the mannose-binding protein. Nature Medicine **1**: 237-243.

Minch, S. L., Kallio, P. T. and Bailey, J. E. 1995. Tissue plasminogen activator coexpressed in Chinese hamster ovary cells with alpha(2,6)-sialyltransferase contains NeuAc-alpha(2,6)Gal-beta(1,4)Glc-N-AcR linkages. Biotechnol. Prog. **11**: 348-351.

Moremen, K. W., Trimble, R. B. and Herscovics, A. 1994. Glycosidases of the asparagine-linked oligosaccharide processing pathway. Glycobiology **4**: 113-125.

Narasimhan, S. 1982. Control of glycoprotein synthesis. J. Biol. Chem. **257**: 10235-10242.

Narasimhan, S., Freed, J. C. and Schachter, H. 1985. Control of glycoprotein synthesis. Bovine milk UDPgalactose:N-acetylglucosamine beta-4-galactosyltransferase catalyzes the preferential transfer of galactose to the GlcNAc beta 1,2Man alpha 1,3- branch of both bisected and nonbisected complex biantennary asparagine-linked oligosaccharides. Biochemistry **24**: 1694-1700.

Nilsson, T., Hoe, M. H., Slusarewicz, P., et al. 1994. Kin recognition between medial Golgi enzymes in HeLa cells. Embo J. **13**: 562-574.

Nilsson, T., Pypaert, M., Hoe, M. H., et al. 1993. Overlapping distribution of two glycosyltransferases in the Golgi apparatus of HeLa cells. J. Cell Biol. **120**: 5-13.

Nilsson, T., Rabouille, C., Hui, N., et al. 1996. The role of the membrane-spanning domain and stalk region of N-acetylglucosaminyltransferase I in retention, kin recognition and structural maintenance of the Golgi apparatus in HeLa cells. J. Cell Biol. **109**: 1975-1989.

Ohno, M., Nishikawa, A., Koketsu, M., et al. 1992. Enzymatic basis of sugar structures of alpha-fetoprotein in hepatoma and hepatoblastoma cell lines: Correlation with activities of alpha-1-6 fucosyltransferase and N-acetylglucosaminyltransferases III and V. Int. J. Cancer **51**: 315-317.

Page, M. J. and Sydenham, M. A. 1991. High level expression of the humanized monoclonal antibody CAMPATH-1H in Chinese hamster ovary cells. Bio/Technology **9**: 64-68.

Palcic, M. M., Ripka, J., Kaur, K. J., et al. 1990. Regulation of N-acetylglucosaminyltransferase V activity: Kinetic comparisons of parental, Rous sarcoma virus-transformed BHK, and L-phytohemagglutinin-resistant BHK cells using synthetic substrates and an inhibitory substrate analog. J. Biol. Chem. **265**: 6759-6769.

Paquet, M. R., Narasimhan, S., Schachter, H., et al. 1984. Branch specificity of purified rat liver Golgi UDP-galactose:N-acetylglucosamine beta-1,4-galactosyltransferase. J. Biol. Chem. **259**: 4716-4721.

Paulson, J. C. and Colley, K. J. 1989. Glycosyltransferases. Structure, localization, and control of cell type-specific glycosylation. J. Biol. Chem. **264**: 17615-17618.

Pels Rijcken, W. R., Overdijk, B., Van den Eijnden, D. H., et al. 1995. The effect of increasing nucleotide-sugar concentrations on the incorporation of sugars into glycoconjugates in rat hepatocytes. Biochem. J. **305**: 865-870.

Rabouille, C., Hui, N., Hunte, F., et al. 1995. Mapping the distribution of Golgi enzymes involved in the construction of complex oligosaccharides. J. Cell Science **108**: 1617- 1627.

Rao, A. K. and Mendicino, J. 1978. Influence of glycopeptide structure of the regulation of galactosyltranferase activity. Biochemistry **17**: 5635-5638.

Rearick, J. I., Sadler, J. E., Paulson, J. C., et al. 1979. Enzymatic characterization of beta-D-galactoside alpha2-3 sialyltransferase form porcine submaxilliary gland. J. Biol. Chem. **254**: 4444-4451.

Reff, M. E., Carner, K., Chambers, K. S., et al. 1994. Depletion of B cells *in vivo* by a chimeric mouse human monoclonal antibody to CD20. Blood **83**: 435-445.

Rossmann, C., Sharp, N., Allen, G., et al. 1996. Expression and purification of recombinant, glycosylated human interferon-alpha-2B in murine myeloma NS0 cells. Prot. Expres. Purif. **7**: 335-342.

Rothman, J. E. and Orci, L. 1992. Molecular dissection of the secretory pathway. Nature **355**: 409-415.

Rothman, J. E. and Wieland, F. T. 1996. Protein sorting by transport vesicles. Science **272**: 227-234.

Russo, R. N., Shaper, N. L., Taatjes, D. J., et al. 1992. Beta-1,4-galactosyltransferase: a short NH-2-terminal fragment that includes the cytoplasmic and transmembrane domain is sufficient for Golgi retention. J. Biol. Chem. **267**: 9241-9247.

Sambanis, A., Lodish, H. F. and Stephanopoulos, G. 1991. A model of secretory protein trafficking in recombinant AtT-20 cells. Biotechnol. Bioeng. **38**: 280-295.

Schachter, H. 1986. Biosynthetic controls that determine the branching and microheterogeneity of protein- bound oligosaccharides. Biochem. Cell Biol. **64**: 163- 181.

Schachter, H., Brockhausen, I. and Hull, E. 1989. High-performance liquid chromatography assays for N-acetylglucosaminyltransferases involved in N- and O-glycan synthesis. Methods Enzymol. **179**: 351-397.

Shao, M. C. and Wold, F. 1988. The effect of the protein matrix on glycan processing in glycoproteins. Kinetic analysis of three rat liver Golgi enzymes. J. Biol. Chem. **263**: 5771-5774.

Shao, M. C. and Wold, F. 1995. The effect of the protein matrix proximity on glycan reactivity in a glycoprotein model. Eur. J. Biochem. **228**: 79-85.

Sheares, B. T. and Robbins, P. W. 1986. Glycosylation of ovalbumin in a heterologous cell: analysis of oligosaccharide chains of the cloned glycoprotein in mouse L cells. Proc. Natl. Acad. Sci. U S A **83**: 1993-1997.

Shelikoff, M., Sinskey, A. J. and Stephanopoulos, G. 1996. A modeling framework for the study of protein glycosylation. Biotechnol. Bioeng. **50**: 73-90.

Spellman, M. W., Basa, L. J., Leonard, C. K., et al. 1989. Carbohydrate structures of human tissue plasminogen activator expressed in Chinese hamster ovary cells. J. Biol. Chem. **264**: 14100-14111.

Stanley, P. and Campbell, C. A. 1984. A dominant mutation to ricin resistance in Chinese hamster ovary cells induces UDP- GlcNac: Glycopeptide β-4-N-Acetylglucosaminyltransferase III activity. J. Biol. Chem. **261**: 13370- 13378.

Stanley, P. 1992. Glycosylation engineering. Glycobiology **2**: 99-107.

Starbuck, C. and Lauffenburger, D. A. 1992. Mathematical model for the effects of epidermal growth-factor receptor trafficking dynamics on fibroblast proliferation responses. Biotechnol. Prog. **8**: 132-143.

Tabas, I. and Kornfeld, S. 1979. Purification and characterization of a rat liver Golgi alpha-mannosidase capable of processing asparagine-linked oligosaccharides. J. Biol. Chem. **254**: 11655-11663.

Taniguchi, N., Nishikawa, A., Fujii, S., et al. 1989. Glycosyltransferase assays using pyridylaminated acceptors: N-acetylglucosaminyltransferase III, IV, and V. Methods Enzymol. **179**: 397-408.

Velasco, A., Hendricks, L., Moremen, K. W., et al. 1993. Cell type-dependent variation in the subcellular distribution of alpha-mannosidase I and II. J. Cell Biol. **122**: 39-51.

Watson, E., Bhide, A. and Van Halbeek, H. 1994. Structure determination of the intact major sialylated oligosaccharide chains of recombinant human erythropoietin expressed in Chinese hamster ovary cells. Glycobiology **4**: 227-237.

Wiest, D. L., Burkhardt, J. K., Hester, S., et al. 1990. Membrane biogenesis during B cell differentiation: Most endoplasmic reticulum proteins are expressed coordinately. Journal Of Cell Biology **110**: 1501-1512.

Wyss, D. F. and Gerhard, W. 1996. The structural role of sugars in glycoproteins. Current Opinion Biotechnol. **7**: 409-416.

Yagamaguchi, N. and Fukuda, M. N. 1995. Golgi retention mechanism of beta-1,4-galactosyltransferase: membrane-spanning domain-dependent homodimerization and association with alpha- and beta-tubulins. J. Biol. Chem. **270**: 12170-12176.

Yoshimura, M., Nishikawa, A., Ihara, Y., et al. 1995. Suppression of lung metastasis of B16 mouse melanoma by N-acetylglucosaminyltransferase III gene transfection. Proc. Nat. Acad. Sci. U.S.A. **92**: 8754-8758.

Youakim, A. and Shur, B. D. 1993. Effects of overexpression of beta-1,4-galactosyltransferase on glycoprotein biosynthesis in F9 embryonal carcinoma cells. Glycobiology **3**: 155-163.

2.10 Tables

Table I. Values of index *i* assigned to each oligosaccharide species.

Oligosaccharide	*i*	Oligosaccharide	*i*
M_9	1	$M_3Gn_3'G$	18
M_8	2	M_3Gn_4G	19
M_7	3	M_5GnGn^b	20
M_6	4	M_4GnGn^b	21
M_5	5	M_3GnGn^b	22
M_5Gn	6	$M_3Gn_2Gn^b$	23
M_4Gn	7	$M_3Gn_3Gn^b$	24
M_3Gn	8	$M_3Gn_3'Gn^b$	25
M_3Gn_2	9	$M_3Gn_4Gn^b$	26
M_3Gn_3	10	M_5GnGn^bG	27
M_3Gn_3'	11	M_4GnGn^bG	28
M_3Gn_4	12	M_3GnGn^bG	29
M_5GnG	13	$M_3Gn_2Gn^bG$	30
M_4GnG	14	$M_3Gn_3Gn^bG$	31
M_3GnG	15	$M_3Gn_3'Gn^bG$	32
M_3Gn_2G	16	$M_3Gn_4Gn^bG$	33
M_3Gn_3G	17		

Table II. Apparent dissociation constants.

Enzyme	K_m (μM)	Source	Acceptor	Reference
ManI	100	rat liver	M_8 *	Tabas and Kornfeld, 1979
GnTI	260	CHO cells	M_5	Chaney and Stanley, 1986
GnTII	190	rat liver	M_3Gn	Schachter et al., 1989
GnTIII	190	rat	M_3Gn_2**	Taniguchi et al., 1989
GnTIV	3,400	rat	M_3Gn_2**	Taniguchi et al., 1989
GnTV	130	human lung	M_3Gn_2**	Gu et al., 1993
GalT	130	rat liver	M_3Gn_2	Paquet et al., 1984

* The core consisted of only one Gn.

** Reducing end-Gn was pyridylaminated.

Table III. Apparent maximal velocities for CHO cells.

Enzyme	V_m (pmol(mg protein)$^{-1}$(h)$^{-1}$)	V_m (pmol(10^6 cells)$^{-1}$(h)$^{-1}$)	Reference
GnTI	12,400	450	Dunphy and Rothman, 1983 Dunphy et al., 1981
GnTII	4,000	140	Dunphy and Rothman, 1983 Dunphy et al., 1981
GnTIII	2,300 - 3,700	80 - 130 *,**	Stanley and Campbell, 1984
GnTV	250	10 *	Heffernan et al., 1993
GalT	16,000	580 *	Stanley and Campbell, 1984

* The conversion of V_m from a value based on protein mass to a value based on cell number, calculated from data for GnTI and GnTII, has been extrapolated to the other enzymes.

** For Lec10 mutant CHO cells

Table IV. Summary of kinetic parameters for enzyme-catalyzed reactions used in the simulations.

Reaction *	K_m (μM)	V_m (pmol(10^6 cells)$^{-1}$(h)$^{-1}$)	Reaction *	K_m (μM)	V_m (pmol(10^6 cells)$^{-1}$(h)$^{-1}$)
1	100	300	18	50	580
2	100	300	19	40	580
3	100	300	20	4,000	0 - 4,000
4	100	300	21	4,000	0 - 4,000
5	260	450	22	4,000	0 - 4,000
6	200	300	23	190	0 - 4,000
7	100	300	24	190	0 - 4,000
8	190	140	25	190	0 - 4,000
9	130	10	26	190	0 - 4,000
10	3,400	10	27	4,000	580
11	3,400	10	28	4,000	580
12	90	10	29	4,000	580
13	4,000	580	30	500	580
14	4,000	580	31	220	580
15	4,000	580	32	200	580
16	130	580	33	140	580
17	70	580			

* The reactions are numbered as in Figure 2.

2.11 Figures

Fig. 1. Structures of common types of N-linked oligosaccharides and nomenclature. M stands for mannose; Gn, N-acetylglucosamine (GlcNAc); G, galactose; Gn^b, bisecting GlcNAc; R, Asn-Gn-β1,4-Gn or Asn-Gn-β1,4-(α1,6-fucose)-Gn. R-M is called the oligosaccharide "core." The square brackets indicate that at least one Gn is linked to a G. The oligosaccharide nomenclature used in this work consists of enumerating the M and Gn residues attached to the R group, indicating the presence of a bisecting GlcNAc by including a Gn^b, and indicating if the oligosaccharide is galactosylated by including a G. The two types of tri-antennary oligosaccharides are differentiated by adding an apostrophe to the Gn_3 term.

Fig. 2. Central reaction network on the N-linked glycosylation pathway. This set of Golgi-localized reactions determines the major types of structures into which N-linked oligosaccharides are normally classified. The enzyme catalyzing each reaction is shown and all reactions have been numbered. The reaction numbers are used to denote the kinetic parameters associated with each reaction (see Table IV for example).

Fig. 3. Predicted dependence of the mole fractions of bi- and tri'-antennary N-linked oligosaccharides on the glycoprotein productivity. The base values of the paramaters described in the model parameters section were used.

Fig. 4. Dependence of the mole fraction of high mannose oligosaccharides on the glycoprotein productivity for two different values of the Golgi mannosidase I (ManI) maximum velocity $v_{m,1}$.

Fig. 5. Mole fractions of different types of bisected oligosaccharides resulting from the expression of GnTIII at different activity levels in CHO cells. A glycoprotein productivity of 500 pmol/10^6 cells/day was used for the simulations.

Fig. 6. Effect of overexpressing a relocated GnTIII, with a Golgi distribution identical to that of GalT, on the bisected-complex oligosaccharide mole fraction. The solid line corresponds to the simulated trend for a wild-type GnTIII, with a spatial distribution identical to those of other GnT enzymes included in this model. A glycoprotein productivity of 500 pmol/10^6 cells/day was used for the simulations.

Fig. 7. Effect of overexpressing a relocated GnTIII, with a Golgi distribution identical to that of GalT, on the selectivity of bisected-complex oligosaccharides. The selectivity is defined as the ratio of the mole fraction of desired bisected-complex oligosaccharides to the sum of mole fractions of bisected-complex oligosaccharides plus undesired bisected-hybrid oligosaccharides. The solid line corresponds to the simulated trend for a wild-type GnTIII, with a spatial distribution identical to those of other GnT enzymes included in this model. A glycoprotein productivity of 500 pmol/10^6 cells/day was used for the simulations.

Fig. 8. Effect of co-expressing GnTIII with GnTII alone, or with GnTII and Man II, on the mole fraction of bisected-complex oligosaccharides.

Fig. 9. Effect of a ten-fold increase in the Michaelis constants for all GnTIII-catalyzed reactions on the bisected-complex oligosaccharide mole fraction. The solid line corresponds to the simulated trend for a glycoprotein substrate with Michaelis constants identical to those estimated for free oligosaccharide substrates. A glycoprotein productivity of 500 pmol/10^6 cells/day was used for the simulations.

Figure 1.

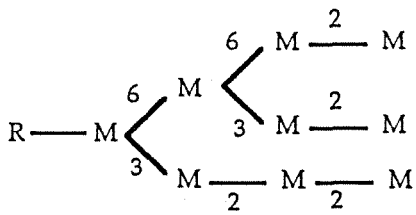

M_9. High-mannose

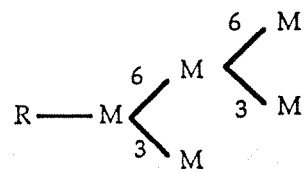

M_5. High-mannose

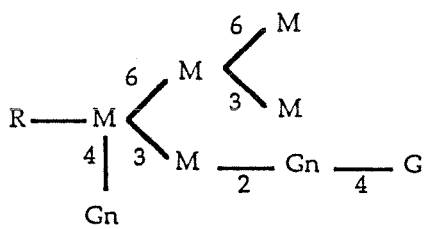

M_5GnGn^bG. Bisected hybrid

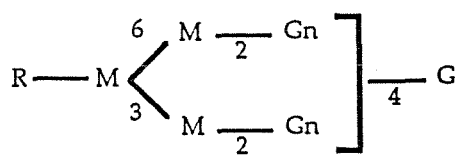

M_3Gn_2G. Bi-antennary complex

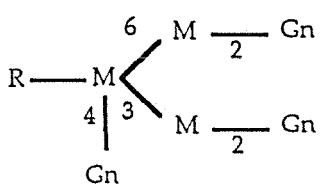

$M_3Gn_2Gn^b$. Bisected bi-antennary complex

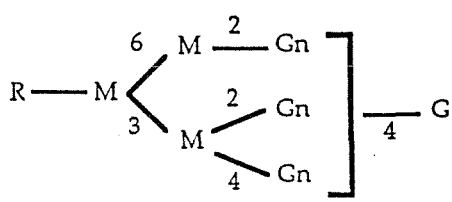

M_3Gn_3G. Tri-antennary complex

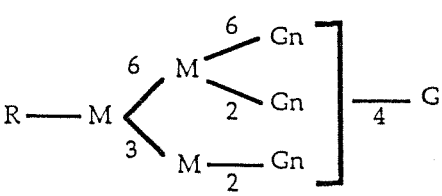

$M_3Gn_3'G$. Tri'-antennary complex

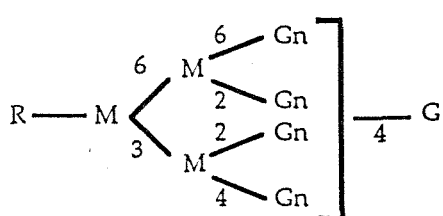

M_3Gn_4G. Tetra-antennary complex

Figure 2.

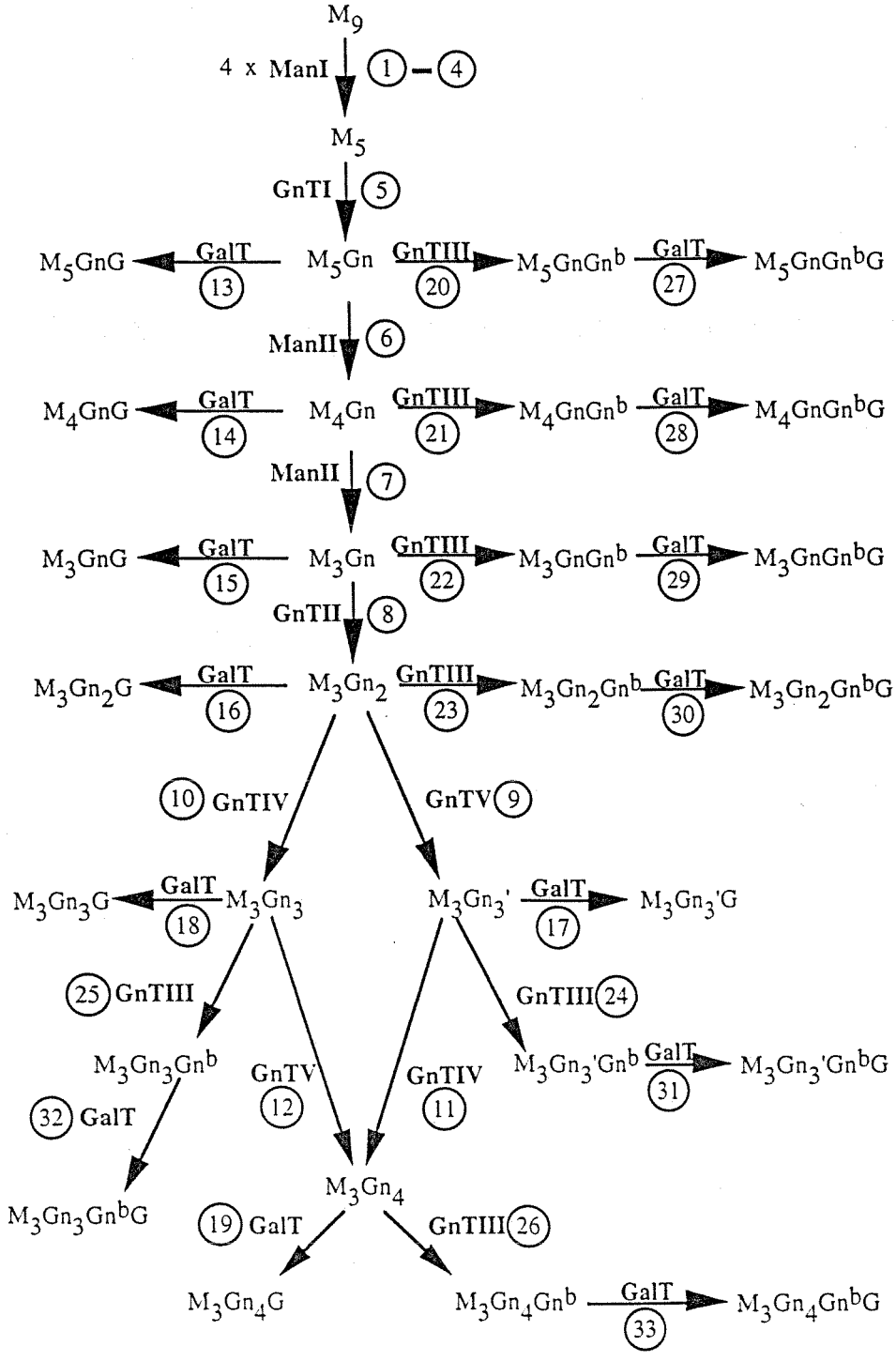
M9
4 x ManI
1
4
M5
GnTI
5
M5GnG
GalT
13
M5Gn
GnTIII
20
M5GnGnb
GalT
27
M5GnGnbG
ManII
6
M4GnG
GalT
14
M4Gn
GnTIII
21
M4GnGnb
GalT
28
M4GnGnbG
ManII
7
M3GnG
GalT
15
M3Gn
GnTIII
22
M3GnGnb
GalT
29
M3GnGnbG
GnTII
8
M3Gn2G
GalT
16
M3Gn2
GnTIII
23
M3Gn2Gnb
GalT
30
M3Gn2GnbG
10
GnTIV
GnTV
9
M3Gn3G
GalT
18
M3Gn3
M3Gn3'
GalT
17
M3Gn3'G
25
GnTIII
GnTIII
24
M3Gn3Gnb
GnTV
12
GnTIV
11
M3Gn3'Gnb
GalT
31
M3Gn3'GnbG
32
GalT
M3Gn4
M3Gn3GnbG
19
GalT
GnTIII
26
M3Gn4G
M3Gn4Gnb
GalT
33
M3Gn4GnbG

Figure 3.

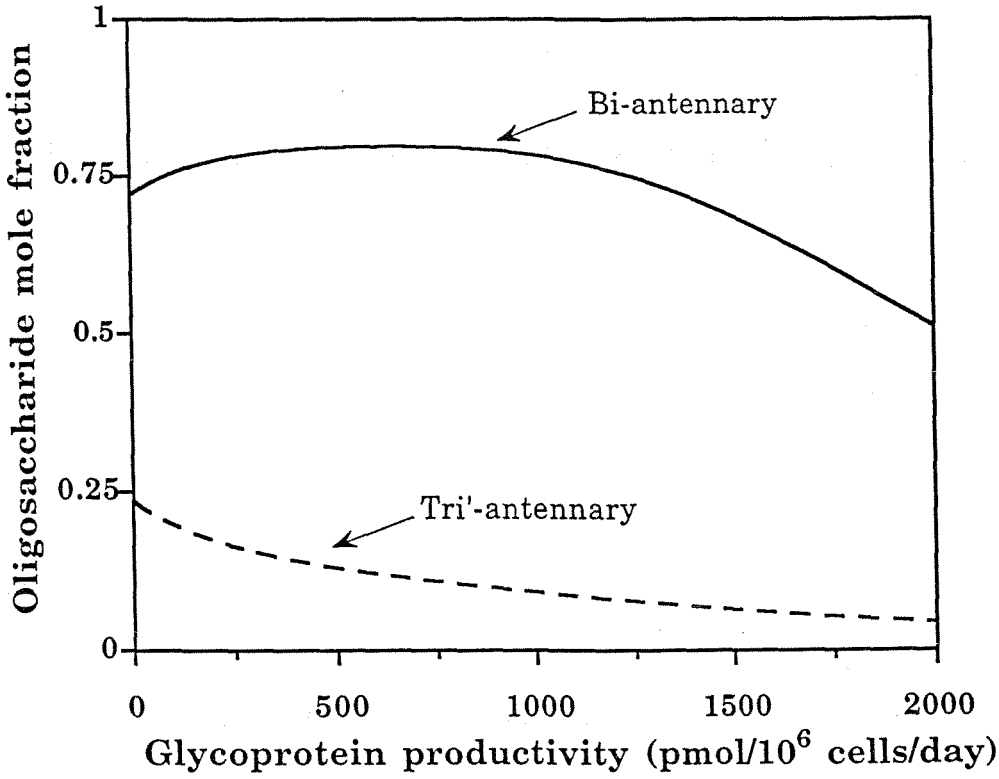
1
0.75
0.5
0.25
0
Oligosaccharide mole fraction
Bi-antennary
Tri'-antennary
0
500
1000
1500
2000
Glycoprotein productivity (pmol/10^6 cells/day)

Figure 4.

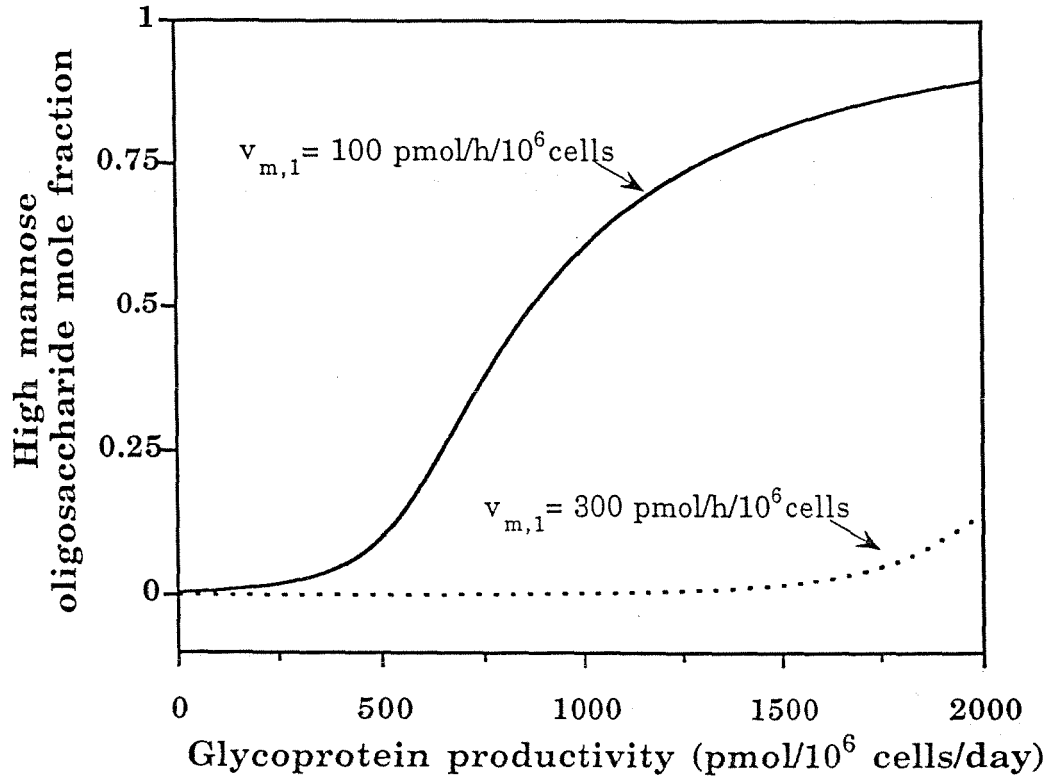
1
0.75
0.5
0.25
0
High mannose oligosaccharide mole fraction
$v_{m,1}$= 100 pmol/h/10^{6}cells
$v_{m,1}$= 300 pmol/h/10^{6}cells
0
500
1000
1500
2000
Glycoprotein productivity (pmol/10^6 cells/day)

Figure 5.

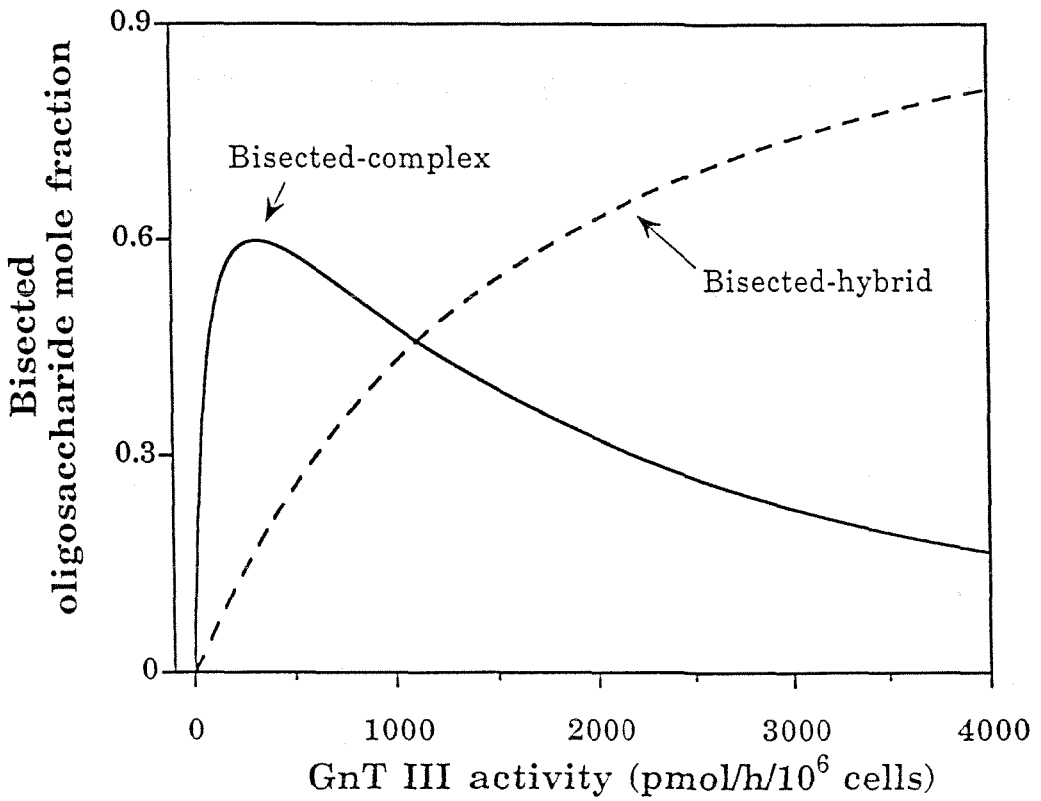
Bisected oligosaccharide mole fraction
0.9
0.6
0.3
0
Bisected-complex
Bisected-hybrid
0
1000
2000
3000
4000
GnT III activity (pmol/h/10^6 cells)

Figure 6.

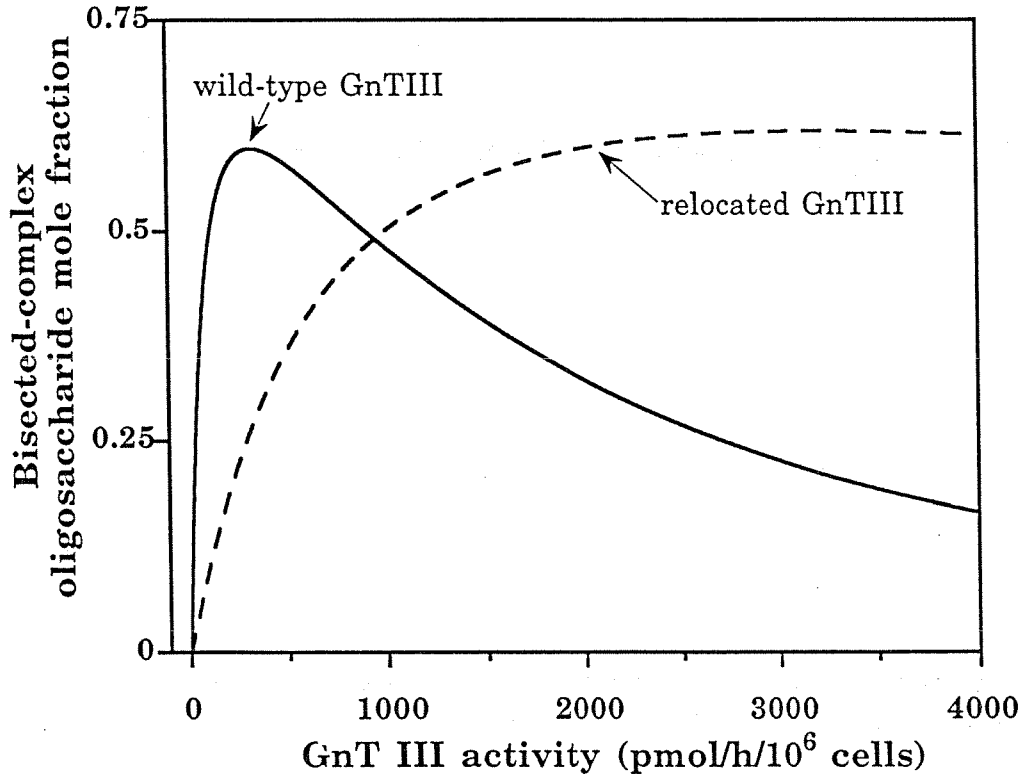
0.75
0.5
0.25
0
Bisected-complex oligosaccharide mole fraction
wild-type GnTIII
relocated GnTIII
0
1000
2000
3000
4000
GnT III activity (pmol/h/10^6 cells)

Figure 7.

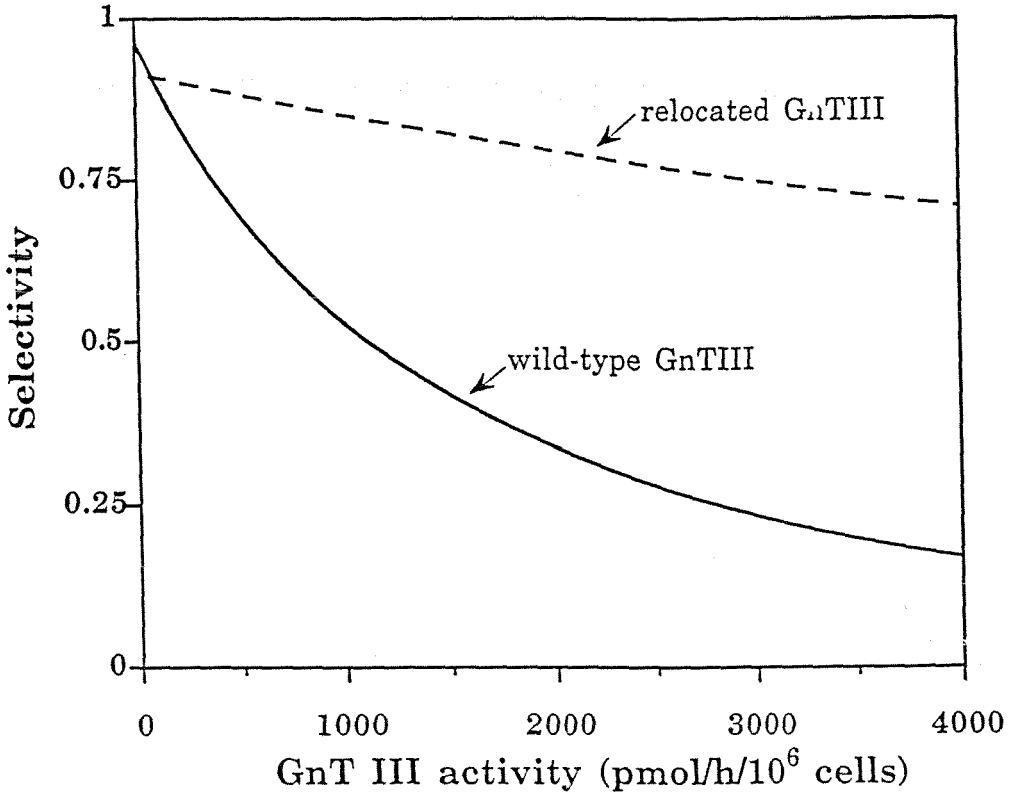
1
0.75
0.5
0.25
0
Selectivity
relocated GnTIII
wild-type GnTIII
0
1000
2000
3000
4000
GnT III activity (pmol/h/10^6 cells)

Figure 8.

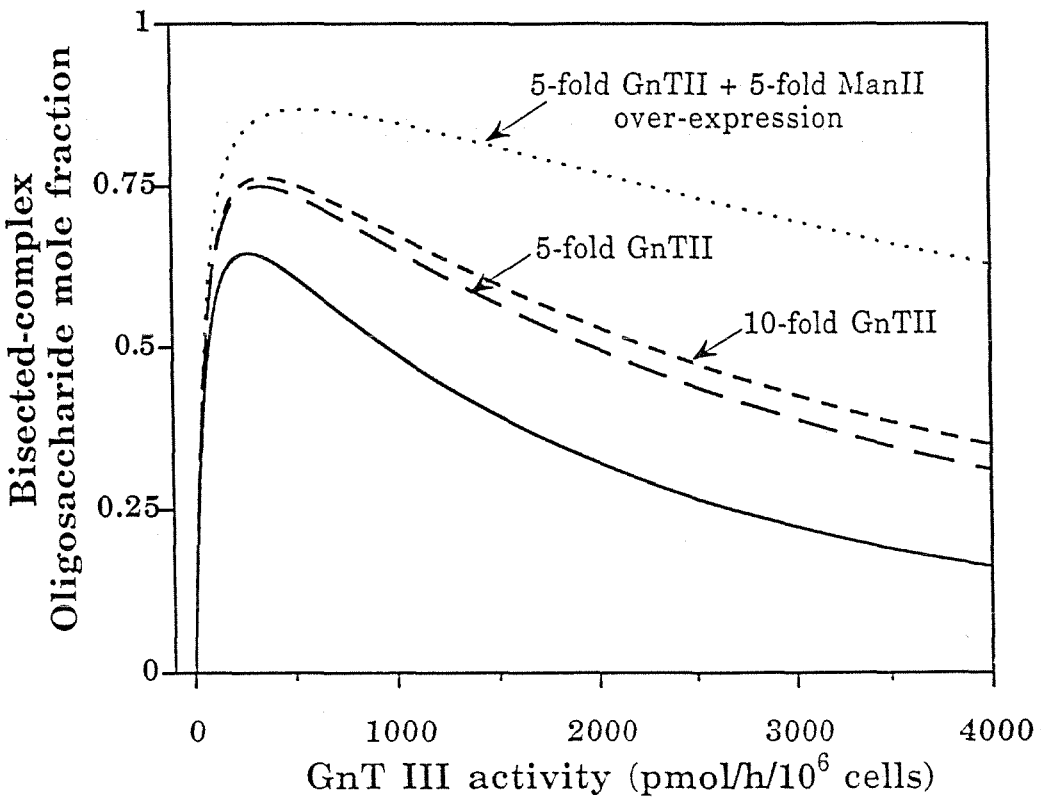
Bisected-complex Oligosaccharide mole fraction
1
0.75
0.5
0.25
0
5-fold GnTII + 5-fold ManII over-expression
5-fold GnTII
10-fold GnTII
0
1000
2000
3000
4000
GnT III activity (pmol/h/10^6 cells)

Figure 9.

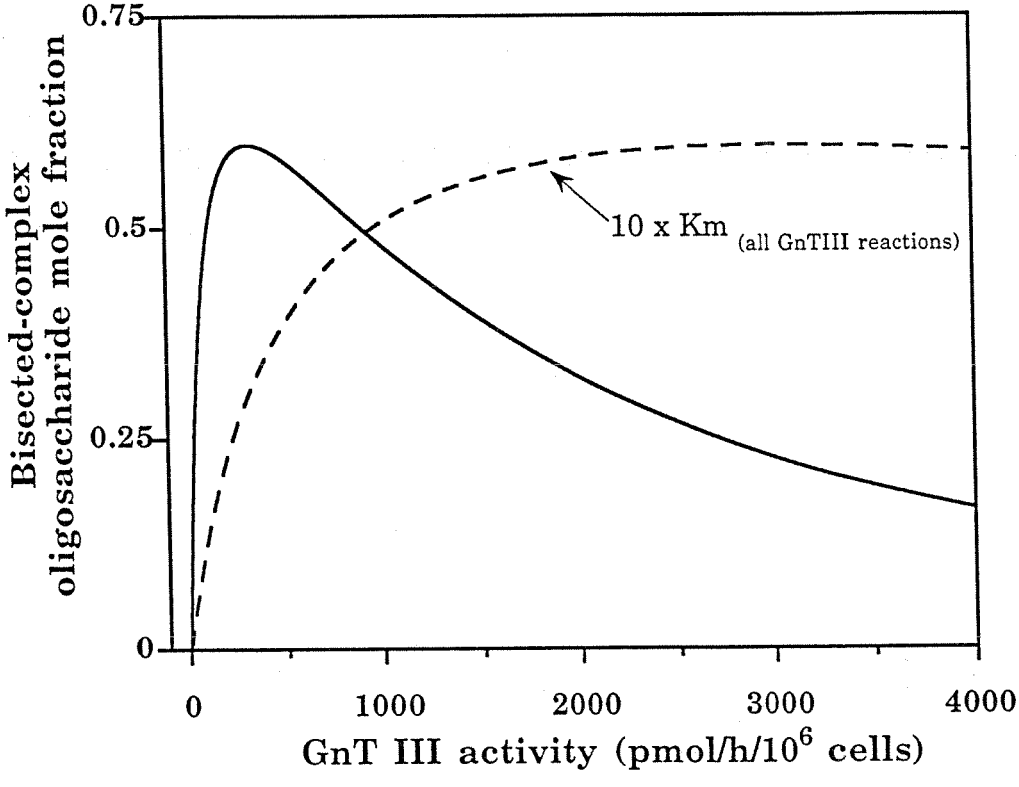
0.75
0.5
0.25
0
Bisected-complex oligosaccharide mole fraction
10 x Km (all GnTIII reactions)
0
1000
2000
3000
4000
GnT III activity (pmol/h/10^6 cells)

CHAPTER III

Tetracycline-Regulated Overexpression of Glycosyltransferases in Chinese Hamster Ovary Cells

3.1 Summary

To investigate the effects of GnTIII overexpression experimentally, a CHO cell line with tetracycline-regulated expression of this glycosyltransferase was established. The amount of GnTIII in these cells could be controlled simply by manipulating the concentration of tetracycline in the culture medium. Using this system, it was found that overexpression of GnTIII to high levels led to growth inhibition and was toxic to the cells. Another CHO cell line with tetracycline-regulated overexpression of GnTV, a distinct glycosyltransferase, showed the same inhibitory effect, indicating that this may be a general feature of glycosyltransferase overexpression. This phenomenon has not been reported previously, probably due to the widespread use of constitutive promoters. The growth effect sets an upper limit to the level of glycosyltransferase overexpression, and may thereby also limit the maximum extent of modification of poorly accessible glycosylation sites. The heterologous GnTIII was localized in the Golgi complex of CHO cells by means of immunoelectron microscopy using an antibody against a peptide epitope tag added to the carboxy-terminus of the enzyme. The enzyme concentrated on one side of the Golgi, apparently the *trans*-side, mainly in cisternal elements. There may be significant competition for complex oligosaccharide acceptors between GalT and GnTIII distributed in this way. A statistical immunogold analysis of many cell sections, relative to an established Golgi-marker, would be valuable to establish the quantitative GnTIII distribution.

3.2 Introduction

The glycosylation of recombinant therapeutic proteins produced in animal cells can be engineered by overexpression of glycosyltransferase genes in the host cells (Bailey, 1991). Previous work in this field has only used constitutive expression of the glycosyltransferase genes, and little attention has been paid to the expression level. However, this variable could play an important role when trying to maximize the proportions of beneficial glycoforms within the glycoform population of a recombinant protein. A case where control of glycosyltransferase gene expression level could be useful is the maximization of therapeutic antibody glycoforms carrying bisected oligosaccharides (see Chapter II). Simulations of the expected qualitative trends in the fraction of these glycoforms upon overexpression of N-acetylglucosaminyltransferase III (GnTIII) in CHO cells suggest that there could be an optimal range of expression level. Here the establishment and characterization of a CHO cell line with regulated GnTIII gene expression is described.

To establish a system with fine control of glycosyltransferase gene expression, various inducible eukaryotic promoters can be used. The systems used to date are responsive to heavy metal ions, hormones, or conditions such as a heat shock. However, these inducers are either toxic to the host cell and/or yield pleiotropic effects. The tetracycline-regulated expression system (Gossen and Bujard, 1992) avoids these unwanted side-effects and allows control of expression level over a wide range. It incorporates regulatory elements of a bacterial tetracycline resistance operon (Fig. 1). Cells are engineered initially to give stable, constitutive production of a tetracycline-controlled transactivator (tTA). tTA consists of the tetracycline repressor fused to the C-terminal domain of VP16, a herpes virus transactivator protein. Then the gene whose expression is to be regulated is subcloned in a vector under the control of a minimal human cytomegalovirus promoter. The promoter is preceeded upstream by multiple copies of the tetracycline operator. The minimal promoter together with the tetracycline operator sequences is referred to as tet-promoter.

Transfection of tTA-producing cells with the vector leads to expresssion of the target gene. The expression level is very low in the absence of transactivation. The C-terminal domain of VP16 provides this activation when the tTA fusion protein binds, through the tetracycline repressor protein portion, to the tetracycline operator DNA upstream of the minimal promoter. Tetracycline binds to the repressor protein, producing a conformational change which disables binding to the operator DNA, and thereby eliminating activation of the minimal promoter by the VP16 C-terminal domain. Different tetracycline concentrations in the medium lead to different equilibrium concentrations of uncomplexed repressor and, therefore, to different frequencies of the transcription activation event. An advantage of this system is that non-toxic concentrations of tetracycline are sufficient to reduce expression of the target gene to the basal level associated with the minimal promoter.

The establishment of CHO cells with tetracycline-regulated GnTIII expression and their use to study the effects of glycosyltransferase overexpression in the host cells is described here. An additional cell line with tetracycline-regulated GnTV expression was established in parallel and used to compare the effects that these two different glycosyltransferases have on the host cells.

3.3 Materials and Methods

Bacterial strains and media

E. coli strains XL-1 Blue and DH5α were grown either on LB agar plates or in LB broth.

Mammalian cell lines and media

CHO-DUKX (M-159) cells (obtained from Dr. Martin Page, Wellcome, UK) were cultured in FMX-8 medium (Cell Culture Technologies, Switzerland) supplemented with 10% (v/v) fetal calf serum (Boehringer Mannheim), 3g/l HEPES and 1% (v/v) antibiotic/antimycotic solution (Gibco). Cells were grown as monolayers in stationary T-flasks, using 0.2 ml of medium/cm^2 of culture surface. The cultures were maintained in an incubator at 37 ^oC under a 5% CO_2 atmosphere. For sub-culturing, cells were detached from T-flasks by addition of Cell Dissociation Solution (Sigma).

Plasmids

Plasmid vectors pUHD15-1, for constitutive expression of the tetracycline-transactivator (tTA); pUHD10-3, for tetracyline-regulated expression of any inserted gene; and pUGH16-3, for tetracycline regulated expression of β-galactosidase (*lac*Z) (Gossen and Bujard, 1992) were obtained from Dr. Hermann Bujard (University of Heidelberg). Plasmid vectors pBluescriptIIKS(+)-GnTIII, carrying the rat GnTIII cDNA (Nishikawa et al., 1992), and pSKV3-GnTV, carrying the human GnTVcDNA (Saito et al., 1995), were obtained from Dr. Naoyuki Taniguchi (University of Osaka, Japan). Plasmid vectors pSV2Neo and pPur, for constitutive expression of genes conferring resistance to neomycin and puromycin respectively, were purshased from Clontech. Plasmid pBluescriptIIKS(+) was purchased from Stratagene.

DNA manipulations

General DNA manipulations were carried out according to standard methods (Sambrook et al., 1989). DNA fragments were extracted from agarose gels using a DNA Extraction kit (Quiagen). DNA cycle sequencing was carried out by Heidi Ernst (Institute of Biotechnology, ETH-Zürich) using Thermo Sequenase (Amersham), fluorescent T7(-40) forward and reverse primers (MGW Biotech, Germany), and an automated DNA sequencer (Li Cor). DNA for transfection into mammalian cells was purified using a Midi DNA Purification kit (Qiagen).

Polymerase chain reactions (PCRs)

PCRs were carried out using HiFi Taq DNA polymerase from an Expand™ High Fidelity PCR kit (Boehringer Mannheim). The composition of the PCR mixes was defined according to instructions from the polymerase supplier. Oligonucleotide primers were synthesized by Microsynth (Switzerland).

Construction of glycosyltransferase expression vectors

C-myc epitope-encoding DNA (Nilsson et al., 1993) was added to the 3' end of the GnTIII cDNA by PCR amplification. The product was subcloned into pBluescriptIIKS(+) for sequencing, and finally subcloned into pUHD10-3 to generate plasmid vector pUHD10-3-GnTIIIm. The GnTV cDNA was directly subcloned into pUHD10-3 to generate plasmid vector pUHD10-3-GnTV.

The c-myc epitope-encoding sequence was added by a two-step sequential PCR approach. The same forward primer was used in both PCR steps. It hybridizes with the unique *NdeI* restriction site towards the downstream end of the GnTIII cDNA, and included a *BamH*I site for subcloning. Its sequence was 5' ctcgaa**ggat cc**cttcgccttc**catatgc** 3', with the restriction sites highlighted in bold characters. The first reverse primer hybridized with the GnTIII carboxy-terminus-encoding sequence and included the first 22

bases coding for the c-myc epitope tag. Its sequence was 5' cagagatcagcttttgttcc ggg**gccctccgttgtatccaactt** 3', with the part that hybridizes to rat GnTIII cDNA given in bold. The second reverse primer contained the entire human c-myc epitope-(EQKLISEEDL) encoding sequence separated from the GnTIII carboxy-terminus-encoding sequence by an additional proline codon, and included the stop codon plus an *Xba*I site for subcloning. Its sequence was 5' gtgtgt**tctaga**ctacaggtcttcttcagag-atcagcttttgttccgg 3', with the *Xba*I site shown in bold characters and the stop codon underlined.

PCRs were carried out as previously described, using 10 temperature cycles with an annealing temperature of 50 °C to obtain the first product, and 15 temperature cycles with an annealing temperature of 55 °C for the second product. The product of the first PCR was purified by agarose gel electrophoresis and gel extraction (Qiagen) and used as the template for the second PCR. The final PCR product was subcloned into pBluescriptIIKS+ and sequenced by cycle sequencing to check if any mutations had been introduced. The remaining upstream portion of the GnTIII cDNA was subcloned into this plasmid, then the reassembled, modified cDNA was subcloned into plasmid vector pUHD10-3 between the *EcoR*I and *Xba*I sites. To construct the other glycosyltransferase expression vector, GnTV cDNA was recovered from vector pSKV3-GnTV using *Xba*I and partial *EcoR*I digestions and subcloned directly into pUHD10-3.

SDS-PAGE and electroblotting to PVDF membranes

Cells dissociated from culture plates were harvested by centrifugation at 400 x g for 5 minutes and washed with 0.5 ml cold PBS. The cell pellet was resuspended in 30 µl of lysis buffer containing 50 mM MOPS-NaOH, 2% (v/v) Triton X-100, 1 mM $MgCl_2$, 1 mM dithiotreitol, 10% (w/v) sucrose and 150 mM NaCl and subjected to two 1-minute cycles of sonification in a Branson Sonifier (at 80-90% output). Between cycles, the cells were incubated on ice for 1 minute. The resulting lysate was incubated on ice for 15

minutes. Insoluble material was removed by centrifugation at 1000 x g for 10 minutes at 4 °C. Total protein content of the clarified lysate was determined with the BCA reagent (Pierce) following the microtiter plate protocol suggested by the supplier.

Between 5 and 20 µg of lysate was diluted two-fold with sample buffer containing 0.125 M Tris HCl, 4% (w/v) SDS, 20% (v/v) glycerol and 10% (v/v) 2-mercaptoethanol, pH 6.8 and boiled for 10 minutes. After cooling down, bromophenol blue was added to 0.01% (v/v), and the sample was subjected to electrophoresis through a 8.75% polyacrylamide gel under reducing conditions. At the end of the electrophoresis, the gel was equilibrated for 20 minutes in electroblotting buffer (25 mM Tris-HCl, 190 mM glycine, 20% (v/v) methanol, pH 8.8). The resolved proteins in the gel were electroblotted to a PVDF membrane (ImmobilonP^{SQ}, Millipore) for 3.5 h at 200mA, using the above buffer. The membranes were then probed with either antibody or lectins as described below.

Western and lectin blots

Non-specific binding sites on the PVDF membrane were blocked by overnight incubation at 4 °C with 0.5% (w/v) blocking reagent (Boehringer Mannheim) in Tris-buffered saline (TBS). Membranes were washed 2 to 3 times for 10 minutes with TBS containing 0.1% (v/v) Tween 20 (TBS-T).

For analysis with lectins, the TBS containing 1 mM $MgCl_2$, 1 mM $MnCl_2$ and 1 mM $CaCl_2$ (lectin buffer) was used for the third wash. Membranes were then incubated for 1 h at room temperature with a solution of biotinylated E-PHA (Oxford Glycosciences) at a concentration of 25 µg/ml in lectin buffer or L-PHA-digoxigenin (Boehringer Mannheim) at 50 µg/ml in the same buffer.

For western analysis, membranes were incubated for 1 h at room temperature with the anti-c-myc monoclonal antibody 9E10 (a gift from Prof. Dr. J. A. Robinson, University of Zürich) at a concentration of 2 µg/ml in TBS-T (GnTIII western blots) or with an anti-

GnTV rabbit polyclonal antibody (a gift from Dr. M. Pierce, University of Georgia, USA) diluted 1000-fold in TBS-T (GnTV western blots).

Membranes were washed three times with TBS-T and incubated for 1 h with either anti-biotin-alkaline phosphatase (Boehringer Mannheim) diluted 1000-fold in TBS-T (detection via E-PHA), anti-digoxigenin-alkaline phosphatase (Boehringer Mannheim) diluted 1000-fold in TBS-T (detection via L-PHA), anti-mouse IgG-horse radish peroxidase (Amersham) diluted 10000-fold in TBS-T (detection of GnTIII), or anti-rabbit IgG-horse radish peroxidase (Amersham) diluted 10000-fold in TBS-T (detection of GnTV). Membranes were subsequently washed three times with TBS-T. For analysis with lectins, the membrane was washed one more time with 0.1 M Tris, 0.05 M $MgCl_2$ and 0.1 M NaCl, pH 9.5 then incubated with the same buffer plus 0.375% (v/v) X-phosphate (Boehringer Mannheim) and 0.5% (v/v) NBT (Boehringer Mannheim). When color developed, the membranes were washed with water and air dried. For western analysis, bound antibody was detected using an enhanced chemiluminescence kit (ECL kit, Amersham) following the manufacturer's instructions.

Transfection of DNA into CHO cells

DNA, either complexed with cationic liposomes (Lipofectamine^{TM}, Gibco), or co-precipitated with hydroxyapatite (calcium phosphate DNA transfection method) was transfected into CHO cells. Transfections using Lipofectamine^{TM} were carried out according to the manufacturer's instructions. Calcium phosphate DNA transfections were carried out using an efficient version of this method (Jordan and Wurm, 1996) with some additional modifications. Briefly, 24 h before transfection cells were seeded to approximately 40% confluency in a T25 flask and incubated at 37 ^{o}C overnight. The next day the medium was replaced with fresh culture medium 1 h before transfection. For each flask with cells to be transfected, a solution of DNA, $CaCl_2$ and water was prepared by mixing 15 µg of total plasmid vector DNA, 75 µl of a 1 M solution of $CaCl_2$, and adding

water to a final volume of 150 µl. To this solution, 150 µl of a 50 mM HEPES, 280 mM NaCl, 1.5 mM Na_2HPO_4 solution at pH 7.05 was added, mixed by vortexing for 5 s, and left to stand at room temperature for 25 s. This brief incubation led to the formation of very fine DNA/hydroxyapatite co-precipitates, which were then diluted with 5 ml of culture medium containing 2% (v/v) fetal calf serum (FCS). The resulting suspension was added to the cells in the T25 flask in place of the existing culture medium, and the cells were incubated for 5 h at 37 °C. The medium was then replaced with 5 ml of a 15% (v/v) glycerol solution in culture medium containing 2% (v/v) FCS and the cells were left for 30 s at room temperature, before a final medium exchange to 5 ml of culture medium containing 10% (v/v) FCS. The final medium was used to wash the cells prior to the last medium exchange. The cells were then incubated at 37 °C until assayed or transferred to other culture flasks or dishes.

Harvesting CHO cell clones by an agarose overlay method

Low density cultures of drug resistant clones were grown, yielding widely distanced clones attached to the surface of the culture dish. The positions of the clones were marked on the outside surface of the dish. The culture medium was then replaced with a sterile solution of 1% (w/v) Agarplaque™ (Pharmingen) in phosphate buffered saline (PBS) at 37 °C, which was then left to harden at room temperature for approximately 20 minutes. A small hole was made in the hardened gel at the position of each clone to be picked, by using a cut pipette tip placed on a 0-200 µl pippete (Gilson), applying suction slowly and simultaneously removing the resulting agar plug. 5 µl of Cell Dissocation solution (Sigma) at 37 °C was added to each hole and after 5 minutes the clones were resuspended using a 0-20 µl pipette (Gilson). The resuspended cells were transferred to wells of a 96-well culture plate (Falcon) containing 200 µl of cell culture medium supplemented with 10% (v/v) FCS plus the drug used for selection of stable transfectants and then incubated overnight at 37 °C. The next day the medium was replaced with fresh culture medium

containing the drug for selection and incubation was continued at 37 °C until the clones had grown enough to be transferred to larger culture plates.

Generation of CHO cells expressing the tetracycline-transactivator (tTA)

CHO cells were co-transfected with pUHD15-1, a vector for constitutive expression of the tTA gene, and pSV2Neo, a vector for constitutive expression of a neomycin resistance gene. Stable, drug-resistant clones were selected and screened for adequate levels of tTA expression. Tetracycline-regulated expression of a β-galactosidase gene was used as a marker for tTA expression.

One well of a 6-well culture plate (Falcon) was seeded with CHO cells to approximately 30-40% confluency, incubated for 24 h at 37 °C, then the cells were co-transfected with vectors pUHD15-1 and pSV2Neo using a lipofection method. The DNA used for transfection was purified over anion exchange columns of a Midi DNA Purification kit (Qiagen) and co-transfected in a molar ratio of 15:1 of pUHD15-1:pSV2Neo. The total amount of DNA used per transfection was 6 µg. Two days after transfection, the cells were transferred to a T75 flask, and Gentamycin (G418, Boehringer Mannheim) was added to the culture medium at a concentration of 400 µg/ml. The medium was replaced every three days for two weeks until G418 resistant clones had grown. The cells were resuspended and individual cells were transferred to wells of a 96-well cell culture plate (Falcon) using a cell sorter (FACS Star Plus, Beckton Dickenson, operated by Eva Niederer, Zentrallabor für Zellsortierung, ETH-Zürich).

Clones were grown until three wells of a six-well plate could be seeded to approximately 30% confluency. A lipofection method was used to transfect the cells in two wells per clone with the β-galactosidase expression vector, pUHG16-3. The cells in the third well was kept as a stock. After transfection, 1 µg/ml tetracycline (final concentration) was added to one of each pair of transfectants, and the cells were incubated for 72 h at 37 °C. The intracellular level of β-galactosidase activity in each transfectant was

then measured using ONPG (Sigma) as a substrate (Sambrook et al., 1989). The clone with the highest level of β-galactosidase acitivity in the absence of tetracycline, named CHO-tTA, was chosen for futher work.

Generation of CHO cells with stable, tetracycline-regulated expression of GnTIII and GnTV

Two T-25 flasks were seeded with CHO-tTA cells to approximately 40% confluency and incubated at 37 °C overnight. The next day, the cells in one flask were co-transfected with vectors pUHD10-3-GnTIIIm and pPur, and in the other with vectors pUHD10-3-GnTV and pPur, using the calcium phosphate transfection method. The DNA used for transfections was linearized, pUHD10-3-based expression vectors with *Pvu*I and pPur with *Pvu*II, then purified over anion exchange columns of a Midi DNA Purification kit (Qiagen). The linearized vectors were co-transfected in a molar ratio of 15:1 of pUDH10-3-GnTIIIm:pPur or pUDH10-3-GnTV:pPur, and the total amount of DNA used per transfection was 15 μg.

Immediately after transfection, tetracycline was added to the culture medium to a concentration of 2 μg/ml. One day after transfection the cells from each flask were transferred to two culture dishes with a diameter of 15 cm each (Falcon), keeping tetracycline at 2 μg/ml, and one day after transfer, puromycin (Clontech) was added to the culture medium to a concentration of 7.5 μg/ml. The medium was replaced every three days until puromycin resistant clones of adequate size for picking had grown. Thirty individual clones were picked from each pair of culture dishes, using the agar-overlay method, and transferred to a 96-well culture plate. The clones were grown in the presence of tetracycline, until one well of a 24-well plate, and two wells of a six-well plate could be seeded to approximately 10% confluency for several clones. The cells in the 24-well plate were kept as stocks of each clone.

Cells in one of each pair of wells from the 6-well plates were cultured in the absence of tetracycline for 4 days, while the other cells were cultured in the presence of 2μg/ml of tetracycline. After this incubation period, the approximate level of confluency was estimated and the cells harvested, lysed, and analysed for tetracycline-regulated expression of the respective glycosyltransferase using the SDS-PAGE and western blot procedures described above. Lectin binding to cellular glycoproteins was used to visualize the extent of modification by the heterologous glycosyltransferase. Clones with high levels of expression in the absence of tetracycline and low levels of expression in the presence of tetracycline were selected, expanded, and stocks were frozen. Clonal purity was ensured by subcloning from a single clone for each glycosyltransferase by limited dilution, giving clones CHO-tet-GnTIIIm and CHO-tet-GnTV respectively, which were used for further work.

Indirect immunofluorescence and confocal light microscopy

CHO-tet-GnTIIIm and CHO-tet-GnTV cells were seeded in 60 mm-diameter culture dishes (Falcon) to approximately 5-10% confluency, and grown for 48 h at 37 °C with different concentrations of tetracycline per dish in the range of 0 - 2000 ng/ml. The culture medium was completely removed by aspiration and the dishes were then washed three times with PBS. The cells were then fixed by incubation with fresh 2% (w/v) paraformaldehyde in PBS for 15 minutes at room temperature. Afterwards, the cells were washed with PBS, incubated for 5 minutes with 0.1 M glycine in PBS for quenching, and washed again with PBS. The cells were then permeabilized by incubating for 15 minutes in PBS containing 0.1% (v/v) Triton X-100 and, as a blocking agent, 2% (w/v) bovine serum albumin (PTB buffer). This solution was replaced with the primary antibody dissolved in PTB buffer (9E10 antibody at 20 μg/ml for GnTIII detection via the c-myc epitope tag, and anti-GnTV polyclonal antibody diluted 100-fold for GnTV detection), and the cells were incubated for 1 h.

The cells were washed three times with PTB buffer and incubated for 45 minutes with the secondary antibody solution containing either anti mouse IgG-Texas Red (Vector Laboratories, USA) for detection of GnTIII or anti rabbit IgG-Texas Red (Vector Laboratories, USA) for detection of GnTV. Both antibodies were diluted 150-fold in PTB buffer. The cells were washed three times with PTB buffer and embedded in 90% glycerol, pH 9.0. Cells were visualized using a MRC-600 Laser scanning confocal imaging system (Bio-Rad) operated by Peter David (ETH-Zürich). Images were processed on a Silicon Graphics Workstation using IMARIS software (Bitplane AG, Switzerland).

Immunoelectron microscopy

CHO cell fixation, sample preparation, ultrathin sectioning, immunolabelling, and visualization were performed as follows (Nilsson et al., 1993). CHO cells were fixed for 3 h at room temperature using 2% (w/v) paraformaldehyde and 0.2% (v/v) gluteraldehyde in 0.2 M sodium phosphate buffer, pH 7.4, washed three times with PBS, incubated for 10 minutes with 50 mM NH_4Cl in PBS, and washed once again in PBS. The fixed cells were scraped with a rubber scraper, pelleted by centrifugation, resuspended in 10% gelatin in PBS, and pelleted again by centrifugation. Excess gelatin was removed and the embedded pellet was infiltrated overnight at 4 °C with a 2.1 M sucrose solution in PBS. Small fragments of the infiltrated pellet were mounted on aluminum studs and flash frozen in liquid nitrogen. 100-nm thick sections were cut at -90 °C in a microtome with a cryo-attachment and transferred onto formvar- and carbon-coated 100-mesh grids. Grids were then transferred to a 35-mm dish with PBS.

The following steps were performed at room temperature and involved carefully transferring grids onto the surface of drops of different solutions placed over a sheet of parafilm. Sections were blocked on a 300 µl drop of 0.8% (w/v) bovine serum albumin, 1% (w/v) fish skin gelatin in PBS (blocking buffer) for 30 minutes and then each grid was

placed for 30 minutes on a 8 µl drop of anti-myc rabbit polyclonal antibody (a gift from Dr. Tommy Nilsson, EMBL-Heidelberg) diluted 1:3 in blocking buffer. After incubating with the primary antibody, the sections were washed four times by placing the grids on 300 µl drops of PBS for 5 minutes each time. Washed sections were incubated for 15 minutes on a 100 µl drop of anti-rabbit IgG conjugated to 10 nm-gold particles (British Biocell, Cardiff, UK) diluted 100-fold in blocking buffer. After incubation with the secondary antibody, the sections were washed four times with PBS and five times with triple distilled water.

Sections were embedded and positively stained by incubation on 2% methyl cellulose containing 0.3% uranyl acetate drops on ice and air dried. The contrasted, dried sections were then examined at 80 kV in a Zeiss EM10 electron microscope. Images magnified 31,500-fold were photographed.

3.4 Results and Discussion

Establishment of CHO cell lines with tetracycline-regulated overexpression of glycosyltransferases

The strategy used for establishment of glycosyltransferase overexpressing cell lines consisted of first generating an intermediate CHO cell line constitutively expressing the tetracycline-controlled transactivator (tTA) at an adequate level for the system to work (Yin et al., 1996). This level had to be high enough to activate high levels of transcription, in the absence of tetracycline, from the minimal promoter upstream of the glycosyltransferase genes. CHO cells were co-transfected with a vector for constitutive expression for tTA, driven by the human cytomegalovirus (hCMV) promoter/enhancer, and a vector for expression of a neomycin-resistance (Neo^R) gene. An excess of the tTA-expression vector was used and neomycin-resistant clones were isolated.

In mammalian cells, co-transfected DNA integrates adjacently at random locations within the chromosomes, and expression depends to a large extent on the site of integration and also on the number of copies of intact expression cassettes. A mixed population of clones with different expression levels of the transfected genes is generated (Yin et al., 1996). Selection for neomycin resistance merely selects for integration of an intact Neo^R expression cassette, while the use of an excess of the tTA-expression vector increases the probability of finding clones with good expression of tTA. The mixed population of clones has to be screened using a functional assay for tTA expression (Gossen and Bujard, 1992; Yin et al., 1996). This was done by transfection of each clone with a second vector harboring a reporter gene, *lac*Z, under the control of the tet-promoter and screening for tetracycline-regulated (tet-regulated), transient expression (i.e., one to three days after transfection) of β-galactosidase activity. CHOt17, which showed the highest level of tet-regulated β-galactosidase activity among 20 screened clones, was selected for further work.

CHOt17 cells were tested for tet-regulated expression of GnTIII by transfecting the cells with vector pUHD10-3-GnTIIIm and comparing the relative levels of GnTIII after incubation of the cells in the presence and absence of tetracycline for 36 h. GnTIII levels were compared by western blot analysis, using a monoclonal antibody (9E10) which recognizes the c-myc peptide epitope tag at the carboxy-terminus of GnTIII. The tag had been introduced through a modification of the glycosyltransferase gene using PCR amplification. Various reports have demonstrated addition of peptide epitope tags to the carboxy-termini of glycosyltransferases, a group of enzymes sharing the same topology, without disruption of localization or activity (Nilsson et al., 1993; Rabouille et al., 1995). Figure 2 shows that in clone CHOt17 GnTIII accumulation is significantly higher in the absence than in the presence of tetracycline. An additional clone, CHOt2, which gave weaker activation of transcription in the β-galactosidase activity assay, was tested in parallel (Fig. 2). GnTIII and β-galactosidase expression levels follow the same pattern of tetracycline-regulation for both of these clones. The range of tetracycline concentrations where GnTIII expression can be quantitatively controlled was found to be from 0 to 100 ng/ml (Fig. 3). This result agrees with previous research using different cell lines and genes (Yin et al., 1996).

To generate a stable cell line with tet-regulated expression of GnTIII, CHOt17 cells were co-transfected with vector pUHD10-3-GnTIIIm and vector, pPUR, for expression of a puromycin resistance gene. In parallel, CHOt17 cells were co-transfected with pUHD10-3-GnTV and pPUR vectors to generate an analogous cell line for this other glycosyltransferase. A highly efficient calcium phosphate transfection method was used and the DNA was linearized at unique restriction sites outside the eucaryotic expression cassettes, to decrease the probability of disrupting these upon integration. By using a host in which the levels of tTA expressed had first been proven to be adequate, the probability of finding clones with high expression of the glycosyltransferases in the absence of tetracycline is increased.

Stable integrants were selected by puromycin resistance, keeping tetracycline in the medium throughout clone selection to mantain glycosyltransferase expression at basal levels. For each glycosyltransferase, 16 puromycin resistant clones were grown in the presence and absence of tetracycline, and 8 of each were analyzed by western blot analysis (Fig. 4). The majority of the clones showed good regulation of glycosyltransferase expression. One of the GnTIII-expressing clones showed a relatively high basal level in the presence of tetracycline (Fig. 4 B, clone 3), which suggests integration of the expression cassete close to an endogenous CHO-cell enhancer; while two puromycin-resistant clones showed no expression of GnTIII in the absence of tetracycline (Fig. 4 B, clones 6 and 8). Among the clones showing good regulation of expression, different maximal levels of glycosyltransferase were observed. This may be due to variations in the site of integration or number of copies integrated. Activity of the glycosyltransferases was verified by E-PHA and L-PHA lectin binding to endogenous cellular glycoproteins derived from various clones grown in the presence and absence of tetracycline (Fig. 5). Lectins are proteins which bind to specific oligosaccharide structures. E-PHA lectin binds to bisected oligosaccharides, the products of GnTIII-catalyzed reactions, and L-PHA binds to tri-and tetra-antennary oligosaccharides produced by GnTV-catalyzed reactions (Merkle and Cummings, 1987). For each glycosyltransferase, a clone with high expression in the absence, but with undetectable expression in the presence, of tetracycline (clone 6, Fig. 4 A, CHO-tet-GnTV, and clone 4, Fig. 4 B, CHO-tet-GnTIIIm) was selected for further work.

Inhibition of growth due to glycosyltransferase overexpression

During screening of GnTIII- and GnTV-expressing clones in the absence of tetracycline, approximately half of each set of clones showed a strong inhibition of growth. The extent of growth-inhibition varied among clones, and comparison with expression levels estimated from western blot analysis (Fig. 4) suggested a correlation between the degree of growth-inhibition and glycosyltransferase overexpression. This correlation was firmly established by growing the final clones, CHO-tet-GnTIIIm and CHO-tet-GnTV, in different concentrations of tetracycline. A strong inhibition of growth was evident after two days of culture at low levels of tetracycline (Fig. 6). Growth-inhibited cells displayed a small, rounded morphology instead of the typical extended shape of adherent CHO cells. After a few days, significant cell death was apparent from the morphology of the growth-inhibited cells.

Growth-inhibition due to glycosyltransferase overexpression has not hitherto been reported in the literature, probably due to the widespread use of constitutive promoters. Those clones giving constitutive expression of a glycosyltransferase at growth-inhibiting levels would be lost during the selection procedure. This was avoided here by keeping tetracycline in the medium, i.e., basal expression levels, throughout selection. Prior to selection, the frequency of clones capable of expressing glycosyltransferases to growth-inhibiting levels using traditional mammalian vectors based on the constitutive hCMV promoter/enhancer would be expected to be lower. This is due to the fact that, for any given gene, the pUHD10-3 vector in CHO cell lines selected for high constitutive levels of tTA gives significantly higher expression levels than constitutive hCMV promoter/enhancer-based vectors, as observed by others (Yin et al., 1996) and us (data not shown).

Inhibition of cell growth could be due to a direct effect of overexpression of membrane-anchored, Golgi-resident glycosyltransferases independent of their *in vivo* catalytic activity, e.g., via misfolding in the endoplasmic reticulum (ER) causing saturation of elements

which assist protein folding in the ER. This could possibly affect the folding and secretion of other essential cellular proteins. Alternatively, inhibition of growth could be related to increased *in vivo* activity of the glycosyltransferase leading to a change of the glycosylation pattern, in a function-disrupting fashion, of a set of endogenous glycoproteins necessary for growth under standard *in vitro* culture conditions.

Independent of the underlying mechanism, the growth-inhibition effect has two consequences for engineering the glycosylation of animal cells. First, it implies that co-transfection of constitutive glycosyltransferase expression vectors together with vectors for the target glycoprotein product is a poor strategy. Other ways of linking expression of these two classes of proteins, e.g., through the use of multiple constitutive promoters of similar strength or use of multicistronic, constitutive expression vectors, should also be avoided. In these cases, clones with very high, constitutive expression of the target glycoprotein, a prerequisite for an economical bioprocess, would also have high expression of the glycosyltransferase and would be eliminated during the selection process. Linked, inducible expression could also be problematic for industrial bioprocesses, since the viability of the growth-arrested cells would be compromised by the overexpression of the glycosyltransferase.

The second consequence is that it imposes an upper limit on glycosyltransferase overexpression for glycosylation engineering approaches. Clearly, the conversions of many glycosyltransferase-catalyzed reactions in the cell, at the endogenous levels of glycosyltransferases, are very high for several glycosylation sites. However, glycosylation sites where the oligosaccharides are somewhat inaccesible or are stabilized in unfavorable conformations for specific glycosyltranferases also exist. For example, it has been observed that addition of bisecting GlcNAc is more restricted to the oligosaccharides attached to the Fc region than to those located on the variable regions of human IgG antibodies (Savvidou et al., 1984). Glycosylation engineering of these restricted sites could be affected by such a limit on glycosyltransferase expression. Although this would imply

aiming for an "unnatural" distribution of glycoforms, these could be of benefit for special therapeutic applications of glycoproteins.

It would be useful to determine if the growth-inhibiting effect is additive. If so, the limit could become more important for glycosylation engineering approaches involving several glycosyltransferases.

Localization of GnTIII in CHO cells

Indirect immunofluorescence of CHO-tet-GnTIII cells with anti-myc (9E10) antibody and a Texas-Red conjugated secondary antibody, visualized using confocal microscopy, showed an asymmetrical, perinuclear staining pattern typical of Golgi-resident proteins (Fig. 7). At high levels of expression, the pattern was very intense, but still perinuclear and asymmetrical, though the cell morphology was round and small. CHO-tet-GnTV cells labelled with an anti-GnTV polyclonal antibody showed a similar pattern (data not shown).

The spatial distribution of GnTIII within the Golgi complex has not yet been reported in the literature. Here it was examined in CHO-tet-GnTIIIm cells grown at 40 ng/ml of tetracycline for 4 to 5 days, where no growth inhibition was observed. This was done by immunoelectron microscopy using an anti-myc polyclonal antibody and a gold particle-conjugated anti-rabbit secondary antibody (Fig. 8). The Golgi distribution of myc-tagged rat GnTIII in CHO-tet-GnTIIIm cells grown under these conditions was quite polarized, the protein being found mainly in cisternal compartments.

The Golgi stack in CHO cells consists of flattened cisternal elements increasing in length from the *cis* to the *trans* side. After the *trans*-cisterna, the next Golgi region is the *trans*-Golgi network, characterized by the presence of numerous vesicles and tubules (Russo et al., 1992). In some cell sections, the Golgi may appear horseshoe shaped, and in these cases the *trans*-region is normally in the middle with the *cis* regions at the top and bottom (Russo et al., 1992). From morphological appearance it seems that GnTIII in these cells has a spatial distribution polarized towards the *trans*-side (Fig. 8).

The qualitative result obtained here for GnTIII distribution suggests a peak of GnTIII with a maximum more to the *trans*-side than those reported for GnTI or ManII. GnTIII localized in this way would show a more significant overlap with GalT than GnTI and ManII show (see Physical Model section in Chapter II). Overlap with GalT could have an impact on attempts to maximize bisected oligosaccharides through glycosylation engineering, since GalT can compete with GnTIII for bi-antennary oligosaccharide substrates (see Fig. 6 in Chapter II). In fact, it has been reported recently that a 50% reduction of GalT activity in a human B cell line, achieved through disruption of one copy of the GalT gene, increased the level of bisected oligosaccharides on a secreted glycoprotein from approximately 50 to 90% (Omae et al., 1997).

Since GnTI and ManII overlap to some extent with GalT in the trans-Golgi cisterna (Rabouille et al., 1995), they would overlap to a similar or even higher extent with GnTIII if distributed as observed here. High level overexpression of GnTIII with such a distribution could still lead to the synthesis of bisected hybrid oligosaccharides (see Chapter II). The qualitative spatial distribution is a preliminary result which requires corroboration by a statistical analysis of many more cell sections. Ideally, statistical immunogold quantitation relative to an established marker (such as GalT) should be done (Rabouille et al., 1995).

3.5 Acknowledgements

This research was supported by the Swiss Priority Program in Biotechnology (SPP BioTech). We thank Dr. Tommy Nilsson and his group (particularly Sabine Rötgger) at EMBL-Heidelberg for providing instruction and the resources to carry out the immuno-electron microscopy work; Peter David for operation of the confocal imaging system; Dr. Naoyuki Taniguchi for providing us with the rat GnTIII and human GnTV cDNAs; and Dr. Michael Pierce, for anti-GnTV polyclonal antibodies.

3.6 References

Bailey, J. E. 1991. Toward a science of metabolic engineering. Science **252:** 1668- 1675.

Gossen, M. and Bujard, H. 1992. Tight control of gene expression in mammalian cells by tetracycline- responsive promoters. Proc. Natl. Acad. Sci. USA **89:** 5547- 5551.

Jordan, M. and Wurm, F. M. 1996. Transfecting mammalian cells: Optimization of critical parameters affecting calcium-phosphate precipitate formation. Nucl. Acids Res.**24:** 596-601.

Merkle, R. K. and Cummings, R. D. 1987. Lectin affinity chromatography of glycopeptides. Methods Enzymol. **138:** 232-259.

Nilsson, T., Pypaert, M., Hoe, M. H., et al. 1993. Overlapping distribution of two glycosyltransferases in the Golgi apparatus of HeLa cells. J. Cell Biol. **120:** 5-13.

Nishikawa, A., Ihara, Y., Htakeyama, M., et al. 1992. Purification, cDNA cloning, and expression of UDP-N-acetylglucosamine:β-D-mannoside β-1,4N-acetylglucosaminyl-transferase III from rat kidney. J. Biol. Chem. **267:** 18199-18204.

Omae, F., Yamada, K., Abe, R., et al. 1997. Expression of glycosyltransferases. Glycoconjugate J. **14:** S45.

Rabouille, C., Hui, N., Hunte, F., et al. 1995. Mapping the distribution of Golgi enzymes involved in the construction of complex oligosaccharides. J. Cell Science **108:** 1617- 1627.

Russo, R. N., Shaper, N. L., Taatjes, D. J., et al. 1992. Beta-1,4-Galactosyltransferase: A short NH-2-terminal fragment that includes the cytoplasmic and transmembrane domain is sufficient for Golgi retention. J. Biol. Chem. **267:** 9241-9247.

Saito, H., Gu, J., Nishikawa, A., et al. 1995. Organization of the human N-acetylglucosaminyltransferase V gene. Eur. J. Biochem. **233:** 18-26.

Sambrook, J., Fritsch, E. F. and Maniatis, T. 1989. Molecular cloning: A laboratory manual. Cold Spring Harbor Laboratory Press, Cold Spring Harbor.

Savvidou, G., Klein, M., Grey, A. A., et al. 1984. Possible role for peptide-oligosaccharide interactions in differential oligosaccharide processing at asparagine-107 of the light chain and asparagine-297 of the heavy chain in a monoclonal IgG1kappa. Biochemistry **23:** 3736-3740.

Yin, D. X., Zhu, L. and Schimke, R. T. 1996. Tetracycline-controlled gene expression system achieves high-level and quantitative control of gene expression. Anal. Biochem. **235:** 195-201.

3.7 Figures

Fig. 1. Schematic representation of the tetracycline-regulated expression of a glycosyltransferase. The glycosyltransferase gene is placed under the control of a minimal human cytomegalovirus (hCMVmin) promoter and transfected into cells which constitutively express a chimeric, tetracycline-controlled transactivator (tTA). In the absence of tetracycline, tTA can bind, via its tetracycline repressor domain, to tetracycline operator DNA (tetO) placed upstream of the hCMVmin promoter. The other domain of tTA, the C-terminal portion of a herpes simplex virus transactivator protein (VP16), can activate transcription of the glycosyltransferase gene from the hCMVmin promoter when tTA is bound to tetO DNA. Tetracycline added to the medium binds to the repressor domain of tTA and prevents binding of the repressor to tetO DNA, thereby eliminating transactivation.

Fig. 2. Western blot analysis of tetracycline-regulated expression of GnTIII in two different tTA-producing CHO clones. CHOt2 (lanes A and B) and CHOt17 (lanes C and D) cells were transfected with the pUDH10-3-GnTIIIm expression vector and cultured for 36 h in the absence (lanes A and C) or presence of tetracycline, at a concentration of 400 ng/ml (lanes B and D). Cell lysates were then preprared for western blot analysis probing with an antibody (9E10), which recognizes specifically the c-myc tag added to GnTIII at its carboxy-terminus.

Fig. 3. Determination of the range of tetracycline concentrations where myc-tagged GnTIII expression can be controlled. CHOt17 cells were transfected with the pUDH10-3-GnTIIIm expression vector and then cultured for 48 h in the presence of the indicated concentrations of tetracycline. GnTIII levels in cell lysates from these cultures were

compared using western blot analysis. GnTIII was detected via the c-myc tag using 9E10 antibody.

Fig. 4. Screening of CHO clones for stable, tetracycline-regulated expression of GnTV (A) or myc-tagged GnTIII (B) glycosyltransferases by western blot analysis. CHOt17 cells were co-transfected with a vector for expression of puromycin resistance (pPUR) and either pUHD10-3-GnTV (A) or pUDH10-3-GnTIIIm (B) and stable CHO clones were selected for resistance to puromycin (7.5 μg/ml), in the presence of tetracycline (2 μg/ml). Eight clones (1-8) for each glycosyltransferase were cultured for 48 h in the absence or presence (+) of tetracycline (2 μg/ml) and analysed by western blot using either an anti-GnTV antibody (A) or an anti-myc (9E10) antibody (B).

Fig. 5. Verification of activity of heterologous GnTV (A) and GnTIII (B) glycosyltransferaseas *in vivo* by lectin blot analysis. Cellular glycoproteins from various stable clones (numbered as in Fig. 4), cultured in the absence or presence (+) of tetracycline (2 μg/ml), were resolved by SDS-PAGE, blotted to a membrane, and probed with either L-PHA (A) or E-PHA (B) lectins. These lectins bind with higher affinity to the oligosaccharide products of reactions catalyzed by GnTV and GnTIII, respectively, than to the oligosaccharide substrates of these reactions. A molecular weight marker (MWM) was run in parallel. A comparison of lectin blots in A and B indicates a broader range of substrates, among the endogenous CHO cell glycoproteins, for GnTIII (B) than for GnTV (A).

Fig. 6. Inhibition of cell growth upon glycosyltransferase overexpression. CHO-tet-GnTIIIm cells were seeded to 5 - 10% confluency and cultured in the absence (A and B) or presence (C and D) of tetracycline. Cultures were photographed 45 (A and C) and 85 (B and D) hours after seeding.

Fig. 7. Immunolocalization of myc-tagged GnTIII visualized by confocal microscopy. CHO-tet-GnTIIIm cells, cultured in the presence of 3 (A) or 50 (B) ng/ml of tetracycline, were fixed, permeabilized, and labeled with anti-myc 9E10 antibody. Labelled cells were subsequently incubated with Texas-Red-secondary antibody conjugates and inspected by confocal microscopy. The observed perinuclear, assymetrical staining pattern is typical for Golgi-localized proteins.

Fig. 8. Golgi distribution of myc-tagged GnTIII by immuno-electron microscopy. Thin frozen sections of CHO-tet-GnTIIIm cells, which had been cultured in the presence of 40 ng/ml of tetracycline, were labelled with an anti-myc polyclonal antibody followed with a secondary antibody coupled to 10 nm-diameter gold particles. Labelled sections were embeded and positively stained with methylcellulose containing uranyl acetate, and examined in an electron microscope. Under these conditions, biological membranes enclosing cellular compartments appear as light lines against a darker background, while the localized gold particles show as very dark small circles. A rather polarized GnTIII-distribution was observed in both extended- (A) and horse shoe-shaped (B) Golgi sections.

Figure 1.

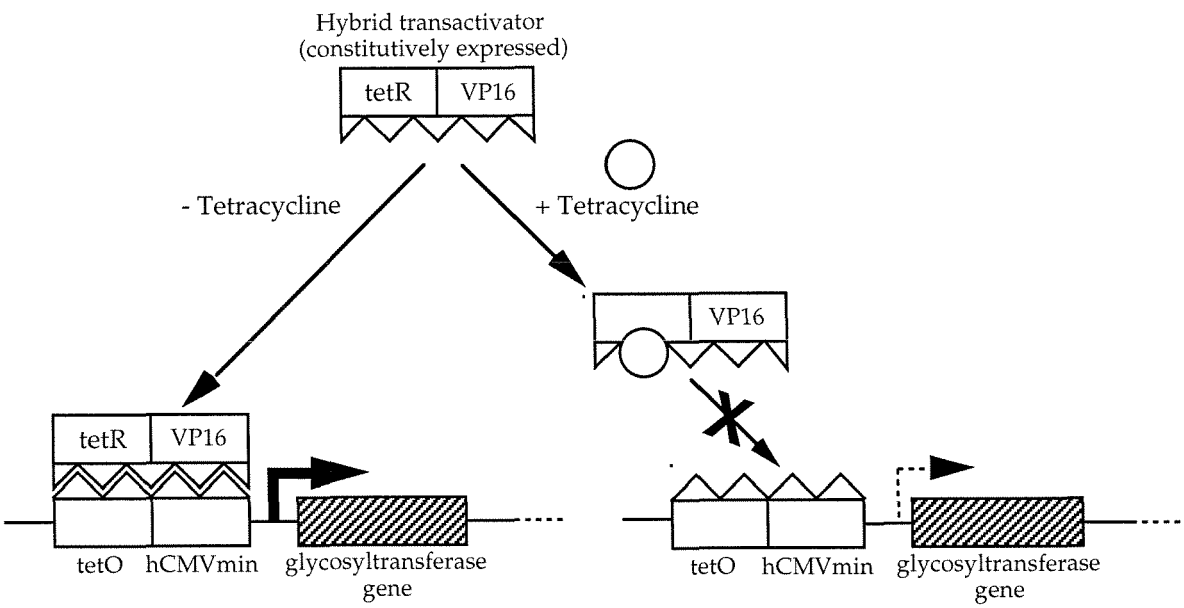
Hybrid transactivator
(constitutively expressed)
tetR
VP16
- Tetracycline
+ Tetracycline
VP16
tetR
VP16
tetO
hCMVmin
glycosyltransferase
gene
tetO
hCMVmin
glycosyltransferase
gene

Figure 2.

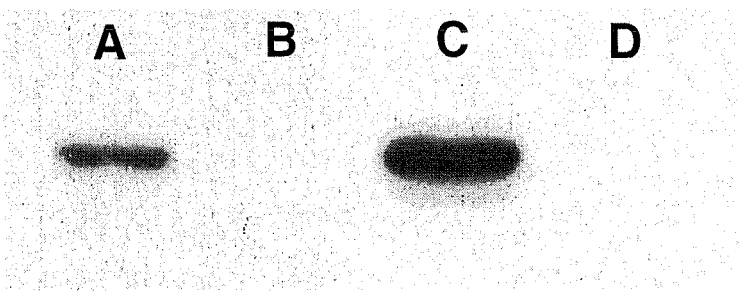

Figure 3.

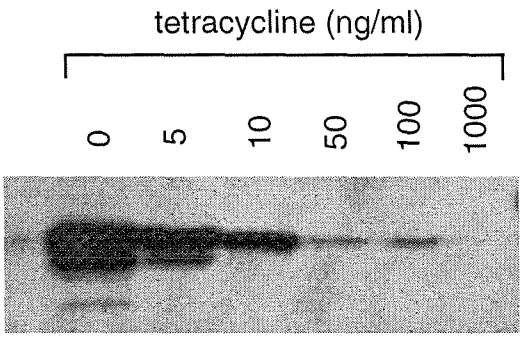

Figure 4.

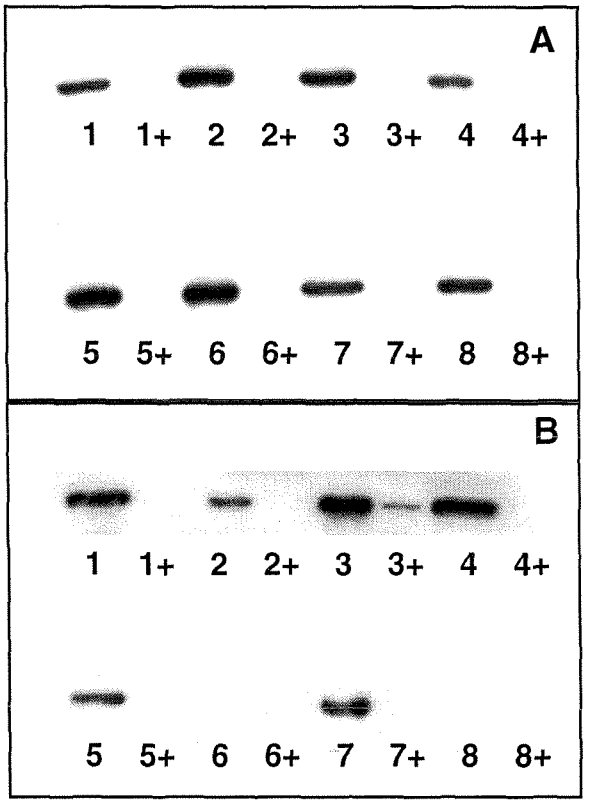

Figure 5.

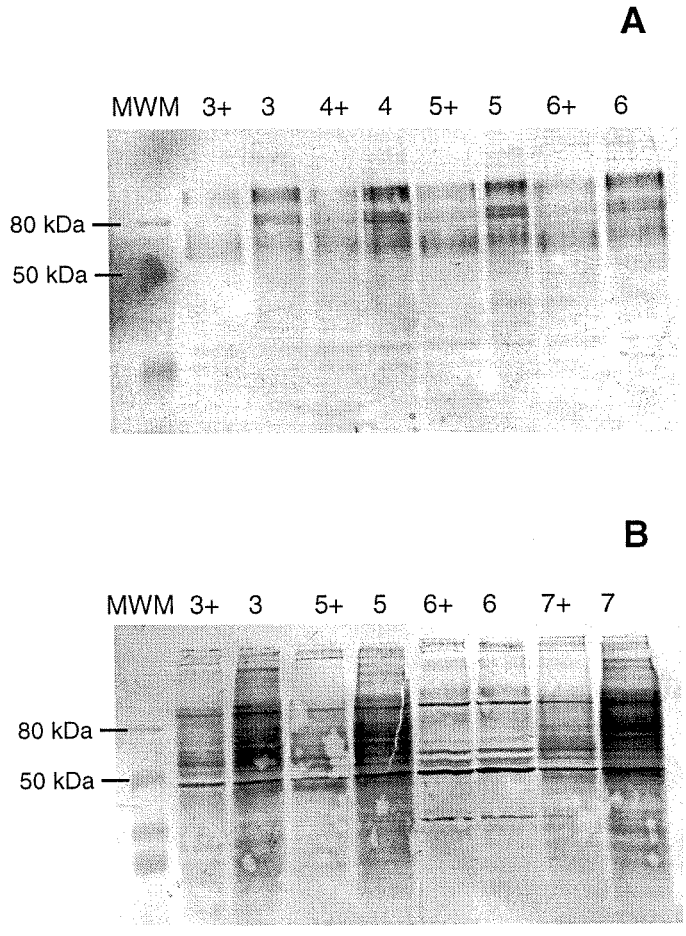

Figure 6.

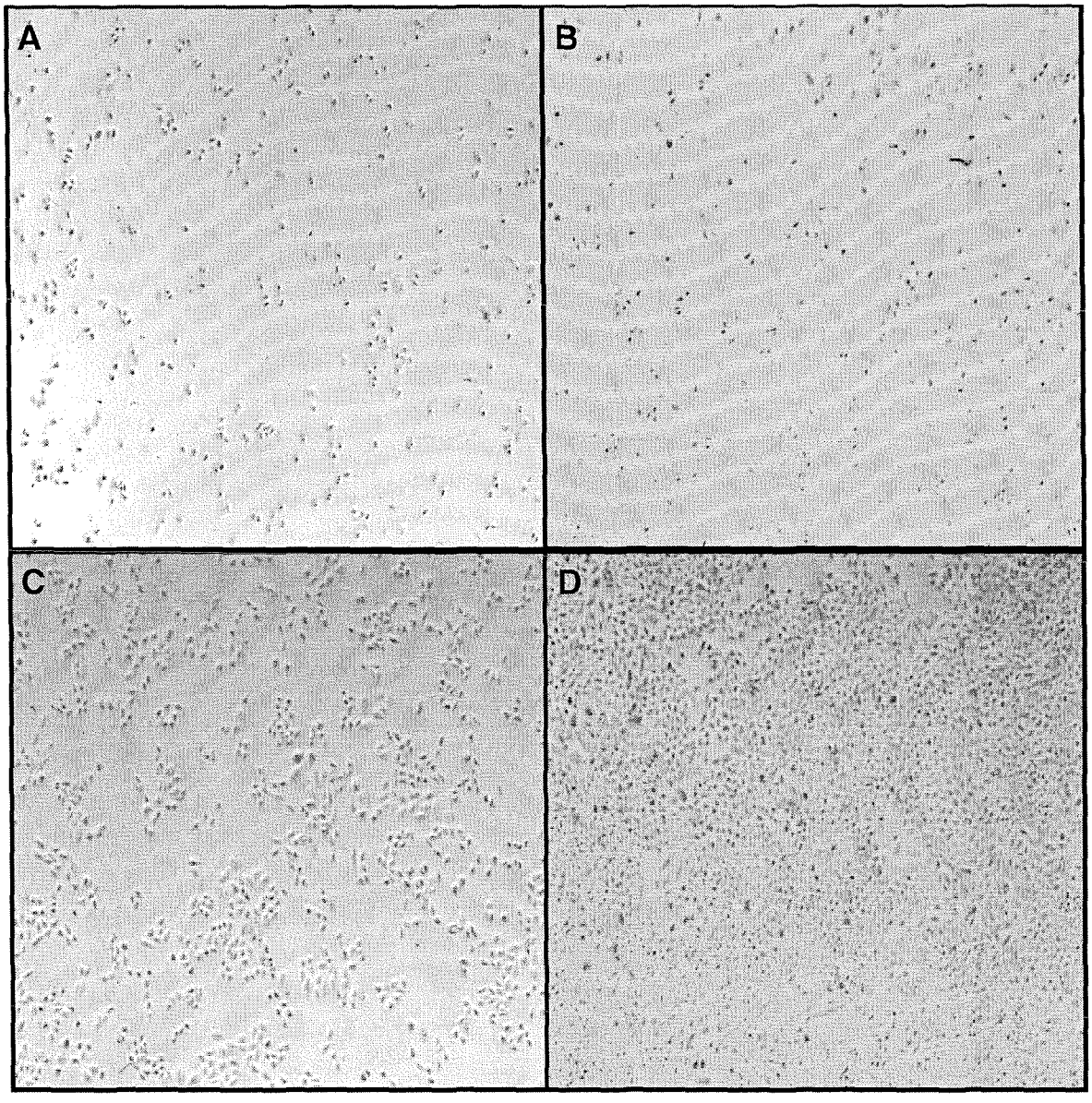

Figure 7. A

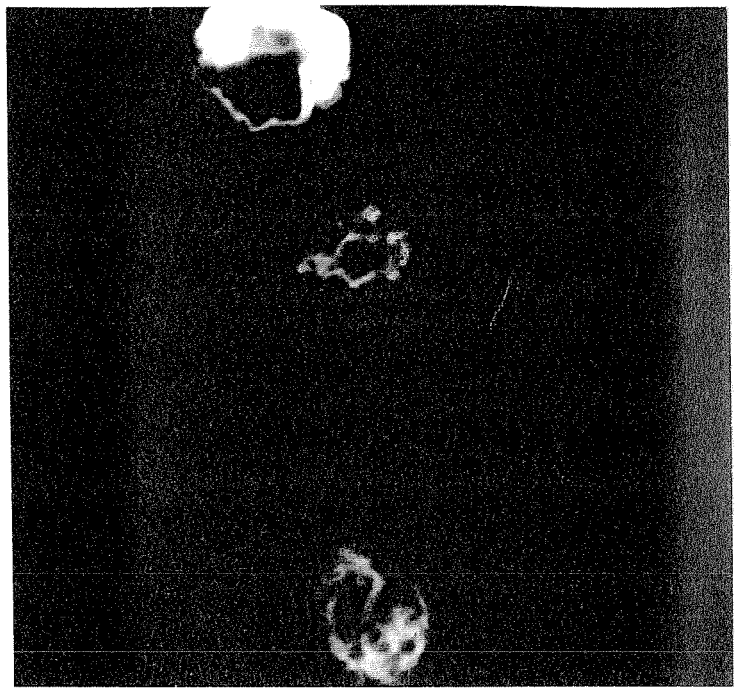

Figure 7. B

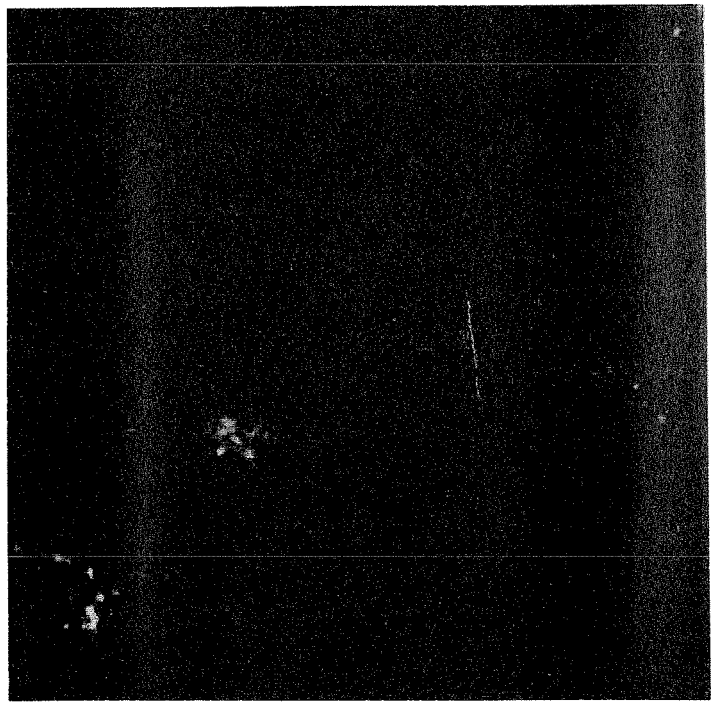

Figure 8. A

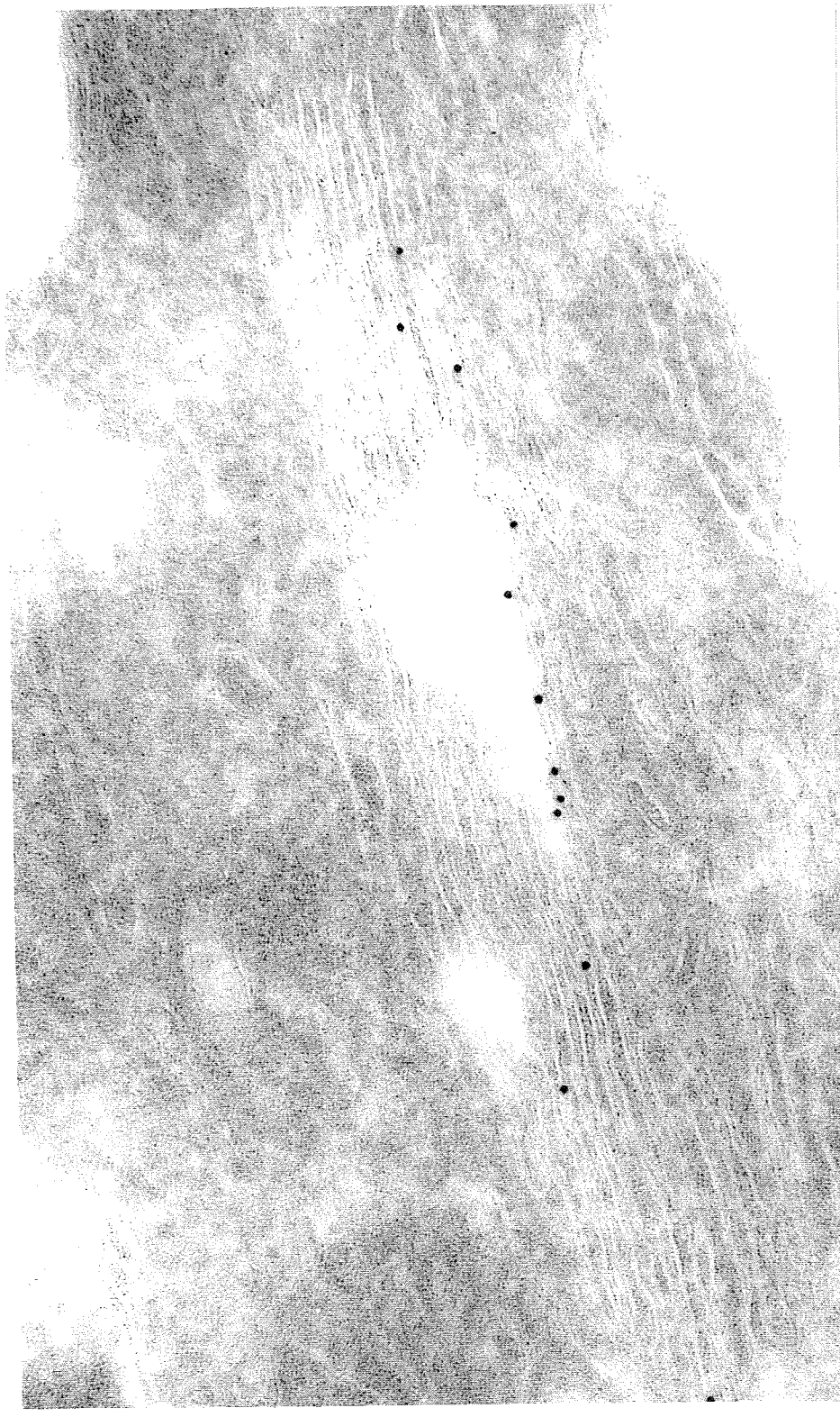

Figure 8. B

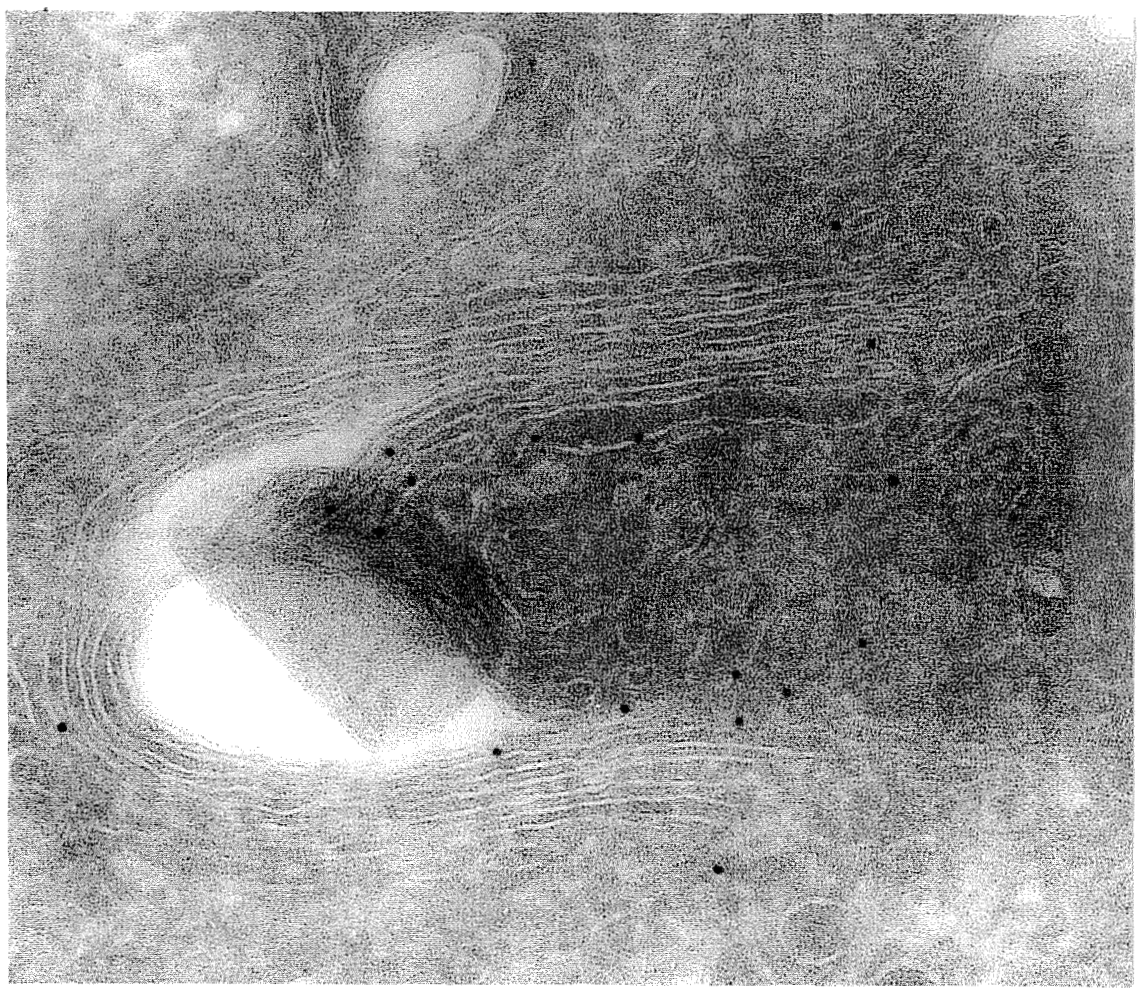

CHAPTER IV

Engineering the Glycosylation of a Therapeutic Antibody in Chinese Hamster Ovary Cells

4.1 Summary

The glycosylation pattern of chCE7, an anti-neuroblastoma therapeutic monoclonal antibody (mAb), was engineered in CHO cells with tetracyline-regulated expression of GnTIII. A set of mAb samples differing in their glycoform distribution was produced by controlling GnTIII expression in a range between basal and toxic levels, and their glycosylation profiles were analyzed by MALDI/TOF-MS of neutral oligosaccharides. Measurement of the ADCC activity of these samples showed an optimal range of GnTIII expression for maximal chCE7 *in vitro* biological activity, and this activity correlated with the level of Fc-associated bisected, complex oligosaccharides. Expression of GnTIII within the biotechnologically practical range, i.e., where no significant growth inhibition and toxicity are observed, led to a consumption of more than 90% of non-bisected, non-galactosylated bi-antennary complex oligosaccharides, but, at most, 50% was converted to the target bisected, complex structures for this set of chCE7 samples. The rest could have been diverted to bisected hybrid by-products and/or consumed by competing GalT to produce non-bisected, galactosylated oligosaccharides. Direct profiling by MALDI/TOF-MS cannot distinguish between the latter two classes of oligosaccharides, but the growth of the associated MALDI/TOF-MS peaks upon GnTIII overexpression, with concomitant reduction of bisected complex-peaks, suggests the formation of bisected hybrid products. The new optimized variants of chCE7 are promising candidate reagents for the treatment of neuroblastoma and should be tested and developed further. The strategy presented here may also be applicable to other therapeutic IgGs.

4.2 Introduction

Clinical trials of unconjugated monoclonal antibodies (mAbs) for the treatment of some types of cancer have recently yielded encouraging results (Deo et al., 1997; Dillman, 1997). A chimeric, unconjugated IgG1 has been approved for low-grade or follicular B-cell non-Hodgkin's lymphoma (Dillman, 1997), while another unconjugated mAb, a humanized IgG1 that targets solid breast tumors, has also shown promising results in phase III clinical trials. The antigens of these two mAbs are highly expressed in their respective tumor cells and the antibodies mediate potent tumor destruction by effector cells *in vitro* and *in vivo*. In contrast, many other unconjugated mAbs with fine tumor specificities cannot trigger effector functions of sufficient potency to be clinically useful (Frost et al., 1997; Surfus et al., 1996). For some of these weaker mAbs, adjunct cytokine therapy is currently being tested. Addition of cytokines can stimulate antibody-dependent cellular cytotoxicity (ADCC) by increasing the activity and number of circulating lymphocytes (Frost et al., 1997; Surfus et al., 1996). ADCC, a lytic attack on antibody-targeted cells, is triggered upon binding of lymphocyte receptors to the constant region (Fc) of antibodies (Deo et al., 1997).

A different, complementary approach to increase ADCC activity of unconjugated IgG1s would be to engineer the Fc region of the antibody to increase its affinity for the lymphocyte receptors (FcγRs). Protein engineering studies have shown that FcγRs interact with the polypeptide chain in the lower hinge region of the IgG CH2 domain (Lund et al., 1996). FcγR binding also requires the presence of oligosaccharides covalently attached at the conserved Asn 297 in the CH2 region (Lund et al., 1996; Wright and Morrison, 1997), suggesting that either both oligosaccharide and polypeptide contribute directly to the interaction site or that the oligosaccharide is required to maintain an active CH2 polypetide conformation (Lund et al., 1996). Modification of the oligosaccharide structure can therefore be explored as a means to increase the affinity of the interaction.

An IgG molecule contains two N-linked oligosaccharide sites in its Fc region, one on each heavy chain. As for any glycoprotein, an antibody is produced as a population of glycoforms which share the same polypeptide backbone but have different oligosaccharides attached to the glycosylation sites. The oligosaccharides normally found in the Fc region of serum IgG are of complex bi-antennary type (Wormald et al., 1997), with low levels of terminal sialic acid and bisecting N-acetylglucosamine (GlcNAc), and a variable degree of terminal galactosylation and core fucosylation (Fig. 1). The minimal carbohydrate structure required for FcγR binding lies within the oligosaccharide core (Lund et al., 1996). Removal of terminal galactoses results in approximately a two-fold reduction in ADCC activity, indicating some role for these residues in FcγR receptor binding (Lund et al., 1996).

The mouse- and hamster-derived cell lines used in industry and academia for production of unconjugated therapeutic mAbs normally attach oligosaccharide determinants to Fc sites. However, IgGs expressed in these cell lines lack the bisecting GlcNAc found in low amounts in serum IgGs (Bergweff et al., 1995; Lifely et al., 1995). In contrast, a humanized IgG1 (CAMPATH-1H), produced in a rat myeloma cell line, carried a bisecting GlcNAc in some of its glycoforms (Lifely et al., 1995). The rat cell-derived antibody reached a similar *in vitro* ADCC activity as CAMPATH-1H antibodies produced in standard cell lines, but at significantly lower antibody concentrations.

The CAMPATH antigen is normally present at high levels on lymphoma cells, and the chimeric mAb has high ADCC activity in the abscence of a bisecting GlcNAc (Lifely et al., 1995). Our goal was to study the impact of a bisecting GlcNAC on the ADCC mediated by IgG1s with low basal activity levels. For this purpose we chose a chimeric anti-neuroblastoma IgG1 (chCE7) which has low ADCC activity when produced by SP2/0 recombinant mouse myeloma cells. ChCE7 recognizes a tumor-associated, 190-kDa, membrane-glycoprotein and reacts strongly with all neuroblastoma tumors tested to date. It has a high affinity for its antigen (K_A of 10^{10} M^{-1}) and, due to its high tumor-

specificity, it has been used routinely as a diagnostic tool in clinical pathology (Amstutz et al., 1993). As for other antibodies with low ADCC activity, only a radiolabelled version has been investigated as a therapeutic agent in human patients. This trial showed good tumor localization of chCE7 and a lack of negative side-effects (Dörr et al., 1993).

In the N-linked glycosylation pathway, bisecting GlcNAc is added by the enzyme β(1,4)-N-acetylglucosaminyltransferase III (GnTIII) (Schachter, 1986). In order to synthesize bisected oligosaccharides in CHO cells, which normally lack GnTIII (Stanley and Campbell, 1984), a CHO cell line expressing a heterologous cDNA (Nishikawa et al., 1992) for this enzyme was first established. For this purpose a tetracycline-regulated mammalian expression system was used (Chapter III). Cultures of this cell line expressing different levels of GnTIII can be obtained simply by controlling the level of tetracycline in the culture medium. ChCE7 samples produced in these cultures should differ in the proportion of glycoforms carrying bisected oligosaccharide products, at least within a certain range of GnTIII expression. Comparison of the ADCC activities of these samples should allow a correlation between expression of the GnTIII gene in CHO cells and the ADCC activity of the modified antibody.

4.3 Materials and Methods

Bacterial strains and media

E. coli strain XL-1 Blue was grown either on LB agar plates or in LB broth.

Mammalian cell lines and media

CHO-tet-GnTIIIm cells (see Chapter III) were cultured in FMX-8 medium (Cell Culture Technologies, Switzerland) supplemented with 10% (v/v) fetal calf serum (Boehringer Mannheim), 3 g/l HEPES, 1% (v/v) antibiotic/antimycotic solution (Gibco), 400 μg/ml G418, and 7.5 μg/ml puromycin. Tetracycline-hydrochloride was added to the medium at a concentration of 2 μg/ml unless noted otherwise. Cells were grown as monolayers in stationary T-flasks, using 0.2 ml of medium/cm^2 of flask surface. The cultures were maintained in an incubator at 37 °C under a 5% CO_2 atmosphere. For sub-culturing, cells were detached from T-flasks by addition of Cell Dissociation Solution (Sigma).

Plasmids

Plasmid vectors 10CE7VH and 98CE7VL, for expression of heavy (IgG1) and light (kappa) chains respectively of anti-human neuroblastoma chimeric antibody chCE7 (Amstutz et al., 1993), were obtained from Dr. Hanspeter Amstutz (Central Laboratory, Swiss Red Cross, Bern). These vectors contain chimeric genomic DNA including the mouse immunoglobulin promoter/enhancer, mouse antibody variable regions, and human antibody constant regions. Mammalian expression vectors pcDNA3.1(+) and pZeoSV2 were purshased from Invitrogen. Plasmid pBluescriptIIKS(+) was purshased from Stratagene.

DNA manipulations

General DNA manipulations were carried out according to standard methods (Sambrook et al., 1989). DNA fragments were extracted from agarose gels using a DNA Extraction kit (Quiagen). DNA cycle sequencing was carried out by Heidi Ernst (Institute of Biotechnology, ETH-Zürich) using Thermo Sequenase (Amersham), fluorescent T7(-40) forward and reverse primers (MGW Biotech, Germany), and an automated DNA sequencer (Li Cor). DNA for transfection into mammalian cells was purified using a Midi DNA Purification kit (Qiagen).

Polymerase chain reactions (PCRs)

PCRs were carried out using *Pwo* DNA polymerase (Boehringer Mannheim). The composition of the PCR mixes was defined according to instructions from the polymerase supplier. Twelve cycles of denaturation-annealing-polymerization were performed. Oligonucleotide primers were synthesized by Microsynth (Switzerland).

Construction of vectors for expression of chimeric antibodies in CHO cells

Chimeric heavy and light chain chCE7 genes were reassambled, sequenced and subcloned into the pcDNA3.1(+) vector. In reassembly all introns were removed, the leader sequences were replaced with synthetic ones, and unique restriction sites joining the variable and constant region sequences were introduced. Details of PCR primers used in these constructions are given in Figures 2 and 3.

Introns from the heavy constant region were removed by splicing with overlap-extension-PCR (Clackson et al., 1991). Briefly, in a first PCR step, using vector 10CE7VH as a template, three individual DNA fragments were generated from separate reaction mixtures. These fragments encoded respectively CH1 plus half of the hinge domain, the rest of the hinge plus all of the CH2 domain, and the CH3 domain; and included overlapping sequences added as 5' tags to PCR primers. The three fragments

were gel purified, mixed together and used as a template for a second PCR; generating a product encoding the whole constant heavy region. Unique restriction sites, *Hind*III and *Nhe*I upstream, and *BamH*I downstream, were introduced via the PCR primers. The final DNA fragment was digested with *Hind*III and *BamH*I and subcloned into pBluescriptIIKS(+) to give plasmid pBlue-CH.

The variable heavy region was amplified by a first PCR step using vector 10CE7VH as a template. This step added a portion of a synthetic leader sequence (Reff et al., 1994) and removed the intron between the leader and variable heavy sequences. The gel purified product was used as a template for a second PCR step which added the rest of the leader sequence and introduced a *Hind*III site upstream and *Nhe*I and *EcoR*I sites downstream. The product was digested with *Hind*III and *EcoR*I and subcloned into plasmid pBluescriptIIKS(+) to give plasmid pBlue-VH.

The heavy variable and constant regions in plasmids pBlueVH and pBlueCH were sequenced by DNA cycle sequencing to check if any mutations had been introduced. pBlueVH was then digested with *Hind*III and *Nhe*I, pBlueCH with *Nhe*I and *BamH*I, and the products encoding the variable and constant heavy regions, respectively, were subcloned together into vector pDNA3.1(+) to generate the final chCE7 heavy chain expression vector pchCE7H.

The light variable and constant sequences were likewise amplified by PCR, this time using vector 98CE7VL as a template. The constant light sequence was amplified in a single PCR step which introduced *Hind*III and *BsiWI* sites upstream and a *BamH*I site downstream. The product was digested with *Hind*III and *BamH*I and subcloned into pBluescriptIIKS(+) to give plasmid pBlue-CL. The variable light sequence was amplified by a sequential two-step PCR procedure analogous to that applied to the variable heavy sequence, which replaced the natural leader sequence by a murine Ig kappa leader sequence from vector pSecTag (Invitrogen), removed the intron, and introduced a *Hind*III site

upstream and *BsiW*I and *Eco*RI sites downstream. The final product was digested with *Hind*III and *Eco*RI then subcloned into pBluescriptIIKS(+) to give plasmid pBlue-VL.

The light variable and constant regions in plasmids pBlueVL and pBlueCL were sequenced by DNA cycle sequencing to check if any mutations had been introduced. pBlueVL was then digested with *Hind*III and *BsiW*I, pBlueCL with *BsiW*I and *BamH*I, and the products encoding the variable and constant light regions, respectively, were subcloned together into vector pDNA3.1(+) to generate the final chCE7 light chain expression vector, pchCE7L.

Generation of CHO-tet-GnTIIIm cells expressing chCE7 antibody

A T-25 flask was seeded with CHO-tet-GnTIIIm cells to approximately 40% confluency, incubated for 24 h at 37 °C, then the cells were co-transfected with vectors pchCE7H, pchCE7L, and pZeoSV2 using the calcium phosphate transfection method (see Chapter III). The DNA used for transfection had been linearized, CE7 expression vectors with *Sfu*I and pZeoSV2 with *Hind*III, then purified over anion exchange columns of a Midi DNA Purification kit (Qiagen). The linearized vectors were co-transfected in a molar ratio of 7:7:1 of pchCE7H:pchCE7L:pZeoSV2, and the total amount of DNA used per transfection was 15 μg. One day after transfection, the cells were transferred to two culture dishes with a diameter of 15 cm each, and one day after transfer Zeocin (Invitrogen) was added to the culture medium at a concentration of 400 μg/ml. The medium was replaced every three days until Zeocin resistant clones of adequate size for picking had grown. Eighty individual clones were picked using the agar-overlay cloning method (see Chapter III) and transferred to a 96-well cell culture plate. Six days after seeding the 96-well plate, the culture medium of each clone was assayed for chimeric antibody expression using an ELISA assay specific for human IgG constant region (Lifely et al., 1995). The five most productive clones were grown further from T-25 cultures and

the secreted antibody levels were measured again to judge the stability of the clones. One clone, CHO-tet-GnTIIIm-chCE7, was chosen for further work.

Production of chCE7 antibody samples

Four chCE7 antibody samples were derived from parallel CHO-tet-GnTIIIm-chCE7 cultures, each culture containing a different level of tetracycline and therefore expressing GnTIII at different levels. CHO-tet-GnTIIIm-chCE7 cells were seeded to 10% confluency in four different T-75 flasks, each at a different concentration of tetracycline. The levels of tetracycline were 2000, 60, 30, and 15 ng/ml. Three days later each culture was transferred to a T-150 flask, again seeding to 10% confluency and using the same levels of tetracycline. After four days, the cultures at 2000, 60 and 30 ng/ml of tetracycline, which were near to confluency, were diluted two-fold with the appropiate media and divided in two T-150 flasks while the culture at 15 ng/ml was kept in the original T-150 flask. One day later, four Triple-flasks (Nunc) of each culture at 2000, 60 or 30 ng/ml of tetracycline were seeded using all of the cells from each set of two T-150 flasks. The levels of tetracycline were maintained in the Triple-flasks, and each flask contained 100 ml of culture medium. Triple-flask cultures were grown until confluency, then the culture medium was pooled for each level of tetracycline and stored at 4 ^{o}C. The culture at 15 ng/ml of tetracycline was maintained in the T-150 flask and the medium was replaced at the time when the Triple-flasks were seeded. Two days later this medium was collected and fresh medium was added again for another two days, each time maintaining the level of tetracycline at 15 ng/ml. The two batches of medium at 15 ng/ml of tetracycline were pooled together and stored at 4 ^{o}C. Each time culture medium was collected, cell debris was removed by centrifugation prior to storage.

Purification of chCE7 antibody samples

Antibody was purified from culture medium by Protein A affinity chromatography followed by buffer exchange on a cation exchange column. All purification steps were conducted at room temperature. Culture medium was passed at a flow rate of 1 ml/min through a 1 ml HiTrap Protein A column (Pharmacia Biotech) which had been equilibrated with 10 ml of 20 mM sodium phosphate, 20 mM sodium citrate, pH 7.5 (buffer A). The column was then washed at a flow rate of 1 ml/min with 10 ml of 20 mM sodium phosphate, 20 mM sodium citrate, 500 mM sodium chloride, 0.01% Tween 20, pH 7.5 (buffer B). A further wash was carried out at a flow rate of 0.2 ml/min using 2 ml of buffer B supplemented with 1 M urea (buffer C). A linear pH gradient was then applied at a flow rate of 0.2 ml/min, from 100% buffer C to 100% buffer D (20 mM sodium citrate, 500 mM sodium chloride, 0.01% (v/v) Tween 20, 1 M urea, pH 2.5). The absorbance at 280 nm was monitored and 0.5 ml fractions were collected into tubes containing 25 µl of 1 M phosphate, pH 8.0. Fractions were stored at 4 °C. The chCE7 peak was identified by the ELISA assay described previously and the corresponding fractions were pooled. Under these conditions, chCE7 eluted from the column at approximately pH 4. In this region of the chromatogram, the absorbance dropped to baseline level in a control chromatographic run using culture medium from the parental CHO-tet-GnTIIIm cells lacking the chCE7 genes, grown under identical conditions.

Affinity purified chCE7 samples were diluted ten-fold with 50mM MES pH 5.0, and passed at a flow rate of 1 ml/min through a 1 ml ResourceS cation exchange column (Pharmacia Biotech) equilibrated with the above buffer. Antibodies were eluted by a step change to phosphate buffered saline (PBS). The concentration of each sample was estimated by measuring the absorbance at 280 nm in a quartz cuvette against PBS as a blank, and using a conversion factor of 1.35 A.U.ml/mg IgG. The samples were stored at -20 °C. Proteins were resolved by SDS-PAGE under reducing conditions and purity was judged from Coomassie Blue staining of the gel.

Binding of antibodies to neuroblastoma cells

Binding assays were performed by Dr. Ilse Novak-Hofer of the Paul Scherrer Institute (Villingen, Switzerland). Binding affinity to human neuroblastoma cells was estimated from displacement of ^{125}I-labelled chCE7 derived from SP2/0 mouse myeloma cells, by the CHO-produced samples (Amstutz et al., 1993).

ADCC activity assay

ADCC activity assays were performed by Dr. Radmila Moudry (Central Laboratory, Swiss Red Cross, Bern). Briefly, lysis of IMR-32 human neuroblastoma cells (target) by human lymphocytes (effector), at a target:effector ratio of 1:19, during a 16 h incubation at 37 ^{o}C in the presence of different concentrations of chCE7 samples, was measured via retention of a fluorescent dye (Kolber et al., 1988). The percentage of cytotoxicity was calculated relative to a total lysis control, resulting from exposure of the target to a detergent, after subtraction of the signal in the absence of antibody.

Oligosaccharide analysis by MALDI/TOF-MS

The four CHO-derived antibody samples, denoted CE7-2000t, -60t, -30t, and -15t (corresponding to the levels of tetracycline in ng/ml used in the cell cultures for production of the samples), and one SP2/0 mouse myeloma-derived chCE7 sample, CE7-SP2/0 (donated by Dr. Hanspeter Amstutz and produced as described in Amstutz et al., 1993), were analyzed. Samples were treated with *A. urefaciens* sialidase (Oxford Glycosciences) to remove any sialic acid monosaccharide residues. Antibody samples were first equilibrated to 100 mM sodium acetate buffer, pH 5.0 by two sequential steps of ultrafiltration using Ultrafree-0.5-5 kDa MWCO cartridges (Millipore). In each step the volume was reduced from 500 to 10 µl. The amounts of antibody digested were 100 µg of CE7-SP2/0, 75 µg of CE7-2000t and CE7-60t, 50 µg of CE7-30t, and 20 µg of CE7-

15t. Each reaction used 0.2 U of sialidase in a final volume of 40 µl, and an incubation time of 20 h at 37 °C.

The samples were then digested with peptide N-glycosidase F (PNGaseF, Oxford Glycosciences). Sialidase digests were diluted with 460 µl of PNGaseF buffer (20 mM sodium phosphate, 50 mM EDTA, 0.02% sodium azide (w/v), pH 7.5) and concentrated to 10 µl by ultrafiltration as described above. The retentate was diluted to 500 µl and concentrated again by ultrafiltration to 4 µl. One microliter of 2.5% (w/v) SDS/125 mM DTT in PNGaseF buffer was added to each sample and they were boiled for 2 min. After cooling, 2.5 µl of 5% (v/v) Triton X-100 in PNGaseF buffer and 12.5 µl of PNGaseF buffer were added to each sample. Finally 2.5 U (5 µl) of PNGaseF was added and the samples were incubated for 20 h at 37 °C.

Protein, detergents, and salts were removed by passing the digests through microcolumns containing, from top to bottom, 20 µl of SepPak C18 reverse phase matrix (Waters), 20 µl of Dowex AG 50W X8 cation exchange matrix (BioRad), and 20 µl of AG 4X4 anion exchange matrix (BioRad). The microcolumns were made by packing the matrices in a Gel Loader tip (Eppendorf) filled with ethanol (Küster et al., 1997). Ethanol was flushed out under air pressure, and the columns were washed with 300 µl of deionized water. After loading the samples, and collecting oligosaccharides in the flow through liquid, the columns were washed with 100 µl of deionized water to improve the oligosaccharide recovery. This wash was mixed with the previous flow through liquid, filtered using a Kwikspin (Pierce) cartridge fitted with a 0.2 µm polysulfone membrane, and evaporated to dryness at room temperature using a SpeedVac (Savant). The dried oligosaccharides were resuspended in 2 µl of deionized water. One microliter was applied to a MALDI-MS sample plate (Perseptive Biosystems) and 1 µl of a 10 mg/ml dehydrobenzoic acid (DHB, Aldrich) solution in acetonitrile was added and mixed by pippeting. The samples were air dried and the resulting crystals were dissolved in 0.2 µl of ethanol (Harvey, 1993) and allowed to recrystallize by air drying.

The oligosaccharide samples were then analyzed by matrix-assisted laser desorption ionization/time-of-flight-mass spectrometry (MALDI/TOF-MS) using an Elite Voyager 400 spectrometer (Perseptive Biosystems), equipped with a delayed ion extraction MALDI-ion source, in positive ion and reflector modes, with an accelaration voltage of 20 kV. One hundred and twenty eight scans were averaged, moving the laser beam around the whole surface of the sample while shooting.

4.4 Results and Discussion

Production of chCE7 in CHO cells expressing different levels of GnTIII

ChCE7 heavy and light chain expression vectors were constructed incorporating the human cytomegalovirus (hCMV) promoter, the bovine growth hormone termination and polyadenylation sequences, and eliminating all heavy and light chain introns. This vector design was based on reports of reproducible high-level expression of recombinant IgG genes in CHO cells (Reff et al., 1994; Trill et al., 1995). In addition, a unique restriction site was introduced in each chain, at the junction between the variable and constant regions. These sites conserve the reading frame and do not change the amino acid sequence. They should enable simple exchange of the mouse variable regions, for the production of other mouse-human chimeric antibodies (Reff et al., 1994). DNA sequencing confirmed that the desired genes were appropriately assembled, and production of the chimeric antibody in transfected CHO cells was verified with a human Fc-ELISA assay.

CHO-tet-GnTIIIm-chCE7 cells, with stable, tetracycline-regulated expression of GnTIII and stable, constitutive expression of chCE7, were established and scaled-up for production of a set of chCE7 samples. During scale-up, four parallel cultures derived from the same CHO clone were grown, each at a different level of tetracycline and therefore only differing in the level of expression of the GnTIII gene. This procedure eliminates any clonal effects from other variables affecting N-linked glycoform biosynthesis, permitting a rigorous correlation to be established between GnTIII gene expression and biological activity of the glycosylated antibody. The tetracycline concentration ranged from 2000 ng/ml, i.e., the basal level of GnTIII expression, to 15 ng/ml, at which significant growth inhibition and toxicity due to glycosyltransferase overexpression was observed (see Chapter III). Indeed, only a small amount of antibody could be recovered from the latter culture. The second highest level of GnTIII expression, using tetracycline at a concentration of 30 ng/ml, produced only a mild inhibition of

growth. The purified antibody yield from this culture was approximately 70% that from the remaining two lower levels of GnTIII gene overexpression.

The four antibody samples, CE7-2000t, -60t, -30t, and -15t, numbers denoting the associated concentration of tetracycline, were purified by affinity chromatography on Protein A and buffer exchanged to PBS using a cation exchange column. Purity was higher than 95% as judged from SDS-PAGE with Coomassie Blue staining (data not shown). Binding assays to human neuroblastoma cells revealed high affinity to the cells and no significant differences in antigen binding among the different samples (estimated equilibrium dissociation constants varied between 2.0 and 2.7 x 10^{-10} M). This was as expected, since there are no potential N-linked glycosylation sites in the CE7 variable regions.

Oligosaccharide distributions and levels of bisected complex oligosaccharides of different chCE7 samples

Oligosaccharide profiles were obtained by matrix-assisted laser desorption/ionization mass spectrometry on a time-of-flight instrument (MALDI/TOF-MS). Mixtures of neutral N-linked oligosaccharides derived from each of the four CHO-produced antibody samples and from a SP2/0 mouse myeloma-derived chCE7 (CE7-SP2/0) sample were analyzed using 2,5-dehydrobenzoic acid (2,5-DHB) as the matrix (Fig. 4). Under these conditions, neutral oligosaccharides appear essentially as single [M + Na^+] ions, which are sometimes accompanied by smaller [M + K^+] ions, depending on the potassium content of the matrix (Field et al., 1996; Harvey, 1993; Küster et al., 1997).

This type of analysis yields both the relative proportions of neutral oligosaccharides of different mass, reflected by relative peak height, and the isobaric monosaccharide composition of each peak (Küster et al., 1997; Naven and Harvey, 1996). Tentative structures are assigned to peaks based on the monosaccharide composition, knowledge of the biosynthetic pathway, and on previous structural data for oligosaccharides derived from

the same glycoprotein produced by the same host, since the protein backbone and the cell type can have a strong influence on the oligosaccharide distribution (Field et al., 1996). In the case of Fc-associated oligosaccharides, only bi-antennary complex oligosaccharides have been detected in IgGs present in human serum or produced by mammalian cell cultures under normal conditions (Wormald et al., 1997; Wright and Morrison, 1997). The pathway leading to these compounds is illustrated in Figure 5, including the mass of the $[M + Na^+]$ ion corresponding to each oligosaccharide. High mannose oligosaccharides have also been detected on antibodies produced in the stationary and death phases of batch cell cultures (Yu Ip et al., 1994).

The two major peaks in the CE7-SP2/0 sample (Fig. 4A) correspond to masses of fucosylated oligosaccharides with four N-acetylhexosamines (HexNAcs) containing either three (m/z 1486) or four (m/z 1648) hexoses (see Fig. 5, but note that the summarized notation for oligosaccharides in this figure does not count the two GlcNAcs of the core). This composition is consistent with core fucosylated, bi-antennary complex oligosaccharide structures carrying zero or one galactose residues, respectively, typical of Fc-associated oligosaccharides, and as previously observed in NMR analysis of Fc oligosaccharides derived from a chimeric IgG1 expressed in SP2/0 cells (Bergweff et al., 1995).

GnTIII-catalyzed transfer of a bisecting GlcNAc to these bi-antennary compounds, which are the preferred GnTIII acceptors, would lead to oligosaccharides with five HexNAcs (m/z 1689 and 1851, non- and mono-galactosylated, respectively, Fig. 5), which are clearly absent in the CE7-SP2/0 sample. The latter peaks appear when chCE7 is expressed in CHO-tet-GnTIIIm cells. In the CHO-expressed antibodies the four HexNAc-containing peaks are also mainly fucosylated, although a small amount of non-fucosylated structures is evident from the peak at m/z 1339 (see Fig. 5). The level of galactosylation is also not very different between the CHO- and SP2/0-derived material. At the basal level of GnTIII expression (CE7-2000t sample, Fig. 4B), the molecules with five

HexNAcs are present in a lower proportion than those with four HexNAcs. A higher level of GnTIII expression (CE7-60t sample, Fig. 4C) led to a reversal of the proportions in favor of oligosaccharides with five HexNAcs. Based on this trend, bisected, bi-antennary complex oligosaccharide structures can be assigned to compounds with five HexNAcs in these samples. Tri-antennary N-linked oligosaccharides, the alternative five HexNAc-containing isomers, have never been found in the Fc region of IgGs and their syntheses are catalyzed by GlcNAc-transferases discrete from GnTIII.

A further increase in GnTIII expression (CE7-30t sample, Fig. 4D) did not lead to any significant change in the levels of bisected complex oligosaccharides. Another peak (m/z 1543) containing five HexNAcs appears at low, but relatively constant levels in the CHO-GnTIII samples and corresponds in mass to a non-fucosylated, bisected-complex oligosaccharide mass (Fig. 5). The smaller peaks at m/z 1705 and 1867 also correspond to five HexNAc-containing bi-antennary complex oligosaccharides. They can be assigned either to potassium adducts of the peaks at m/z 1689 and 1851 (mass difference of 16 Da with respect to sodium adducts) (Küster et al., 1997) or to mono- and bi-galactosylated, bisected complex oligosaccharides without fucose (Fig. 5). Together, the bisected complex oligosaccharides amount to approximately 25% of the total in sample CE7-2000t and reach approximately 45 to 50% in samples CE7-60t and CE7-30t.

Additional information from the oligosaccharide profiles of chCE7 samples

Although the levels of bisected complex oligosaccharides were not higher in sample CE7-30t, increased overexpression of GnTIII did continue to reduce, albeit to a small extent, the proportions of substrate bi-antennary complex oligosaccharide substrates. This was accompanied by moderate increases in two different, four HexNAc-containing peaks (m/z 1664 and 1810). The latter two peaks can correspond either to galactosylated bi-antennary complex oligosaccharides or to bisected hybrid compounds (see Fig. 6). A combination of both classes of structures is also possible. The relative increase in these peaks is consistent

with the accumulation of bisected hybrid by-products of GnTIII overexpression, as predicted from the mathematical model of N-linked glycoform biosynthesis presented in this thesis (Chapter II). Indeed, the sample produced at the highest level of GnTIII overexpression, CE7-15t, showed a large increase in the peak at m/z 1664, a reduction in the peak at m/z 1810 and a concomitant reduction of complex bisected oligosaccharides to a level of approximately 25% (see peaks with m/z 1689 and 1851 in Fig. 4E and the corresponding structures in Fig. 6). Higher accumulation of non-fucosylated (m/z 1664) bisected hybrid by-products, instead of fucosylated ones (m/z 1810), would agree with the fact that oligosaccharides which are first modified by GnTIII can no longer be biosynthetic substrates for core α1,6-fucosyltransferase (Schachter, 1986).

The peak at m/z 1257 is present at a level of 10 -15% of the total in the CHO-derived samples and at a lower level in CE7-SP2/0 (Fig. 4). It corresponds to five hexoses plus two HexNAcs. The only known N-linked oligosaccharide structure with this composition is a five mannose-containing compound of the high-mannose type. Another high mannose oligosaccharide, a six mannose one (m/z 1420), is also present at much lower levels. As mentioned above, such oligosaccharides have been detected in the Fc of IgGs expressed in the late phase of batch cell cultures (Yu Ip et al., 1994).

Antibody dependent cellular cytotoxicity of chCE7 samples

ChCE7 shows some ADCC activity, measured as *in vitro* lysis of neuroblastoma cells by human lymphocytes, when expressed in CHO-tet-GnTIIIm cells with the minimum level of GnTIII overexpression (Fig. 7, sample CE7-2000t). Raising the level of GnTIII produced a large increase in ADCC activity (Fig. 7, sample CE7-60t). Further overexpression of GnTIII was not accompanied by an additional increase in activity (Fig. 7, sample CE7-30t), and the highest level of expression actually led to reduced ADCC (Fig. 7, sample CE7-15t). Besides exhibiting the highest ADCC activities, both CE7-60t and CE7-30t samples show significant levels of cytotoxicity at very low antibody

concentrations. These results show that there is an optimal range of GnTIII overexpression in CHO cells for ADCC activity, and comparison with oligosaccharide profiles shows that activity correlates with the level of Fc-associated, bisected complex oligosaccharides.

Given the importance of bisected complex oligosaccharides for ADCC activity, it would be useful to engineer the pathway to further increase the proportion of these compounds. Overexpression of GnTIII to levels approaching that used for sample CE7-30t is within the biotechnologically practical range where no significant toxicity and growth inhibiton are observed. At this level of expression, the non-galactosylated, non bisected, bi-antennary complex oligosaccharides, i.e., the preferred, potential GnTIII substrates, are reduced to less than 10% of the total (see m/z 1486 peak, Fig. 4D). However, only 50% are converted to the desired bisected biantennary complex structures. The rest are either diverted to bisected, hybrid oligosaccharide byproducts or consumed by the competing enzyme β1,4-galactosyltransferase, GalT (Fig. 6).

Resolution of the bisected hybrid and the non-bisected, galactosylated complex oligosaccharide peaks by complementary structural analyses would determine how much each potential, undesired route is consuming. The growth of the m/z 1664 and 1810 peaks at high GnTIII overexpression levels suggests that at least a fraction of these peaks corresponds to bisected hybrid oligosaccharides (Fig. 6). In theory, a flux going to bisected hybrid compounds can be reduced by co-overexpression of enzymes earlier in the pathway such as mannosidase II together with GnTIII (see Fig. 8 in Chapter II). On the other hand, competition between GnTIII and GalT for bisected complex oligosaccharide substrates could potentially be biased towards GnTIII-catalyzed reactions, by increasing the intra-Golgi concentration of UDP-GlcNAc while overexpressing GnTIII. GnTIII transfers a GlcNAc from the co-substrate UDP-GlcNAc to the different oligosaccharides. Should the intra-Golgi concentration of UDP-GlcNAc co-substrate be sub-saturating for GnTIII, then increasing it, either by manipulation of the culture medium composition or by genetic

manipulation of sugar-nucleotide transport into the Golgi, could favor GnTIII in a competition for oligosaccharides with GalT. In light of the results showing a polarized Golgi distribution of GnTIII (see Chapter III), this potential competition should not be overlooked (see Fig. 6 in Chapter II).

It remains to be determined whether the increase in ADCC activity results from the increase in both the galactosylated and non-galactosylated, bisected complex oligosaccharides, or only from one of these forms (see peaks at m/z 1689 and 1851 in Fig. 4). If it is found that galactosylated, bisected complex bi-antennary oligosaccharides are the optimal structures for increased ADCC activity, then maximizing the fraction of these compounds on the Fc region would require overexpression of both GnTIII and GalT. Given the competitive scenario discussed previously, the expression levels of both genes would have to be carefully regulated. In addition, it would be valuable to try to re-distribute overexpressed GalT as much as possible towards the TGN instead of the trans-Golgi cisterna. The latter strategy may be realized by exchanging the transmembrane region-encoding sequences of GalT with those of α2,6-sialyltransferase (Chege and Pfeffer, 1990).

The boosted ADCC activity of the bisected chCE7 glycoforms, together with other attributes (Amstutz et al., 1993; Dörr et al., 1993), make this unconjugated mAb an interesting candidate reagent in the treatment of neuroblastoma, the most common solid tumor in children. The strategy presented here may also be applicable to other IgGs, including those which already have high ADCC activity in the absence of a bisecting GlcNAc. In the latter case, the dose required to achieve a therapeutically useful effect could be significantly diminished, having a large impact on the economy of cost-intensive mAb production processes (Bibila and Robinson, 1995; Trill et al., 1995).

4.5 Acknowledgements

This research was supported by the Swiss Priority Program in Biotechnology (SPP BioTech). In addition we would like to thank our collaborators Dr. Hanspeter Amstutz, Radmila Moudry, and Ilse Novak for useful discussions, providing essential materials, and carrying out important assays for this work. We also thank Dr. Naoyuki Taniguchi for providing us with the rat GnTIII cDNA.

4.6 References

Amstutz, H., Rytz, C., Novak-Hofer, I., et al. 1993. Production and characterization of a mouse/human chimeric antibody directed against human neuroblastoma. Int. J. Cancer **53:** 147-152.

Bergweff, A. A., Stroop, C. J., Murray, B., et al. 1995. Variation in N-linked carbohydrate chains in different batches of two chimeric monoclonal IgG1 antibodies produced by different murine SP2/0 transfectoma cell subclones. Glycoconjugate J. **12:** 318-330.

Bibila, T. A. and Robinson, D. K. 1995. In pursuit of the optimal fed-batch process for monoclonal antibody production. Biotechnol. Prog. **11:** 1-13.

Chege, N. W. and Pfeffer, S. R. 1990. Compartmentation of the Golgi complex: Brefeldin-A distinguishes trans Golgi cisternae from the trans Golgi network. J. Cell Biol. **111:** 893-899.

Clackson, T., Güssow, D. and Jones, P. T. 1991. General applications of PCR to gene cloning and manipulation. p. 187-214 In: McPherson, M. J., Quirke P. and Taylor G. R. (ed.), PCR a practical approach. Oxford University Press, Oxford.

Deo, Y. M., Graziano, R. F., Repp, R., et al. 1997. Clinical significance of IgG Fc receptors and FcγR-directed immunotherapies. Immunology Today **18:** 127.

Dillman, R. O. 1997. Magic bullets at last! Finally-approval of a monoclonal antibody for the treatment of cancer!!! Cancer Biother. & Radiopharm. **12:** 223-225.

Dörr, U., Haldemann, A. R., Leibundgut, K., et al. 1993. First clinical results with the chimeric antibody chCE7 in neuroblastoma. Targeting features and biodistribution data. Eur. J. Nucl. Med. **20:** 858.

Field, M., Papac, C. and Jones, A. 1996. The use of high-performance anion-exchange chromatography and matrix-assisted laser desorption/ionization time-of-flight mass spectrometry to monitor and identify oligosaccharide degradation. Anal. Biochem. **239:** 92-98.

Frost, J. D., Hank, J. A., Reaman, G. H., et al. 1997. A Phase I/IB trial of murine monoclonal anti-GD2 antibody 14.2G2a plus interleukin-2 in children with refractory neuroblastoma. Cancer **80:** 317-333.

Harvey, D. J. 1993. Quantitative aspects of the matrix-assisted laser desorption mass spectrometry of complex oligosaccharides. Rapid Commun. Mass Spectrom. **7:** 614-619.

Kolber, M. A., Quinones, R. R., Gress, R. E., et al. 1988. Measurement of cytotoxicity by target cell release and retention of the fluorescent dye bis-carboxyethyl-carboxyfluorescein (BCECF). J. Immunol. Meth. **108:** 255-264.

Küster, B., Wheeler, S. F., Hunter, A. P., et al. 1997. Sequencing of N-linked oligosaccharides directly from protein gels: In-gel deglycosylation followed by matrix-assisted laser desorption/ionization mass spectrometry and normal-phase high-performance liquid chromatography. Anal. Biochem. **250:** 82-101.

Lifely, R. M., Hale, C., Boyce, S., et al. 1995. Glycosylation and biological activity of CAMPATH-1H expressed in different cell lines and grown under different culture conditions. Glycobiology **318:** 813- 822.

Lund, J., Takahashi, N., Pound, J. D., et al. 1996. Multiple interactions of IgG with its core oligosaccharide can modulate recognition by complement and human Fcγ receptor I and influence the synthesis of its oligosaccharide chains. J. Immunol. **157:** 4963-4969.

Naven, T. J. P. and Harvey, D. J. 1996. Effect of structure on the signal strength of oligosaccharides in matrix-assisted laser desorption/ionization mass spectrometry on time-of-flight and magnetic sector instruments. Rapid Commun. Mass Spectrom. **10:** 1361-1366.

Nishikawa, A., Ihara, Y., Htakeyama, M., et al. 1992. Purification, cDNA cloning, and expression of UDP-N-acetylglucosamine:β-D-mannoside β-1,4N-acetylglucosaminyl-transferase III from rat kidney. J. Biol. Chem. **267:** 18199-18204.

Reff, M. E., Carner, K., Chambers, K. S., et al. 1994. Depletion of B cells in vivo by a chimeric mouse human monoclonal antibody to CD20. Blood **83:** 435-445.

Sambrook, J., Fritsch, E. F. and Maniatis, T. 1989. Molecular cloning: A laboratory manual. Cold Spring Harbor Laboratory Press, Cold Spring Harbor.

Schachter, H. 1986. Biosynthetic controls that determine the branching and microheterogeneity of protein- bound oligosaccharides. Biochem. Cell Biol. **64:** 163- 181.

Stanley, P. and Campbell, C. A. 1984. A dominant mutation to ricin resistance in Chinese hamster ovary cells induces UDP- GlcNac: Glycopeptide β-4-N- Acetylglucosaminyl-transferase III activity. J. Biol. Chem. **261:** 13370- 13378.

Surfus, J. E., Hank, J. A., Oosterwijk, E., et al. 1996. Anti-renal-cell carcinoma chimeric antibody G250 facilitates antibody-dependent cellular cytotoxicity with in vitro and in vivo interleukin-2-activated effectors. J. Immunother. **19:** 184-191.

Trill, J. J., Shatzman, A. R. and Ganguly, S. 1995. Production of monoclonal antibodies in COS and CHO cells. Current Opinion Biotechnol. **6:** 553-560.

Wormald, M. R., Rudd, P. M., Harvey, D. J., et al. 1997. Variations in oligosaccharide-protein interactions in immunoglobulin G determine the site-specific glycosylation profiles and modulate the dynamic motion of the oligosaccharides. Biochemistry **36:** 1370-1380.

Wright, A. and Morrison, S. L. 1997. Effect of glycosylation on antibody function: implications for genetic engineering. Tibtech **15:** 26-31.

Yu Ip, C. C., Miller, W. J., Silberklang, M., et al. 1994. Structural Characterization of the N-Glycans of a Humanized Anti-CD18 Murine Immunoglobulin G. Arch. Biochem. Bioph. **308:** 387-399.

4.7 Figures

Fig. 1. Representation of typical, human Fc-associated oligosaccharide structures. A conserved oligosaccharide core, linked to the Asn, is composed of three mannose (Man) and two N-acetylglucosamine (GlcNAc) monosaccharide residues. Additional GlcNAcs are normally β1,2-linked to the α6 Man and α3 Man (α6 and α3 arms, respectively), while the monosaccharide residues in bold, N-acetylneuraminic acid (NeuAc), galactose (Gal), fucose (Fuc), and the bisecting GlcNAc (boxed), can be present or absent.

Fig. 2. Sequences of oligonucleotide primers used in PCRs for the construction of the chCE7 heavy chain gene. Forward and reverse primers are identified by the suffixes .fwd and .rev, respectively. Overlaps between different primers, necessary to carry out secondary PCR steps using as a template the product of a primary PCR step, are indicated. Restriction sites introduced, sequences annealing to the CE7 chimeric genomic DNA, and the synthetic leader sequence introduced, are also indicated. The construction procedure is described in Materials and Methods (section 4.3).

Fig. 3. Sequences of oligonucleotide primers used in PCRs for the construction of the chCE7 light chain gene. Forward and reverse primers are identified by the suffixes .fwd and .rev, respectively. Overlaps between different primers, necessary to carry out secondary PCR steps using as a template the product of a primary PCR step, are indicated. Restriction sites introduced, sequences annealing to the CE7 chimeric genomic DNA, and the leader sequence introduced, are also indicated. The construction procedure is described in Materials and Methods (section 4.3).

Fig. 4. MALDI/TOF-MS spectra of neutral oligosaccharide mixtures from chCE7 samples produced either by SP2/0 mouse myeloma cells (**A**, oligosaccharides from 50 μg

of CE7-SP2/0), or by CHO-tet-GnTIII-chCE7 cell cultures differing in the concentration of tetracycline added to the media, and therefore expressing the GnTIII gene at different levels. In decreasing order of tetracycline concentration, i.e., increasing levels of GnTIII gene expression, the latter samples are: CE7-2000t (**B**, oligosaccharides from 37.5 μg of antibody), CE7-60t (**C**, oligosaccharides from 37.5 μg of antibody), CE7-30t (**D**, oligosaccharides from 25 μg of antibody) and CE7-15t (**E**, oligosaccharides from 10 μg of antibody).

Fig. 5. N-linked oligosaccharide biosynthetic pathway leading to bisected complex oligosaccharides via a GnTIII-catalyzed reaction. M stands for mannose; Gn, N-acetylglucosamine (GlcNAc); G, galactose; Gn^b, bisecting GlcNAc; f, fucose. The oligosaccharide nomenclature consists of enumerating the M, Gn, and G residues attached to the core oligosaccharide and indicating the presence of a bisecting GlcNAc by including a Gn^b. The oligosaccharide core is itself composed of 2 Gn residues and may or may not include a fucose. The major classes of oligosaccharides are shown inside dotted frames. ManI stands for Golgi mannosidase; GnT, GlcNAc transferase; and GalT, for galactosyltransferase. The mass associated with the major, sodium-associated oligosaccharide ion that is observed in MALDI/TOF-MS analysis is shown beside each oligosaccharide. For oligosaccharides which can potentially be core-fucosylated, the masses associated with both fucosylated (+f) and non-fucosylated (-f) forms are shown.

Fig. 6. N-linked oligosaccharide biosynthetic pathway leading to bisected complex and bisected hybrid oligosaccharides via GnTIII-catalyzed reactions. M stands for mannose; Gn, N-acetylglucosamine (GlcNAc); G, galactose; Gn^b, bisecting GlcNAc; f, fucose. The oligosaccharide nomenclature consists of enumerating the M, Gn, and G residues attached to the common oligosaccharide and indicating the presence of a bisecting GlcNAc by including a Gn^b . The oligosaccharide core is itself composed of 2 Gn residues and may

or may not include a fucose. The major classes of oligosaccharides are shown inside dotted frames. ManI stands for Golgi mannosidase; GnT, GlcNAc transferase; and GalT, for galactosyltransferase. The mass associated with the major, sodium-associated oligosaccharide ion that is observed in MALDI/TOF-MS analysis is shown beside each oligosaccharide. For oligosaccharides which can potentially be core-fucosylated, the masses associated with both fucosylated (+f) and non-fucosylated (-f) forms are shown.

Fig. 7. ADCC activity of different chCE7 samples. Lysis of IMR-32 neuroblastoma cells by human lymphocytes (target:effector ratio of 1:19, 16 h incubation at 37 ^{o}C), mediated by different concentrations of chCE7 samples, was measured via retention of a fluorescent dye. The percentage of cytotoxicity is calculated relative to a total lysis control (by means of a detergent), after subtraction of the signal in the absence of antibody.

Figure 1.

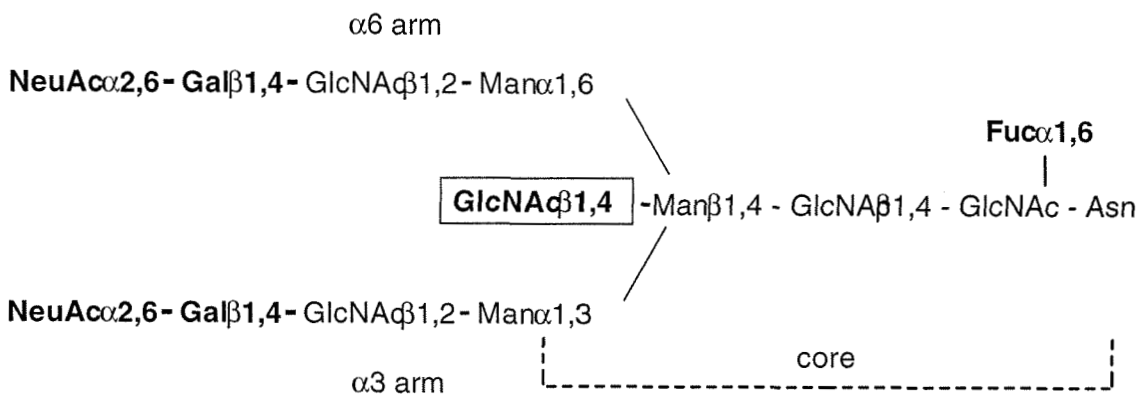
α6 arm
NeuAcα2,6- Galβ1,4- GlcNAcβ1,2- Manα1,6
Fucα1,6
GlcNAcβ1,4
-Manβ1,4 - GlcNAβ1,4 - GlcNAc - Asn
NeuAcα2,6- Galβ1,4- GlcNAcβ1,2- Manα1,3
core
α3 arm

Figure 2.

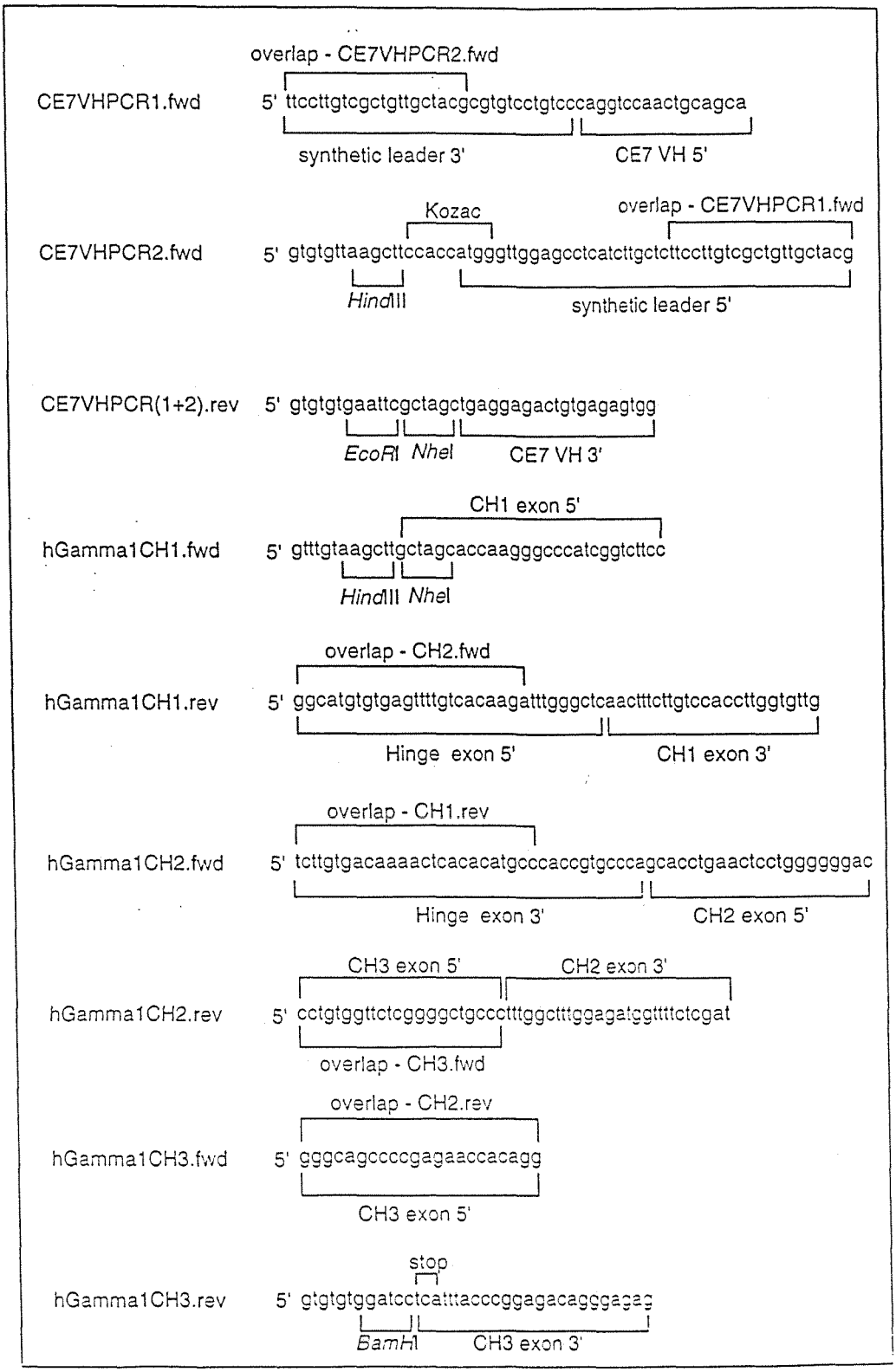
overlap - CE7VHPCR2.fwd
CE7VHPCR1.fwd
5' ttccttgtcgctgttgctacgcgtgtcctgtcccaggtccaactgcagca
synthetic leader 3'
CE7 VH 5'
Kozac
overlap - CE7VHPCR1.fwd
CE7VHPCR2.fwd
5' gtgtgttaagcttccaccatgggttggagcctcatcttgctcttccttgtcgctgttgctacg
HindIII
synthetic leader 5'
CE7VHPCR(1+2).rev
5' gtgtgtgaattcgctagctgaggagactgtgagagtgg
EcoRI NheI
CE7 VH 3'
CH1 exon 5'
hGamma1CH1.fwd
5' gtttgtaagcttgctagcaccaagggcccatcggtcttcc
HindIII NheI
overlap - CH2.fwd
hGamma1CH1.rev
5' ggcatgtgtgagttttgtcacaagatttgggctcaactttcttgtccaccttggtgttg
Hinge exon 5'
CH1 exon 3'
overlap - CH1.rev
hGamma1CH2.fwd
5' tcttgtgacaaaactcacacatgcccaccgtgcccagcacctgaactcctgggggggac
Hinge exon 3'
CH2 exon 5'
CH3 exon 5'
CH2 exon 3'
hGamma1CH2.rev
5' cctgtggttctcggggctgccctttggctttggagatggttttctcgat
overlap - CH3.fwd
overlap - CH2.rev
hGamma1CH3.fwd
5' gggcagccccgagaaccacagg
CH3 exon 5'
stop
hGamma1CH3.rev
5' gtgtgtggatcctcatttacccggagacagggagag
BamH1
CH3 exon 3'

Figure 3.

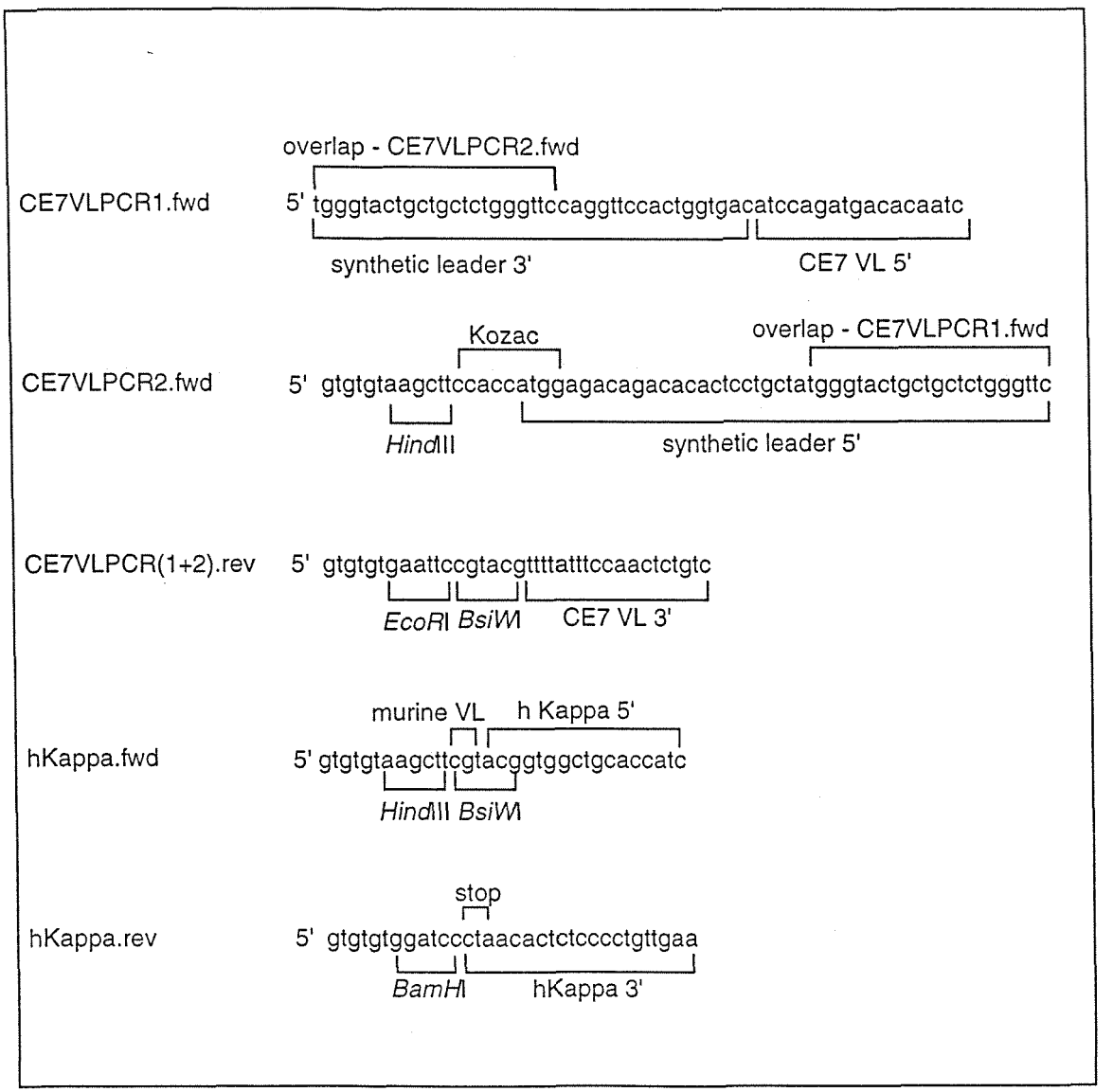
overlap - CE7VLPCR2.fwd
CE7VLPCR1.fwd
5' tgggtactgctgctctgggttccaggttccactggtgacatccagatgacacaatc
synthetic leader 3'
CE7 VL 5'
Kozac
overlap - CE7VLPCR1.fwd
CE7VLPCR2.fwd
5' gtgtgtaagcttccaccatggagacagacacactcctgctatgggtactgctgctctgggttc
HindIII
synthetic leader 5'
CE7VLPCR(1+2).rev
5' gtgtgtgaattccgtacgttttatttccaactctgtc
EcoRI BsiWI
CE7 VL 3'
murine VL
h Kappa 5'
hKappa.fwd
5' gtgtgtaagcttcgtacggtggctgcaccatc
HindIII BsiWI
stop
hKappa.rev
5' gtgtgtggatccctaacactctcccctgttgaa
BamHI
hKappa 3'

Figure 4.

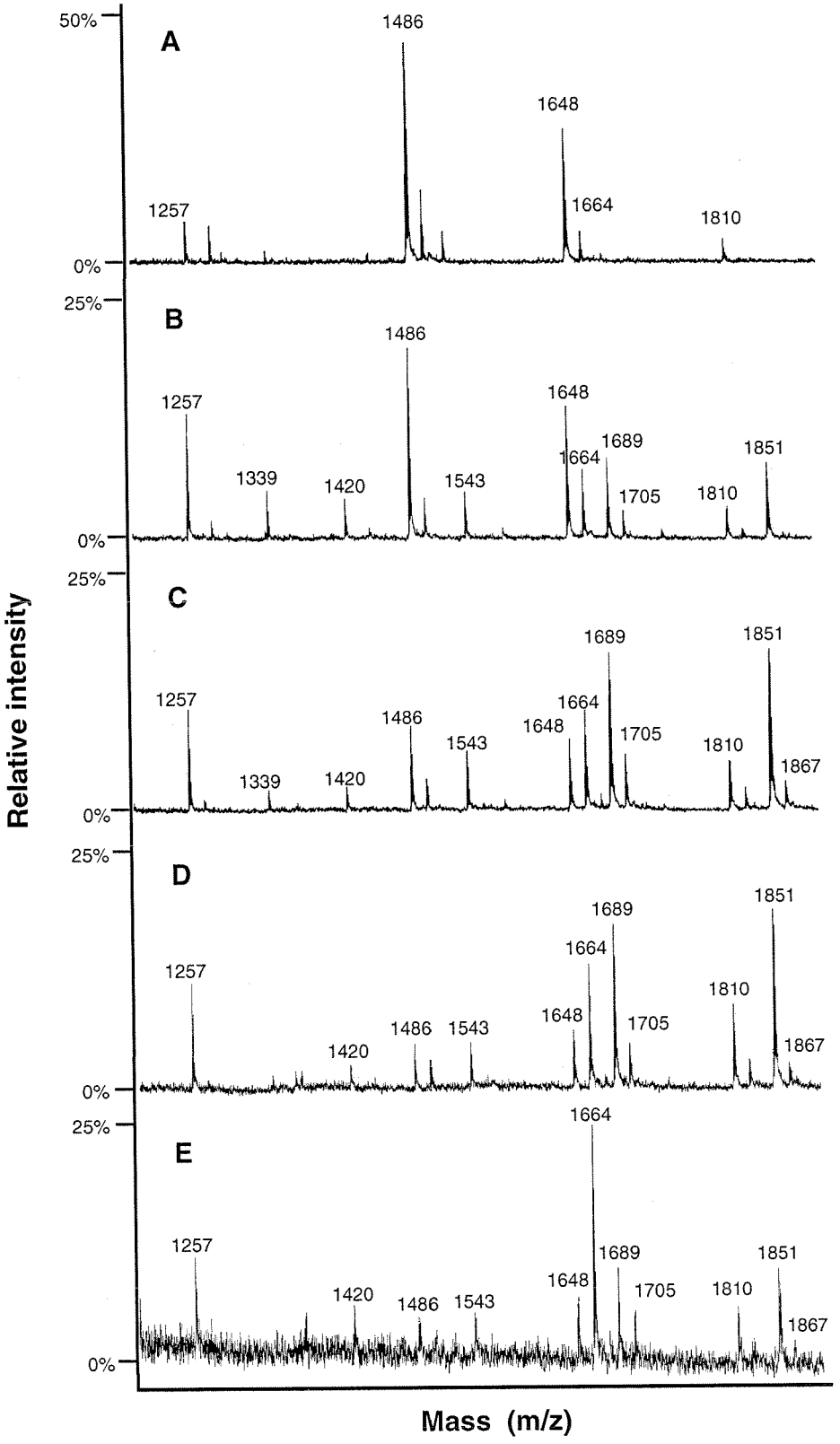
50%
A
1486
1648
1257
1664
1810
0%
25%
B
1486
1257
1648
1689
1664
1851
1339
1420
1543
1705
1810
0%
25%
C
1689
1851
1257
1664
1486
1648
1543
1705
1810
1339
1420
1867
0%
25%
D
1689
1851
1664
1257
1810
1486
1543
1648
1705
1420
1867
0%
25%
E
1664
1257
1689
1851
1648
1420
1705
1810
1486
1543
1867
0%
Relative intensity
Mass (m/z)

Figure 5.

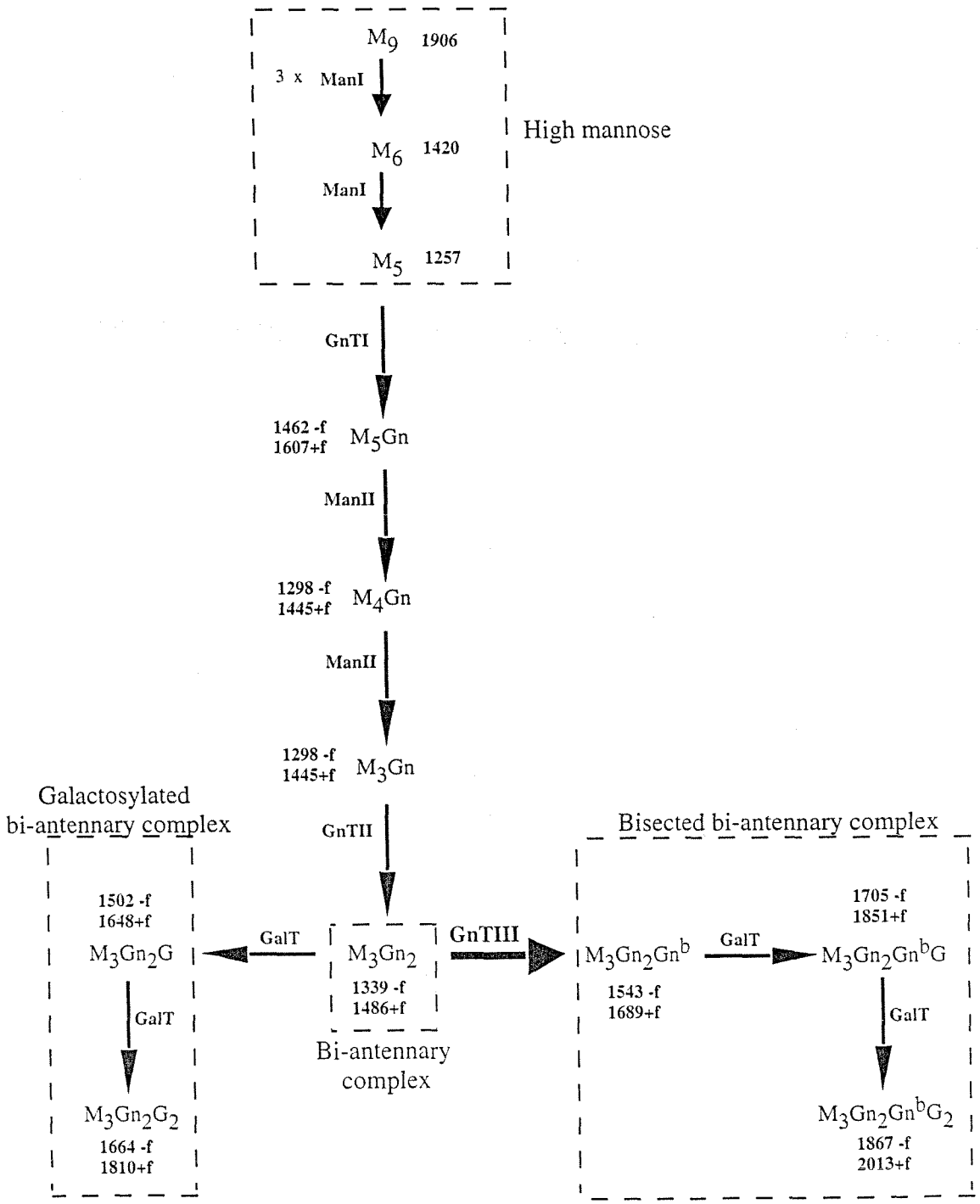
M9 1906
3 x ManI
M6 1420
ManI
M5 1257
High mannose
GnTI
1462 -f
1607+f
M5Gn
ManII
1298 -f
1445+f
M4Gn
ManII
1298 -f
1445+f
M3Gn
GnTII
Galactosylated
bi-antennary complex
1502 -f
1648+f
M3Gn2G
GalT
M3Gn2G2
1664 -f
1810+f
GalT
M3Gn2
1339 -f
1486+f
Bi-antennary
complex
GnTIII
Bisected bi-antennary complex
M3Gn2Gnb
1543 -f
1689+f
GalT
1705 -f
1851+f
M3Gn2GnbG
GalT
M3Gn2GnbG2
1867 -f
2013+f

Figure 6.

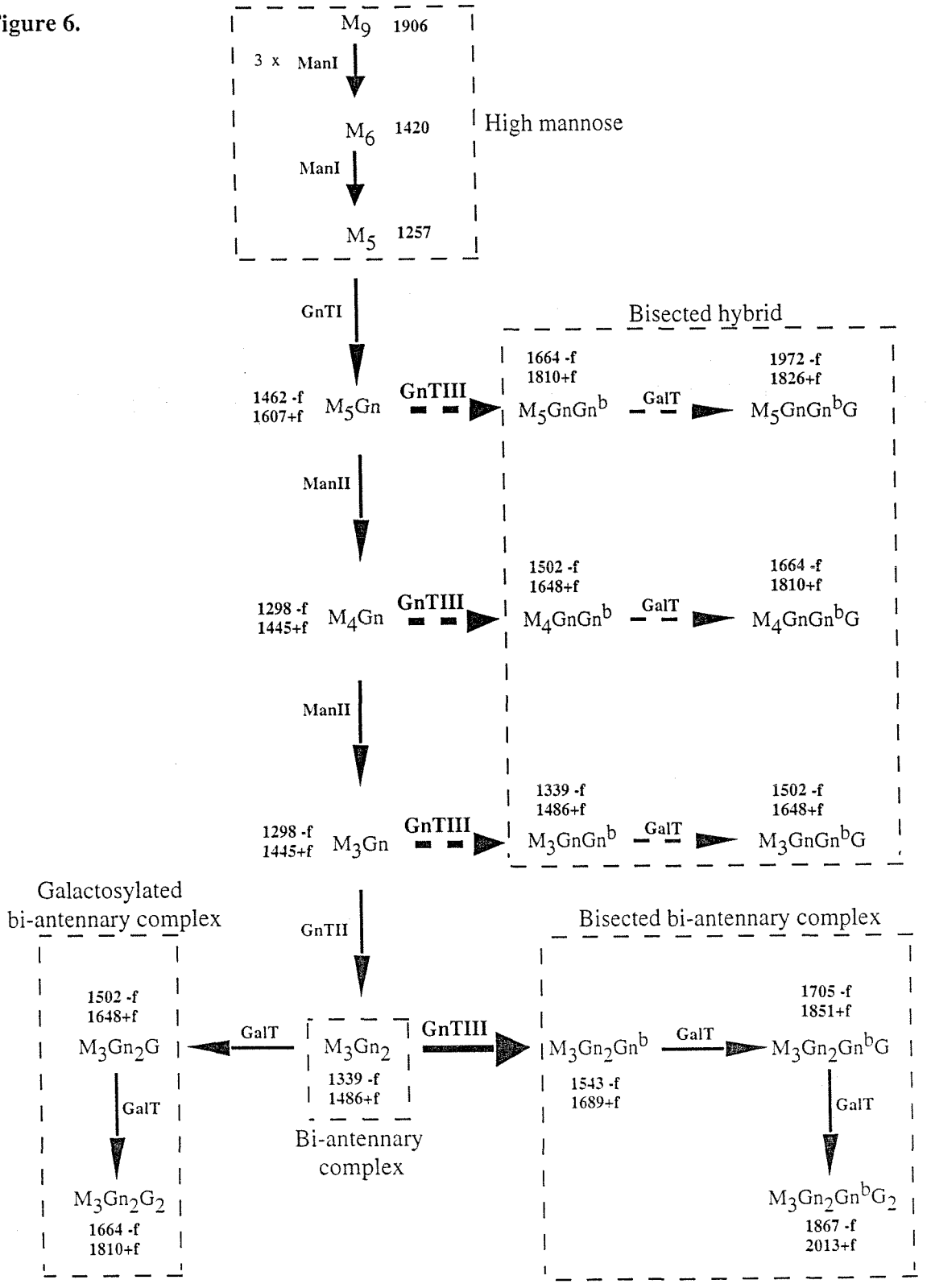
M9 1906
3 x ManI
M6 1420
ManI
M5 1257
High mannose
GnTI
Bisected hybrid
1462 -f
1607+f
M5Gn
GnTIII
1664 -f
1810+f
M5GnGnb
GalT
1972 -f
1826+f
M5GnGnbG
ManII
1298 -f
1445+f
M4Gn
GnTIII
1502 -f
1648+f
M4GnGnb
GalT
1664 -f
1810+f
M4GnGnbG
ManII
1298 -f
1445+f
M3Gn
GnTIII
1339 -f
1486+f
M3GnGnb
GalT
1502 -f
1648+f
M3GnGnbG
Galactosylated
bi-antennary complex
GnTII
Bisected bi-antennary complex
1502 -f
1648+f
M3Gn2G
GalT
GalT
M3Gn2
GnTIII
M3Gn2Gnb
GalT
1705 -f
1851+f
M3Gn2GnbG
1339 -f
1486+f
Bi-antennary
complex
1543 -f
1689+f
GalT
M3Gn2G2
1664 -f
1810+f
M3Gn2GnbG2
1867 -f
2013+f

Figure 7.

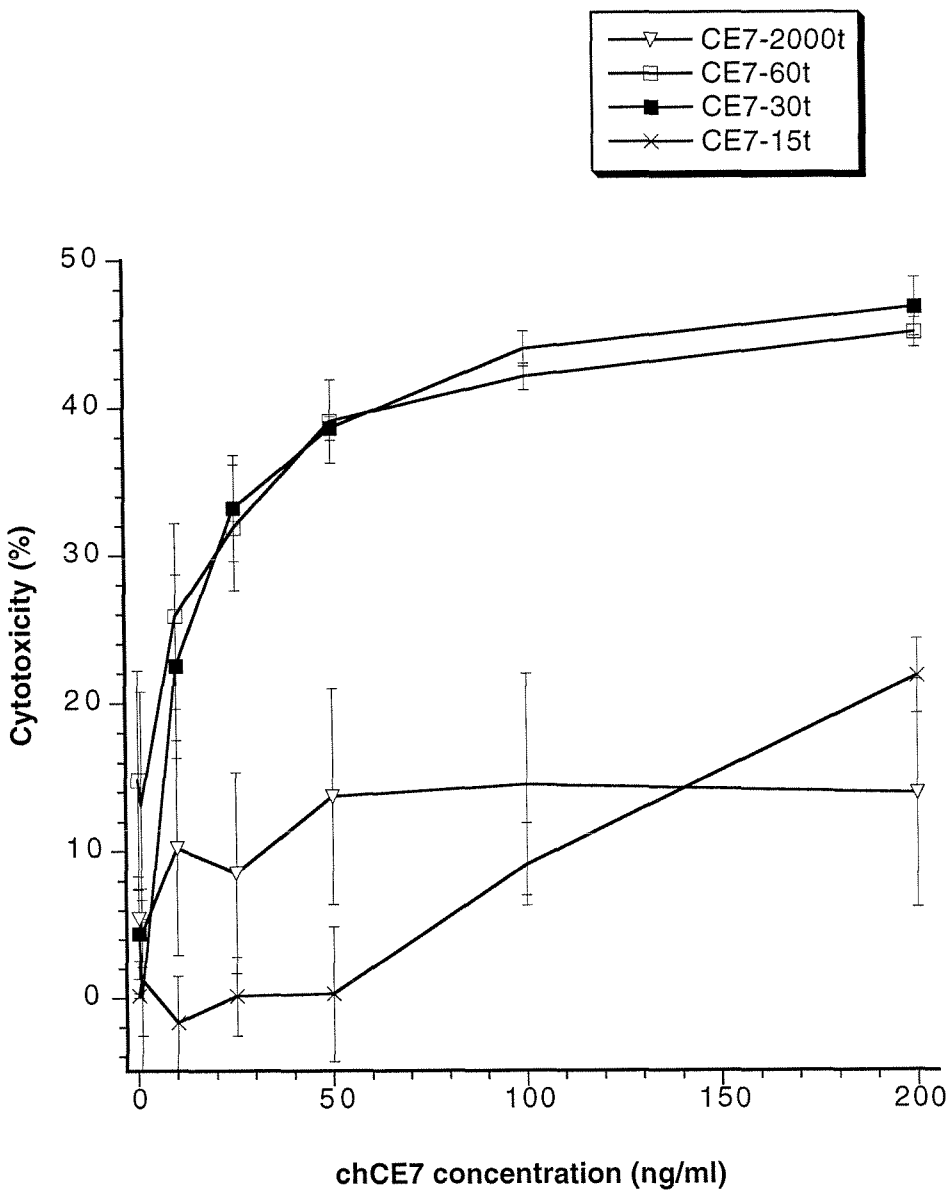
CE7-2000t
CE7-60t
CE7-30t
CE7-15t
Cytotoxicity (%)
50
40
30
20
10
0
0
50
100
150
200
chCE7 concentration (ng/ml)

CHAPTER V

Conclusions

5.1 Summary of Findings and Recommendations for Future Work

The goals of this thesis were to engineer glycoform biosynthesis in CHO cells in order to produce new variants of a therapeutic protein, and to study the extent to which the glycosylation reaction network could be manipulated in an attempt to maximize the proportion of certain glycoforms within the population. An anti-neuroblastoma chimeric IgG1-type mAb (chCE7) was used as a model therapeutic protein and the target glycoforms were those carrying bisected, complex oligosaccharides. Natural IgG antibodies in humans and animals carry these types of oligosaccharides, albeit in a small proportion within the glycoform population, and a recent study suggested that these oligosaccharides could lead to enhanced killing of target cells via ADCC. Therapeutic antibodies produced in CHO cells do not carry bisected oligosaccharides as the cells do not express the gene encoding GnTIII, the glycosyltransferase that catalyzes the biosynthesis of bisected oligosaccharides. We therefore decided to overexpress GnTIII in CHO cells and use the modified cells to produce new variants of chCE7.

A mathematical model of N-linked glycoform biosynthesis was constructed and used to simulate the qualitative effects of GnTIII overexpression. The simulations indicated a maximum level for bisected complex oligosaccharides, and accumulation of hybrid bisected oligosaccharides. CHO cells with stable, tetracycline-regulated overexpression of the GnTIII gene were established. The amount of GnTIII in these cells could be controlled simply by manipulating the concentration of tetracycline in the culture medium. Using this system, it was found that overexpression of GnTIII to high levels led to growth inhibition and was toxic to the cells. Another CHO cell line with tetracycline-regulated overexpression of GnTV, a distinct glycosyltransferase, showed the same inhibitory effect, indicating that this may be a general feature of glycosyltransferase overexpression. This phenomenon has not been reported previously, probably due to the widespread use of constitutive promoters. The growth effect sets an upper limit to the level of

glycosyltransferase overexpression, and may thereby also limit the maximum extent of modification of poorly accessible glycosylation sites.

The heterologous GnTIII was localized in the Golgi complex of CHO cells by means of immunoelectron microscopy using an antibody against a peptide epitope tag added to the carboxy-terminus of the enzyme. The enzyme concentrated on one side of the Golgi, mainly in cisternal compartments, suggesting that GnTIII may spatially distribute as a peak with a maximum between those of GnTI/ManII/GnTII and that of GalT, but still overlapping significantly with all of these enzymes. A statistical immunogold analysis of many cell sections (Nilsson et al., 1993; Rabouille et al., 1995) would be valuable to establish the quantitative GnTIII distribution.

CHO cells with GnTIII expression levels ranging from basal to toxic were used to produce ChCE7 antibody variants differing in their glycoform distributions. Experimental results showed an optimal range of GnTIII expression for maximal chCE7 *in vitro* biological activity, and this activity correlated with the level of Fc-associated bisected, complex oligosaccharides. Expression of GnTIII within the biotechnologically practical range, i.e., where no significant growth inhibition and toxicity are observed, led to a consumption of more than 90% of non-bisected, non-galactosylated bi-antennary complex oligosaccharides, but, at most, 50% was converted to the target bisected, complex structures for this set of chCE7 samples. The rest could have been diverted to bisected hybrid by-products and/or consumed by competing GalT to produce non-bisected, galactosylated oligosaccharides. Direct profiling by MALDI/TOF-MS cannot distinguish between the latter two classes of oligosaccharides, but the growth of the associated MALDI/TOF-MS peaks upon GnTIII overexpression, with concomitant reduction of bisected complex-peaks, suggests the formation of bisected hybrid products.

The new optimized variants of chCE7 are promising candidate reagents for the treatment of neuroblastoma. In future work, production should be scaled-up and clinical trials eventually undertaken. The strategy presented here may also be applicable to other

IgGs, including those with high ADCC activity in the absence of a bisecting GlcNAc (Reff et al., 1994).

It would be desirable to try to further maximize the fraction of bisected complex oligosaccharides. This may possibly be achieved by simultaneous overexpression of ManII mannosidase and GnTIII, perhaps concurrent with an increase in the intra-Golgi level of UDP-GlcNAc cosubstrate.

It remains to be determined whether the increase in ADCC activity results from the increase in both the galactosylated and non-galactosylated, bisected complex oligosaccharides, or only from one of these forms. If glycoforms with galactosylated, bisected complex oligosaccharides are found to be the most active, maximizing these would require simultaneous overexpression of both GnTIII and GalT. Given the competitive scenario discussed previously, the expression levels of both genes would have to be carefully regulated.

Finally, it would be valuable to try to re-distribute overexpressed GalT as much as possible towards the TGN instead of the trans-Golgi cisterna. The latter strategy may be realized by exchanging the transmembrane region-encoding sequences of GalT with those of α2,6-sialyltransferase (Chege and Pfeffer, 1990).

5.2 References

Chege, N. W. and Pfeffer, S. R. 1990. Compartmentation of the Golgi complex: Brefeldin-A distinguishes trans Golgi cisternae from the trans Golgi network. J. Cell Biol. **111:** 893-899.

Nilsson, T., Pypaert, M., Hoe, M. H., et al. 1993. Overlapping distribution of two glycosyltransferases in the Golgi apparatus of HeLa cells. J. Cell Biol. **120:** 5-13.

Rabouille, C., Hui, N., Hunte, F., et al. 1995. Mapping the distribution of Golgi enzymes involved in the construction of complex oligosaccharides. J. Cell Science **108:** 1617- 1627.

Reff, M. E., Carner, K., Chambers, K. S., et al. 1994. Depletion of B cells in vivo by a chimeric mouse human monoclonal antibody to CD20. Blood **83:** 435-445.